A MICROPROCESSOR-BASED SYSTEM OF SIGNAL GENERATION FOR USE IN CLINICAL AUDIOMETRY

by

JACK GOLDBERG

B.S., Massachusetts Institute of Technology
(1973)

SUBMITTED IN PARTIAL FULFILLMENT
OF THE REQUIREMENTS FOR THE
DEGREE OF

MASTER OF SCIENCE

at the

MASSACHUSETTS INSTITUTE OF TECHNOLOGY

September, 1978

Signature of Author .....
Department of Electrical Engineering and Computer Science
September, 1978.

Certified by.....
Thesis Supervisor

Accepted by .....
Chairman, Departmental Committee on Graduate Students

A Microprocessor-Based System of Signal Generation for Use in Clinical Audiometry

by

Jack Goldberg

Submitted to the Department of Electrical Engineering and Computer Science in September, 1978, in partial fulfillment of the requirements for the Degree of Master of Science.

ABSTRACT

A versatile device for the generation of signals used to measure human hearing is described. The design prototype is microprocessor based (Zilog Z-80) with the capability to produce two independent pure tones and narrowband masking noise. The test frequency can sweep logarithmically as required in Bekesy-type testing. Facilities for control of the signal intensity and recognition of subject responses are excluded from this work. As background, knowledge of historical advances in psychoacoustics and technical progress in audiometer design lend perspective to the development of a new system. For present-day clinical use, considerations of quality and practicality indicate that direct digital synthesis of the required waveforms is inappropriate, as are open-loop methods of sine-wave control and discrete-time filtering. In this design, phase-lock and voltage-controlled filtering techniques provide an adequate means of generating the necessary sweepable signals. Pure tone production is accomplished through two computer controlled square wave generators and two low distortion phase-locked sine wave generators. Noise is created by clocked digital logic and shaped by a voltage-controlled two-pole lowpass filter. A unique combination of clock control and voltage control, both derived from phase-locked circuitry, establishes a noise with fixed energy and controllable bandwidth. Four quadrant multiplication is then utilized to create third-octave band masking noise centered around the frequency of one of the pure tones. Sweep speeds of ½, 1, and 2 octaves per minute for frequencies from 75 Hz to 12.8 KHz can be attained by the design. Measured performance characteristics of the system exceed the current requirements of clinical equipment. An inherent tradeoff between sweep speed and frequency range and the limitations of available two- and four-quadrant multipliers are minor disadvantages of the chosen system architecture. Applications include signal generation for manual and Bekesy testing and the production of modulated signals for free-field use.

Thesis Supervisor: Francis F. Lee, Professor, Electrical Engineering and Computer Science, Massachusetts Institute of Technology

ACKNOWLEDGEMENTS

For assistance and support in this project, I wish to thank the following people:

Francis F. Lee, for supervising the work;

Rufus L. Grason, for the interest and enthusiasm which made this project possible;

Joseph Mihaly, Michael Coln, and Webster P. Dove, for critically reviewing and discussing technical ideas;

H.S.Colburn, for esoteric dialogue on random signals; and

Donna J. Selger, whose knowledge of the field of audiology and whose kind support were invaluable.

I further thank Joy Thompson, Carl Thompson, Ralph Goguen and William Handley for help with the typing, editing, and mechanical drawing.

TABLE OF CONTENTS

LIST OF FIGURES

I. INTRODUCTION

The measurement of human hearing is a task which has been recognized as vitally important since the earliest times. The manner of testing, however, underwent essentially no change from ancient times well into the nineteenth century. An audiometric procedure of the earliest type is neatly outlined in Raue's text on medical practice published in 1885:

> "If we want to ascertain the distance at which a patient is able to hear, we must use an instrument which gives a sound always of the same nature and strength, and which can easily be held at different distances from the ear to be examined. Such an instrument is the watch. We commence by holding it at a distance and bring it gradually nearer to the ear until its tick is perceived; the reverse order might give rise to mistakes. As soon as the patient can indicate the tempo of the tick, we are sure that he hears it, and we know the distance in which he hears by exact measurement."

Ideas expressed in this short description were familiar to many even during the time of Aristotle: sound is transmitted through the air to the ear by means of motion; that which produces sound must be vibrating; and individuals with keener hearing can perceive a given sound at greater distances. Of course, a watch is a relatively complex acoustic device which was unavailable in ancient times, yet the reports of using whispers and the click of coins struck together to investigate hearing involve the same basic concepts.

Major developments in the field were infrequent until recent times as is apparent from the fact that procedures such as the watch tick test were widely used for hundreds of years. The reason for this slow initial growth lies in the multidisciplinary nature of the problem. A person's inner perception is known to himself only, therefore audiometrists must work with observable responses to known stimuli. How can we observe, quantify, and

interpret the characteristics of an auditory system? In order to test, one must have sufficient knowledge of the hearing mechanism and the physics of sound to know what features to explore and how to best carry out the procedure, must have access to accurate, specific sound generation and measurement apparatus, and finally must be able to assign meaningful measures to the results of the test. Thus, the fields of mathematics, physics, psychology, and physiology are all of concern. A certain level of understanding within each of these four disciplines was necessary before the links between them could be discovered. Once discovered, the study of psychoacoustics burgeoned.

The twentieth century has witnessed incredible change. Almost everyone in this country has at some time received a hearing test, and a full scale evaluation is readily available. Procedures are widely accepted and standardized. A screening test takes a matter of minutes, and a clinical evaluation seldom takes longer than a few hours. Audiometers of today are sophisticated electroacoustic devices which offer calibrated tones and noises covering about a seven-octave frequency range and a 120 dB dynamic range. They allow the operator to perform dozens of different paradigms and include facilities for both air and bone conduction, free field, and speech testing. Only when the appropriate electroacoustic setup is unavailable are the old tuning fork or whisper techniques employed by audiologists. Our knowledge about the hearing system is far from complete, however. Current research is exploring aspects ranging from the muscular functions in the middle ear to the acoustical/biological transduction present within the cochlea to the cognition of speech sounds. Because of this continuing progress, apparatus for auditory research and eventually

commercial clinical instrumentation, where human engineering and diagnostic value are important, must keep pace.

The bulk of this paper describes the development of an electronic system designed as part of a computer controlled, clinical audiometric instrument. For a broader perspective, an historical survey is included. This section briefly highlights philosophical, scientific, and technological events in areas relating to the measurement of hearing. Following the history, the discussion of the project begins with a statement of its scope and a description of the signal generation requirements of modern clinical equipment. Next, the considerations leading to the final choice of system architecture are reviewed, along with several ideas for future research. Following this, is a more detailed discussion of the theory, performance, and limitations of the circuitry utilized in the prototype. Several applications are also outlined. This versatile system can be used for the entire battery of tests involving controlled pure tone and noise stimuli with voluntary subject responses. Being computer based, many previously unavailable features such as record keeping, arithmetic routines to aid during setup, novel signal generation capabilities, and additional data to assist in diagnosis can be incorporated.

II. HISTORICAL BACKGROUND

Fundamental ideas concerning the nature of sound were proposed at a very early stage in the development of scientific thought. Amongst the first to speculate on the production, propogation, and reception of sound were the ancient philosophers. Aristotle (384-322 B.C.), in his work "De Audibilibus", put forth a germinal theory of sound which implied its wave nature. He maintained that a body emitting sound caused motion in the air, and that the disturbance is propagated by means of "contraction or expansion or compression". A contrasting interpretation of observed acoustical phenomena was held by Lucretius, a Roman philosopher, during the first century, B.C. Lucretius reasoned that sound was particulate, citing evidence such as the existence of echoes, the effects of wind, and the way shouting "scrapes" the throat [Schroeder, 1975].

Writings of the fifth century and later indicate wider acceptance of Aristotle's view, though there were a few, even as late as the Renaissance, who adhered to the particle theory. Accuracy of initial theories is unusual in the history of science. Early notions about sound, such as Aristotle's, were elaborated upon though never seriously revised, which is not the case, for example, regarding primitive theories of light and heat [Lindsay, 1966]. Over the next thousand years, refinement of acoustical concepts was minor, awaiting the evolution of ideas in mathematical mechanics and other fields. During the seventeenth century, significant growth in our understanding of sound was first apparent. Progress was encouraged by an abundance of questions arising out of many aspects of life. Some researchers were interested in musical instruments and

composition. Many were concerned with the problems of the hearing-impaired. Others were scientists curious about the speed of sound or the limits and mechanisms of human hearing. Theoreticians, experimentalists, and designers of apparatus all made contributions.

Figures II-1 and II-2 which follow present a summary of the history of audiometry from ancient times to the present. The first figure is an overview of major accomplishments in acoustics and hearing, and the second figure is a chronology of audiometric apparatus starting with the early mechanoacoustic systems. It should be pointed out that sources of information for this chapter are in general secondary, and thus some minor disagreements, still unresolved here, may exist when compared with other historical reviews. (Lindsay's book, Acoustics: Historical and Philosophical Development, 1966, contains reprints of many original works.) The two summary outlines supplement the text in order to clarify the complex and fascinating interaction of scientific disciplines which has led to our current techniques of hearing measurement.

Audiometry is a clinical study within the area of psychoacoustics. As already pointed out, the measurement of human hearing is a multidisciplinary problem, and thus any study of the history of audiometry is linked with developments in many branches of science. Most of the outstanding work has been accomplished by individuals with knowledge bridging two or more fields. Many areas have had major impact on current techniques in audiometry. These include the mathematics of waves, the mechanics of harmonic motion, the mathematics of signals and system theory, the psychology and statistics of detection theory, the physiology of the

auditory system, the psychological scaling of sensations, and the physics of electronic devices.

Early innovations in methods of measuring hearing, occurring during the eighteenth and nineteenth centuries, were due primarily to an increasing knowledge of psychoacoustics. The mechanical generation of sound was the only means of producing stimuli available in that period, a time rich in developments leading to the first models of hearing and applications of calculus to mechanics, systems theory, and statistics. Mechanoacoustic audiometric systems were never produced in large number; however, many were designed for research purposes. Clinical practice before the twentieth century was generally limited to the use of various tuning fork tests, though psychoacoustics laboratories often had elaborate setups. Most treatises on general medical practice published during the first half of the nineteenth century offer treatments for deafness, but without any hints on how to detect it.

Research in psychoacoustics continued enthusiastically during the early twentieth century, but another factor was then beginning to exert a strong influence on audiometric techniques. Applications of electricity and electronics to the generation and measurement of acoustic signals were being devised at a pace so rapid that progress in the testing of hearing soon became linked to the growth of electroacoustic technology rather than to the comparatively slow advances in related physical, psychological and physiological research. The most important of the new electroacoustic components was the transducer, applied first to the telephone. Audiometers incorporating electric "earphones" were produced during the late 1800's,

but none became popular until an early application of the vacuum tube resulted in the first commercially successful electric audiometer, the Western Electric 2A introduced in 1924 [Bunch, 1941].

Today's audiometers produce generally the same signals that were being strived for in designs of the late nineteenth century. Knowledge about masking has caused some recent changes in audiometric instrumentation, but the need for masking noise was known one hundred years ago, as was the need for both pure-tone and speech stimuli. The diagnostic significance of bone-conduction measures had been recognized before the turn of the century, and the benefits associated with logarithmic scaling of intensity and frequency were formalized around 1860. Were Helmholtz (1821-1894) alive today, he would not at all be surprised at the capabilities of modern audiometers, though the electronic techniques employed and the ease of operation might astound him. The sixty year evolution of the electronic audiometer seems very brief when compared to the centuries of research necessary to devise the first well quantified hearing test.

Any device which produces sound can conceivably be utilized to measure hearing. In ancient times, the only specialized sound generators were musical instruments usually built for artistic rather than scientific application. The human voice, of course, is the most accessible sound source and indeed most hearing problems initially show up as difficulties in understanding spoken language. Speech testing is very important in the diagnosis of hearing problems, especially those having to do with signal processing within the cochlea or auditory perception. Early whisper tests were often conducted in an effort to characterize the severity of a hearing

impairment, but the cognition of speech is a very complex process involving almost the entire auditory apparatus. Without other information, results of whisper tests cannot be considered conclusive, even if the intensity of the voice is well controlled. Another kind of stimulus, easy to specify and produce, and with clear diagnostic significance was needed.

Without theories of audition, early "audiometrists" were guided primarily by practicality in selecting non-speech stimuli for testing. The requisites for an appropriate sound source were simply that it be easy to operate and produce nearly the same sound every time. Clocks, bells, coin clicks, and simple whistles were the earliest choices. There was a tendency to use sounds that were not harsh or noisy; musical sounds, whether tonal or rhythmic, were preferred. Experiences with music have provided many thinkers with a framework for psychoacoustic investigation. Due to interest in musical instruments, the relationship between pitch and frequency was discussed over two thousand years ago, but the factors governing the quality or timbre of tones were not understood then. In order to thoughtfully specify stimuli for testing, researchers had to first comprehend the important features which distinguish different sounds.

J.B.J. Fourier's famous theorem, reported in 1822, had far-reaching impact on the study of acoustics [Lindsay, 1966]. The conclusion that periodic functions can be expressed as a sum of sinusoids implied for the first time that the pure tone is especially significant in hearing. About twenty years later, George Simon Ohm introduced a theory of audition which characterized all musical tones as arising from harmonic vibrations of definite frequency with variation in timbre due to the coexistence of

different harmonics. Furthermore, Ohm believed that the human ear has the ability to analyze a complex tone into a set of harmonically related frequencies. Later, Hermann von Helmholtz's "resonance theory of hearing" (1863) carried these concepts further, hypothesizing for the first time the mechanics of the ear. In accordance with the ear's ability to analyze sound into component frequencies, Helmholtz postulated that various elements of the basilar membrance resonate to certain frequencies. [Green, 1976]

Though the use of pure tones in testing was greatly encouraged by these early theories of audition, the tendency to use them in practice was evident long before. Of all the sources used in audiometry before the twentieth century, except perhaps the human whistle, tuning forks were the purest. Another important advantage in using forks was the ability to test hearing through bone conduction. Ingrassia, an Italian professor in the sixteenth century, observed that a vibrating body when rested against the teeth can be heard. In 1825, Ernst Heinrich Weber first published his experimental result that sometimes when a fork is placed midline on the skull of a person with unilateral loss, the tone is heard better in the impaired ear. This fact served as the basis for the popular Weber test, first introduced into clinical practice in 1834 after realization of its significance in distinguishing conductive from other types of hearing loss. The possibility of investigating both air and bone conduction paths with the same fork was described about twenty years later by Rinne as another diagnostic procedure. [Johnson, 1970]. Several other fork tests have been introduced including the Schwabach test, a bone-conduction procedure in which the hearing sensitivity of the patient is compared with that of the

examiner, and the Bing test which involves closing off the opening of the outer ear canal, which in normals causes the loudness of bone-conduction to increase [Martin, 1975]. Tuning forks provided audiometry with the first popular clinical techniques, and are still occasionally used today.

Vibrating forks, by nature, have very stable frequency and were therefore widely used to study the frequency limits of hearing. Many researchers worked on this question, even before the popularization of forks, but it was Rudolph Koenig (1832-1901) who constructed the most extensive sets. Koenig's "universal tonometer" contained forks that produced frequencies as low as 16 Hz and as high, he claimed, as 90,000 Hz. His estimate of the frequency range of human hearing was approximately from 13 Hz to 17.5 KHz. There were many other valuable contributions as a result of investigation into the range of audible frequencies. Felix Savart built a variable frequency standard modelled after seventeenth century work by Robert Hooke, consisting of a rotating serrated wheel striking a reed, which he used in 1830 to study the range. Other researchers included Seebeck, who invented the present form of the siren, Galton, famous for his calibrated whistles, and Helmoltz. [Beranek, 1949]. Early errors in the determination of the frequency range of hearing can be attributed to the audibility of the harmonics of low frequency sources, and the misspecified frequencies of high frequency sources.

Acoustic stimuli generated by forks and whistles were well specified in terms of frequency, but their intensity was very difficult to control. Being a serious drawback to their application, several systems of calibrated striking for sounding rods or tuning forks were devised,

includng Macfarlan's "pleximeter" in 1922 and Roth's "acoustimeter" in 1934 [Johnson, 1970]. Interest in these techniques diminished as electronic circuits replaced mechanical arrangements, but before that time, the severity of impairment had to be quantified indirectly. The watch-tick test characterized hearing loss in terms of distance, meaningless unless the intensity of the tick, room acoustics, and ambient noise levels were known; and it had the further disadvantage that results based on different watches could not easily be compared. In the Schwabach procedure, the difference in sensitivity between the patient and the examiner, hopefully a person with normal hearing, was specified in seconds. These measures could not be standardized, and accurate measurement of intensity was an active area of concern throughout the nineteenth century. The related investigation into the absolute sensitivity of hearing parallelled advances in the physical measurement of stimuli. Techniques included the use of sensitive flames by Le Conte and Koenig, optical apparatus by Biot and Lissajous, and various graphical instruments. Lord Rayleigh, who is considered by many to have ushered in the era of modern acoustics by writing his authoritative treatise on the field published in 1877, invented the Rayleigh disk, a small light circular plate suspended by a fiber, which, by its deflection, indicates the intensity of an impinging sound wave. [Beranek, 1949]

As the pitch of a sound represents the psychological percept of frequency, the loudness of a sound represents the percept of intensity. Along with interest in measuring the physical intensity of a stimulus, there were many who researched the scaling of loudness. Weber's speculation on the scaling of sensations has led, after over a century, to

our current use of the decibel scale in many areas. In 1834, Weber hypothesized that the just noticeable difference (JND) in a sensation is always equal to a constant fraction of its absolute magnitude. Early experiments with different sensory modalities showed general agreement with this law, and in 1860, a physicist, G. T. Fechner, was led to a mathematical expression that could unite for the first time inner experience with the world of outer events. In his "Elemente der Psychophysik", Fechner concluded that the responses of humans to stimuli vary as the logarithms of those stimuli, a result derived by considering that each JND is a constant portion of the sensory scale. [Hirsh, 1952]. Modern studies have shown considerable disagreement with Fechner's law, yet logarithmic scaling is used widely.

Designing instrumentation with accurately specified stimuli was a considerable problem before the application of electronics. Using electricity, however, required some form of electroacoustic transduction. Numerous physical effects can be exploited to change electrical energy into sound and vice versa. The most widely used transducers have been based on phenomena observed long before their application was apparent: electrostatic and electromagnetic forces. Magnetostriction, discovered by J.P. Joule in 1842 and the piezoelectric effect, first reported by Pierre and Jacques Curie in 1880, were both introduced along with possible application for the generation of sound [Lindsay, 1966]. Alexander Graham Bell is credited with the first application of transducers in communications. His invention of the telephone, patented in 1876 after a long legal battle, marks the beginning of the era of electronic audiometry.

A. Hartmann and D.E. Hughes are both credited with the earliest use of electricity in instruments for the measurement of hearing. Hartmann's "acoumeter" of 1878 and Hughes's "sonometer" of 1879 used the tuning fork as a frequency source. The motion of the fork regularly interrupted a primary circuit. Coupling was accomplished with a rheocord, or sliding induction coil, and in the secondary circuit there was an electromagnetic transducer. The cumbersome nature of these devices, along with their inability to operate at frequencies greater than 1000 Hz outweighed their advantage in terms of intensity control, and therefore neither was widely used. These first design concepts were improved upon by Urbantschitsch in 1884 when he replaced the tuning fork in the primary circuit with an electric buzzer, and Jacobson in 1885, who incorporated a second induction coil for better level control and a pair of tubes for binaural listening. In 1899, Carl Emile Seashore introduced the first audiometer with logarithmic intensity control, by utilizing a series of secondary windings which could be selected with a switch. At the turn of the century, dozens of different audiometers had been introduced. One single impure tone was generally employed when testing hearing with these first electric instruments and all of them were expensive and difficult to operate. [Bunch, 1941]

Researchers of the twentieth century understood the importance of using low distortion tones, adjustable over wide frequency and intensity ranges, yet great technical difficulties stood in the way of producing the desired signals. An interesting step in audiometer evolution was the application of A. Stefanini's electric generator in 1914. His invention created an alternating current by means of a toothed pendulum which fell

through a magnetic field. By adjusting the height of the fall, the frequency could be controlled with ease; however, the system had the disadvantage that the range of frequencies was limited and the duration of the test tone could not be altered independently. [Bunch, 1941]. L.W. Dean and C.C. Bunch [1919] further innovated when they used a newer type of generator, one with a rotating toothed wheel in a magnetic field, to construct the "pitch range audiometer". A motor drove the wheel at variable speed such that tones with fundamental frequency ranging from 30 Hz to 10 KHz could be produced. Dean and Bunch felt that their invention fulfilled the six most important requirements of an audiometer: 1) to produce tones within the full audible frequency range without any gaps; 2) to produce a "relatively pure tone, pure enough for all practical purposes"; 3) to enable the convenient control of intensity from below threshhold to a level on the verge of being painful; 4) to enable the precise recording of both frequency and intensity; 5) to enable a sweep of frequency at fixed intensity as well as a sweep of intensity at fixed frequency; and 6) to be simple and rapid in use.

Almost all subsequent developments in audiometric instrumentation, from 1919 on, have been centered around the use of amplifying circuits. Oscillating circuits had been discovered in the middle of the nineteenth century, but their use in acoustics depended on an adequate means of coupling. The vacuum triode was invented by Lee de Forest in 1906. As an amplifier this device allowed the first application of oscillating circuits to the generation of sound. The Berlin Otological Society witnessed the demonstration of the first vacuum tube sets for testing hearing in November of 1919. One of these devices, presented by Grushke, Greismann and

Schwartzkopf, was later manufactured as the "Otaudion" and was used considerably in Europe [Davis and Merzbach, 1975]. This is apparently the first instrument which used a loudspeaker arrangement, a precursor to modern free-field techniques. John Guttman and the team of Minton and Wilson are both mentioned as the first in America to construct a testing device incorporating the vacuum tube. Guttman's "electric acoumeter" was presented in 1921, and in the following year, studies of hearing conducted with the aid of the device were published. [Johnson, 1970]

Despite earlier efforts by several inventors, Western Electric Company was the first to actually manufacture commercial audiometers. Teams of research scientists and engineers of this company had been serving the technological needs of World War I, and as a result of that involvement, in 1920 they began work on electronic audiometry. The 1-A audiometer was presented by Harvey Fletcher and Edmund P. Fowler at the 1922 meeting of the Americal Laryngological, Rhinological and Otological Society [Davis and Mertzbach, 1975]. This audiometer had a resistive attenuator calibrated logarithmically and achieved a distortion lower than any previous electric instruments. Through his work with Western Electric, Harvey Fletcher introduced the term <u>decibel</u> to the otologic community, as well as demonstrating the first graphical method of documenting hearing loss, the audiogram [Fletcher, 1953].

The cost of the 1-A audiometer was prohibitive ($1500) and it was difficult to use because of its size and complexity; thus it lacked popularity. Western Electric soon introduced the 2-A, a smaller, more affordable unit, thought of as the first successful commercial effort.

Though Western Electric was the only commercial producer of audiometers for a number of years, other practical vacuum tube designs were presented. Hastings and Tucker in 1922 described a device intended for production which is believed never to have been manufactured; Knudsen constructed his "audioamplifier" in 1924, a design which served as the basis for Sonotone's first model. [Bunch, 1941]. These first commercial audiometers were not required to adhere to any standard. The tendency of the early manufacturers, Western Electric, Sonotone, Maico, and A.D.C., was to consult with otologists and thereby produce an instrument suiting their needs. In 1937, Maico introduced an important improvement in design with the D-5. Due to an automatic mechanical arrangement, this device eliminated the necessity of the operator's selecting the proper zero reference point of intensity each time the frequency was changed. This convenience was a significant factor in the popularization of audiometers amongst physicians and institutions. [Watson and Tolan, 1949]. The zero reference level was determined through studies with a large number of listeners and represented a supposed average normal threshold. Disagreement in studies regarding the average thresholds was one of the many reasons that otologists demanded standards for audiometers.

Problems in standardization were apparent even before the era of electronic audiometers. In 1921, the American Academy of Ophthalmology and Otolaryngology set up a committee for the study of tuning forks and hearing tests. Their recommendations included use of the more stable plated forks and five specific frequencies for testing: 32 Hz, 64 Hz, 256 Hz, 512 Hz, and 4096 Hz. Later suggestions on tuning fork standardization involved their rates of decay and harmonic content [Johnson, 1970]. In 1937 the

Council on Physical Therapy of the American Medical Association set up a committee in cooperation with the American Standards Association and several manufacturers to ensure greater accuracy and uniformity in audiometric tests. Thinking primarily about electronic apparatus, the committee established the first absolute values for normal hearing thresholds maintained at the Bureau of Standards. They also set up requirements as to the number of tones produced, their purity, their maximum intensity, and the frequency accuracy. In 1946, the American Standards Association Committee on Acoustical Terminology finally recommended the use of the "even" frequencies that we use today: 125, 250, 500, 750, 1000, etc. The standards committees began receiving products for acceptance as soon as their specifications were announced. [Watson and Tolan, 1949]. In 1941, only three audiometers had been certified and by 1948 there were seven. Major American standards were introduced in the years 1951 and 1969, and the newest revision, drafted May 1978, is expected to be accepted shortly by the American National Standards Institute.

Fig. II-1

Summary of some Historical Events

Relating to Audiometry

A. Ancient Times

6th century BC - Pythagoras observed physical relation between strings which produce tones differing by an octave.

4th century BC - Aristotle postulates wave nature of sound.

1st century BC - Lucretius presents his particulate view of sound.

6th century AD - Boethius writes clearly of the relationship between frequency and pitch.

B. 16th, 17th and 18th centuries

app. 1550 - Giovanni Philippo Ingrassia first observes bone conduction.

app. 1620 - Pierre Gassendi revives atomic theory of sound similar to Lucretius'.

1638 - Galileo Galilei publishes "Dialogues concerning two new sciences" discussing modern scientific basis of relating frequency and pitch.

1650 - Accademia del Cimento of Florence first seriously attempts to measure velocity of sound obtaining value of 1148 ft/sec., in error by over 5%.

1650 - Athansius Kircher concludes that air is <u>not</u> necessary for the propagation of sound.

1660 - Robert Boyle observes that air <u>is</u> a medium for the transmission of sound.

1681 - Robert Hooke invents rotating serrated wheel with reed for sound generation.

1701 - Joseph Sauveur, who worked on the relation between frequency and pitch, first suggests use of the term acoustics.

1711 - John Shore, a trumpeter, invents present form of the tuning fork.

1738 - Academy of Sciences of Paris determines speed of sound to be 332 m/sec, a value accurate to .2%

1747 - Jean Le Rond d'Almbert develops modern form of the acoustic wave equation.

1787 - E.F.F.Chladni publishes treatise describing method of using sand sprinkled on vibrating plate to show nodal lines.

C. Nineteenth century

1807 - Thomas Young describes graphical apparatus consisting of a rotating drum with blackened surface and a stylus for the determination of frequency of vibrating bodies.

1817 - Rene Theophile Hyacinthe Laennec invents the stethoscope.

1819 - Cagniard de la Tour invents the siren.

1820 - J.F. Biot presents optical system with crossed mirrors and resonant tube for determining intensity of sound.

1822 - Jean Baptiste Joseph Fourier derives famous theorem for periodic functions.

1825 - Ernst Heinrich Weber first observes basis of Weber tuning fork test.

1830 - Felix Savart publishes study of frequency range of hearing using toothed wheel apparatus patterned after Hooke's,

arriving at a range of 8 - 24 KHz.

1834 - First tuning fork test, the Weber test, introduced into clinical practice.

1841 - L.F.W.A. Seebeck invents present form of siren.

1842 - James Prescott Joule discovers magnetostriction.

1843 - George Simon Ohm puts forward his theory of audition.

1855 - Adolf Rinne describes his fork test to distinguish conductive loss.

1857 - Edouard-Leon Scott de Martinville invents the "phonautograph", a refinement of Young's apparatus, for visualizing air-borne waves.

1857 - Jules A. Lissajous presents paper describing optical apparatus which enables the determination of phase relations between two signals.

1858 - John LeConte observes phenomena of the sensitive flame.

1860 - Gustav Theodor Fechner hypothesizes logarithmic nature of sensation scaling.

1860 - Rudolph Koenig invents "manometric flame device" incorporating sensitive flame and mirror for visualizing sound waves.

1863 - Hermann von Helmholtz publishes Sensations of Tone in which he describes his "resonance theory of hearing".

1867 - John Tyndall publishes important work on the use of sensitive flames to measure sound intensity.

1870 - A. Toepler and L. Boltzmann present study of auditory threshold using new optical device based on interference bands.

1876 - Alexander Graham Bell patents the invention of the telephone.

1876 - Francis Galton presents his calibrated whistle as a new high-frequency sound source.

1877 - Thomas Alva Edison invents the phonograph.

1877 - Lord Rayleigh, John William Strutt, publishes first edition of Theory of Sound.

1878 - Arthur Hartmann constructs first electric audiometer, called the "acoumeter".

1878 - Eli Whitney Blake uses a telephone and mirror to photograph the sound of human speech.

1880 - Pierre and Jacques Curie discover piezoelectricity.

1882 - Lord Rayleigh invents the Rayleigh disk for the determination of intensity.

1885 - Dagobarth Schwabach publishes study of hearing using his new tuning fork procedure.

1891 - Albert Bing introduces new fork test involving "secondary perception".

1897 - Rudolph Koenig presents his "universal tonometer", containing wide range of tuning forks and uses it to determine audible range to be from about 13 Hz to 17.5 KHz.

D. Early Twentieth century.

1907 - Max Friedrich Meyer presents theory of hearing based on number and frequency of nervous impulses.

1908 - G.W. Pierce constructs first sound level meter.

1916 - Dayton Clarence Miller invents "phonodeik" for filming sound waveforms.

1919 - First vacuum tube audiometers demonstrated in Berlin, including the "Otaudion".

1921 - American Academy of Ophthalmology and Otolaryngology sets up first committee for standardization of tuning forks and hearing tests.

1922 - Western Electric produces first commercial audiometer, the 1-A.

1937 - A.M.A. in cooperation with American Standards Institute sets up first committee for the standardization of audiometers.

1939-1940 - First large-scale tests for auditory threshold conducted at New York and San Francisco Worlds Fairs.

[References for Figure II-1: Beranek, 1949; Davis and Merzbach, 1975; Lindsay, 1966; Johnson, 1970; and Susskind, 1976.]

Fig. II-2
Chronology of Audiometric Apparatus

A. Mechanoacoustic Devices.

1877 - Hormesser of A. Politzer; stimulus was sound of small weight falling on bar.

1877 - Acoumeter of Beerwald; series of bells with automatic striker.

1895 - Acoumeter of A. Lehmann; stimulus was sound of object dropped on platform.

1905 - Objective Audiometer of P. Ostmann; series of tuning forks covering most of audible frequency range.

1922 - Pleximeter of D. Macfarlan; calibrated striking of tuning forks.

1934 - Acoustimeter of Aaron Roth; calibrated forks on revolving turret with swinging hammer.

B. Electric Systems

1878 - Acoumeter of A. Hartmann; first electric type, with tuning fork in primary circuit

1879 - Electric Sonometer of D.E. Hughes; also called "audimeter", with tuning fork in primary.

1882 - Audiometer of Ladriet de Lacharriere; compact with tuning fork, commercial production may have been attempted.

1882 - Audiometer of Boudet de Paris; circuitry unclear.

1884 - Elektrischer Horprufungs Apparat of V. Urbantschitschi; first buzzer type electric circuit.

1885 - Audiometre Elettro-Telefonico of V. Cozzolino; similar to earlier types.

1890 - Electro-acoumetre of V. Cheval; similar to Hughes'.

1899 - Audiometer of Carl Emile Seashore; first to include logarithmic scaling of intensity.

1914 - Audiometer of A. Stefanini; variable frequency type using pendulum generator.

1916 - Audiometer of R. Foy.

1919 - Pitch Range Audiometer of C.C.Bunch and L.W. Dean; variable frequency, motor driven electric generator, 30 Hz - 10 KHz.

C. Instruments with Vacuum Tubes

1919 - Otaudion, as it later was called, of Grushke, Griessmann and Schwartzkopf; one of first two tube types, presented in Berlin, manufactured later in Europe.

1919 - Audiometer of K.L.Schaefer; the other tube type presented in Berlin.

1921 - Electric Acoumeter of J. Guttman; one of first two tube types to appear in America.

1921 - Audio-oscillator of J.P.Minton and J.G.Wilson; the other of the first two tube types in America.

1922 - Audiometer of S. Hastings and W.S.Tucker; never reached production in England.

1922 - 1-A Audiometer of Western Electric (H. Fletcher and E.P. Fowler); first commercial type, calibrated in decibels.

1924 - 2-A Audiometer of Western Electric; cheaper, smaller, more popular than 1-A.

1924 - Audio Amplifier of I.H.Jones and V.O. Knudsen; produced on West Coast and later manufactured by Sonotone.

1936 - 6-A Audiometer of Western Electric; used dynamic receiver and beat frequency oscillator, no batteries.

1936 - Sonotone-Jones-Knudsen Audiometer.

1937 - D-5 Audiometer of Maico; first to automatically correct for "average normal" threshold.

1947 - Audiometer of Georg von Bekesy; innovative sweep frequency, automatic recording system.

1952 - Audiometer of S.N. Reger; built for research purposes, first practical realization of Bekesy design.

1954 - E-800 Audiometer of Grason-Stadler Co.; first commercial Bekesy type.

D. Speech Testing

1904 - Phonographic Acoumeter of W. Sohier-Bryant; first speech type used phonograph, stethoscope, and valve.

app. 1907 - Audiphone of Bristol; with phonograph and resistive attenuator, used in Lexington School for the Deaf.

1927 - 4-A Audiometer of Western Electric; first commercial speech type, used electromagnetic pickup.

[References for Figure II-2: Bunch, 1941; Davis and Merzbach, 1975; Grason-Stadler, 1965; Johnson, 1971; Macfarlan, 1939; Watson and Tolan, 1949.]

III. SIGNAL GENERATING CAPABILITIES IN MODERN AUDIOMETERS:

PROJECT SCOPE

Early audiometers were operated manually. After selection of frequency, the intensity was adjusted and usually manually corrected for reference threshold. The operator was also responsible for selection of the masking level, presentation of the tones and recognition of the subject's responses. While manual audiometry has remained a significant part of the test battery, numerous other procedures have evolved. A new and innovative technique in audiometry was introduced by Georg von Bekesy in 1947. A significant feature of his automatic scheme, now widely used, was the ability of the subject to control the intensity of the stimulus by means of a pushbutton handswitch. In the first audiometer of this type, the level of the tone increased while the switch was depressed and decreased otherwise. Later versions, such as the first commercial Bekesy, the Grason Stadler E-800 (1954), reversed this handswitch action such that the patient could use the button to "push away the tone". The person being tested was instructed to maintain the level of the tone as near to his threshold as possible. Automatic recording was an integral part of the design, as the horizontal and vertical pen motions were mechanically linked to level and frequency controls. Throughout the test, the frequency of the tone was continually swept from 100 Hz to 10,000 Hz, thus the system automatically generated a record of fluctuating level from which the threshold in the entire range could easily be determined. Bekesy's prototype performed the entire test without any operator intervention in

about 15 minutes by sweeping the frequency logarithmically at a rate of slightly less than 1/2 octave per minute. The rate of change of intensity was also a factor in the design of this audiometer. Rates of 90 dB and 220 dB per minute were initially used, and it was discovered that the amount of fluctuation in the tracing, which depends on the attenuation rate, could serve as an aid in differential diagnosis. Masking of the non-test ear had long been recognized as essential in a clinical instrument, and offered a great challenge to designers and researchers for many years. Bekesy incorporated a masking noise in his device which was created by using a chopper to interrupt 60 Hz alternating current. This type of sound was typical in many audiometers of the time, however its periodic nature was later found to be a disadvantage. In order to maintain the proper masking level, it was mechanically linked to the tone level

The Bekesy procedure has undergone some modification since its introduction and now sweep frequency automatic audiometry is an integral part of most clinical test batteries. It is not always possible to administer the Bekesy procedure, due to the sophistication required on the part of the person being tested. Modern instruments, therefore, enable pure tone testing in either the manual or Bekesy modes. Another popular proedure in use today involves loudness balancing, performed for the most part in order to detect an abnormal growth of loudness. The Alternative Binaural Loudness Balance test (ABLB) compares the loudness function of one ear with that of the other in cases of unilateral loss. The equipment must be such that tones of the same frequency can be alternated between the ears with each channel having its own attenuator. In the most common ABLB procedure, the examiner varies the intensity in the test ear while the

patient judges the loudness match, however, some prefer to allow the patient to control the level of the test signal as in Bekesy audiometry. A Monaural Loudness Balance test (MLB) is necessary in cases of bilateral loss. In this procedure, the frequency of the reference tone is chosen to be at a point where the hearing is least impaired. The listener must balance the loudness of a tone of different frequency to the loudness of the reference. Again, either the operator or the subject might be in control of the intensity. The SISI test, Short Increment Sensitivity Index, is another method of investigating abnormal loudness functions, though recent research indicates that it may not be a valid measure. A sound is presented which consists of a pure tone with a small intensity increment superimposed upon it at regular intervals. The size of the just noticeable intensity increment is determined. These are some of the more common paradigms used, however may others are employed experimentally or in special cases (Handbook of Clinical Audiometry, edited by Jack Katz, discusses these procedures in detail.) Figure III-1 shows a block diagram of a currently available clinical audiometer, the Grason-Stadler 1701. This instrument can perform all of the above hearing tests and is indicative of the features required in modern equipment.

Standard specifications for audiometers have changed considerably in the past forty years due to the popularization of different testing methods and the technological growth in electroacoustics. The latest specifications, drafted in May 1978, cover a vast array of features of audiometric equipment. Not only are the signals to be used well specified, but also environmental factors, human engineering factors, calibration methods, and acceptable transducer characteristics are discussed. The

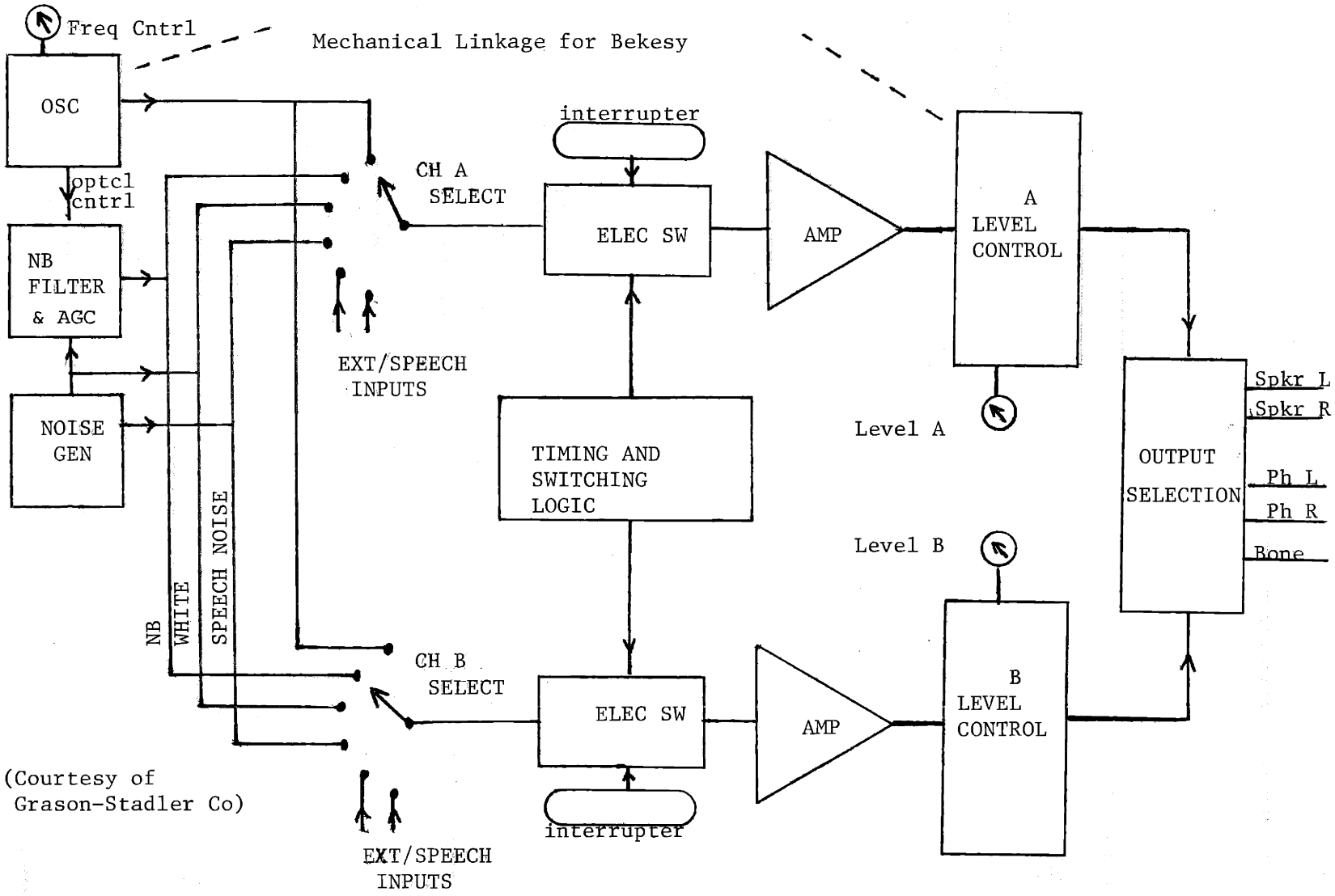

Fig. III-1 Block Diagram of a Currently Available Clinical Instrument

system described in this paper is meant to be a major part of a clinical audiometer designed to exceed the latest applicable specifications and have the ability, due to its microprocessor base, to perform all common paradigms as well as be programmable for special purpose testing. Many other advantages are expected in using a microprocessor within such an instrument, and a few of them are mentioned in the concluding chapter. All signal generating capabilities, with the important exception of level control, and also excluding the relatively simple requirements of pulsing and switching, are encompassed in this work. For Bekesy and manual testing, the system produces logarithmically sweepable and fixed pure tones with accompanying narrowband noise. A second independent pure tone generator is also included for simultaneous presentation of two frequencies, desired for binaural tests of frequency discrimination and other advanced paradigms. Another advantage of incorporating two sine wave generators is the ability to use one of them to modulate the other, a free field application discussed later. Output level is held fixed as frequency changes for each of the three signals. Figure III-2 lists all relevant specifications from the latest American National Standards Institute draft. These guided the project.

Figure III-2

Excerpts from A.N.S.I. Specifications on Audiometric

Signals, Drafted May 1978

Frequency accuracy: The frequency shall remain sensibly constant at a value within ± 3% of the indicated value.

Harmonic Distortion: The maximum level of the harmonics related to the fundamental of the test tone shall not exceed the values given in Table a. Distortion shall be measured at the hearing level listed or at the maximum hearing level setting on the audiometer, whichever is the lower.

Table a. Maximum Permissible Harmonic Distortion

Frequency	125	250 & 8000	500 through 6000
Hearing Level Output (dB)	75	90	110
Second Harmonic	2%	2%	2%
Third Harmonic	2%	2%	2%
Fourth and each Higher Harmonic	0.3%	0.3%	0.3%
All Sub-Harmonics	--	0.3%	0.3%
Total Harmonic Distortion	3%	3%	3%

For air conduction, distortion shall be measured acoustically on an acoustic coupler or artificial ear.

Due to limitations existing on acoustic couplers, artifical ears and mechanical couplers, measurement occurring at frequencies above 4000 Hz do not describe accurately the non-linear properties of the system. Hence, electrical measurements should be made across the terminals of the transducers for frequencies above 4000 Hz.

Extraneous Sound of electrical origin from the Transducer: Extraneous sounds from all causes shall be of such a magnitude that the sound pressure level in any one-third octave band is at least 10 dB below the reference equivalent level for the corresponding test frequency, except that it need not be lower than a level 70 dB below the signal from the "ON" earphone.

Rate of Frequency Change: Where automatic recording facilities of Bekesy type are provided, the following additional requirements shall be met. If a continuous sweep frequency is provided, the preferred rate of change is one octave/minute. If the audiometer provides fixed frequencies, a minimum period of 30 seconds should be allowed at each frequency.

Masking: Audiometers shall provide masking sounds for the pure tone signals indicated. All measurements of the masking noise level shall be made acoustically in the coupler (or in the artificial ear). Analysis of the noise spectrum should be performed with a one-third octave or a narrow band wave analyzer.

Narrow band noise: If the audiometer provides narrow band masking, the noise bands shall be centered geometrically around the test tones. The recommended bandwidths for the masking sound are given in Table b. The average attenuation rate outside the passband should be at least 12 dB per octave up to at least 40 dB stopband attenuation.

Table b. Bandwidths for Narrow Band Masking Sounds

(Pass band upper and lower frequency limits at 3 dB points)

Center frequency Hz	Lower Limit Hz	Upper Limit Hz
250	210-224	280-297
500	420-450	560-595
750	631-668	842-892
1000	841-900	1120-1190
1500	1260-1340	1680-1740
2000	1680-1800	2240-2380
3000	2520-2680	3370-3570
4000	3360-3550	4500-4760
6000*	5040-5360	6740-7140
8000*	6720-7100	9000-9520

*Due to the limitations of the existing couplers and artificial ears, acoustic measurements are not required.

Note: The band limits correspond to one-third octave as a minimum and a half octave as a maximum. These bands are wider than most estimates of critical masking bands, but are recommended in order to minimize the perceived tonality in the masking noise.

Before proceeding with a discussion of various schemes for audiometric signal generation, it is important to review the major features of the standard and understand their implications in the design of modern equipment. Less than five percent of the A.N.S.I. standard deals with quality of signals and some of the sections which do are subject to interpretation. All of the measurements having to do with the signals are to be made acoustically, which implies that for a pure tone, the basic signal generator needs to exceed the standard, as noise and distortion from stages which handle amplification, attenuation, and switching, and from the transducer itself, degrade the performance. Therefore, the goals of this project were set higher than the standard calls for. Absolute frequency accuracy of 3% is usually not a major design problem, but note the wording "the frequency shall remain sensibly constant". Standards often contain phrasing such as this, and in this case it is taken to mean that the signal should have no audible frequency jitter and if the frequency drifts, it should be slow enough so as not to be perceivable during testing. Next, there is a limit of total harmonic distortion of 3% at all frequencies, with distortion to be measured at specified acoustic output levels because electroacoustic components generally perform more poorly at high levels. The output signal may have more or less distortion than the pure tone source due to the filtering and nonlinearities of the transducer, but at the levels specified, the transducers generally perform linearly. A source distortion of 1%, none concentrated at any high harmonics, is certainly adequate to ensure output signal purity and was a design goal here. A signal-to-noise ratio at the transducer of 70 dB is sufficient to satisfy the requirements for non-harmonic extraneous noise. In keeping with the

tendency to have a signal source of higher quality than the output signal need be, a noise level of -80 dB for the pure tones was another of the project's goals. The popularity of Bekesy-type testing is apparent from the inclusion of a recommendation for a sweep speed of one octave per minute. Actually, two other speeds, one-half and 2 octaves per minute, are commonly used. No limits on sweep timing accuracy are given. Fundamental to the acceptance of an audiometer by the field is that it produces a clean sounding, smoothly sweeping signal free of transient sounds and without any properties which might be construed as giving extraneous cues to the person being tested. A listening test is therefore the important final check on signal quality.

Masking is the most complex signal specification included in the new standard. The two major features of the noise are its center frequency, which must be approximately equal to the tone frequency, and its bandwidth, which must be proportional to the pure tone frequency, one-third to one-half octave wide. Many manufacturers use some kind of controlled lowpass filtering technique and then with four quadrant multiplication ensure that the center frequency is correct. Multiplying lowpassed noise by the test tone results in a bandpassed noise signal with bandwidth twice as wide as that of the lowpassed signal and centered around the frequency of the pure tone. Filter control in such a system must be derived from the test tone in a manner which yields a masker of the appropriate bandwidth over a range of three decades. The Grason-Stadler 1701 offers one example of such a scheme (Figure III-1). The lowpass filter consists of two cascaded <u>optically</u> controlled single order sections. To keep the level of the lowpassed noise constant over the frequency range, an automatic gain

control is included before the multiplier. A photoresistor coupled to a lamp whose brightness varies with the oscillator frequency is the basis of each controlled pole. The attenuator control in this instrument is mechanically linked to the frequency as in Bekesy's original arrangement, however, the inclusion of a swept narrowband masker offers a great advantage over earlier periodic masking sounds.

Unfortunately, filter terminology is very confusing because of the variety of applications and measuring techniques employed in different fields. The curves of figure III-3 are meant to clarify the A.N.S.I. draft specification on narrowband masking noise. A center frequency of 1 KHz has been chosen for the examples. The frequency axis need only be scaled to represent the requirements at other audiometric frequencies. The major difficulty in interpretation involves the differences between peaky and non-peaky filters. The definitions assumed here are somewhat arbitrary, but seem to agree with the intent of the writers of the standard. The author recommends that clarifying comments or graphs be included in the forthcoming standard. For a non-peaky filter, such as a Butterworth type, 0 dB is referenced to the peak magnitude, and for filters with ripple in the passband, the average value corresponds to 0 dB, as shown in the figure. Throughout this paper, filter magnitudes are consistently defined in agreement with this convention. According to the standard, the -3 dB points must fall within specified limits. The rolloff characteristics described in the draft are assumed to be related to the appropriate -3 dB point such that for each octave traversed from either specified point there is 12 dB attenuation. Finally, the -40 dB stopband attenuation is indicated on these curves. The dashed curve corresponds to a masker of

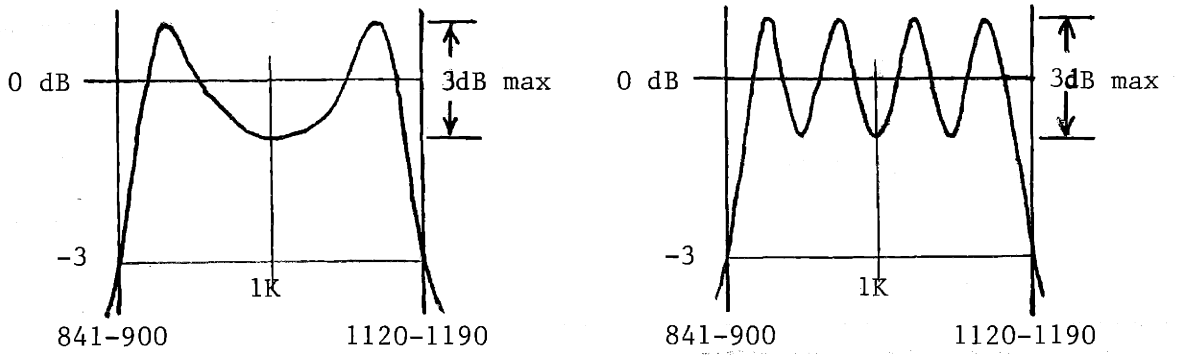

other acceptable passband types for
very narrow band measurements

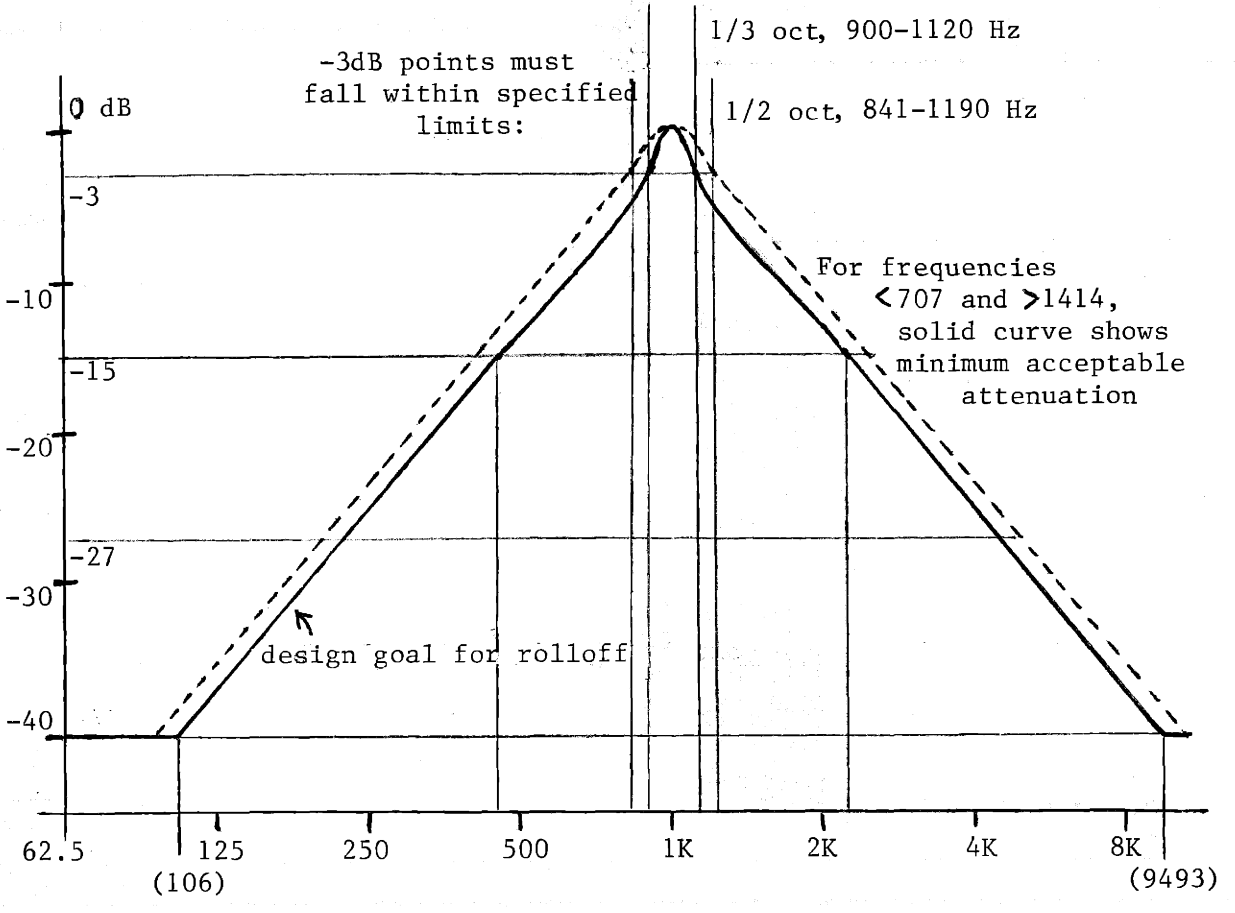

FIGURE III-3 An Interpretation of the Draft Standard
on Narrowband Masking

one-half octave bandwidth, and the other is for a one-third octave masker. For frequencies greater than one-half octave away from the center frequency (<707 Hz and >1414 Hz in the figures), the narrower solid curve was considered to indicate the minimum acceptable attenuation for this work. Remember that spectral characteristics of the noise are to be measured acoustically. When a narrowband analyzer is used to measure noise, there is averaging taking place within the analysis band. Therefore, if 0 dB is referenced to the energy in a narrow band centered at 1,000 Hz, some frequencies within that narrow band may have more energy than the average. The deviation from average depends on the width of the analyzer, the spectral shape, and the type of averaging inherent in the measuring instrument. For this reason, a somewhat arbitrary amount of maximum ripple, 3 dB, is shown in a band around the center frequency in these explanatory curves. As in the case of pure tone characteristics, succeeding stages alter the response. Commonly used audiometric earphones are flat within a couple of decibels from 50 Hz to 2,000 Hz when measured in the specified standard 9-A coupler. However, at higher frequencies, they vary considerably. The TDH-49 with an MX-41/AR cushion , for example, has a peak, referenced to the 1 KHz level, of approximately 2 dB at 3 KHz, and rolls off rapidly at higher frequencies to about -15 dB at 8 KHz. Therefore masking noise generators can show poorer electrical performance than indicated by the curves for frequencies higher than about 3,000 Hz.

A relevant example is described by figure III-4 which shows electrically-measured performance similar to that which could be attained by using a simple set of two cascaded first order lowpass sections and a four quadrant multiplier. (The G-S 1701 uses such a system.) The rolloff

characteristics of this arrangement are sharper than the standard near the center and at higher frequencies, however performance significantly degrades at lower frequencies. Case I is based on a lowpass filter which has a bandwidth of 120 Hz, thereby establishing the -3 dB points at 880 and 1,120 Hz, just within A.N.S.I. limits on the high end. Case II has a bandwidth of 159 Hz, placing the -3 dB points at 841 and 1,159 Hz, meeting the specification at the other extreme. For comparison, the rolloff of the one-third octave, standard curve, set as one of this project's goals, is shown. Note that both of the narrowband spectra shown cross over the standard, one at about 250 Hz, and the other around 400 Hz. The reason for this is that a lowpass filter rolloff of 12 dB per octave is referenced to its own natural frequency, equal to either 187 or 248 Hz in the cases shown. The figure illustrates that when the natural frequency of a two pole section is lower, the resulting narrowband noise comes closer to meeting the desired spectral characteristic. It is apparent, therefore, that a filter more complex than two cascaded first order sections would be necessary for this application. Despite this difficulty, there are other factors, not taken into account in the A.N.S.I. draft, which significantly lessen the apparent problem at low frequencies for a system such as the 1701. These include low frequency attenuation due to acoustic leakage around the cushion seal, which is not evident when an earphone is tested in a 9-A coupler, and the much lessened sensitivity of the ear at low frequencies. A second and minor artifact which occurs in lowpass systems, and is not indicated in the figure, is a zero in the resulting narrowband noise spectrum right around the test tone frequency due to the usual necessity of A.C. coupling somewhere in the signal path before the

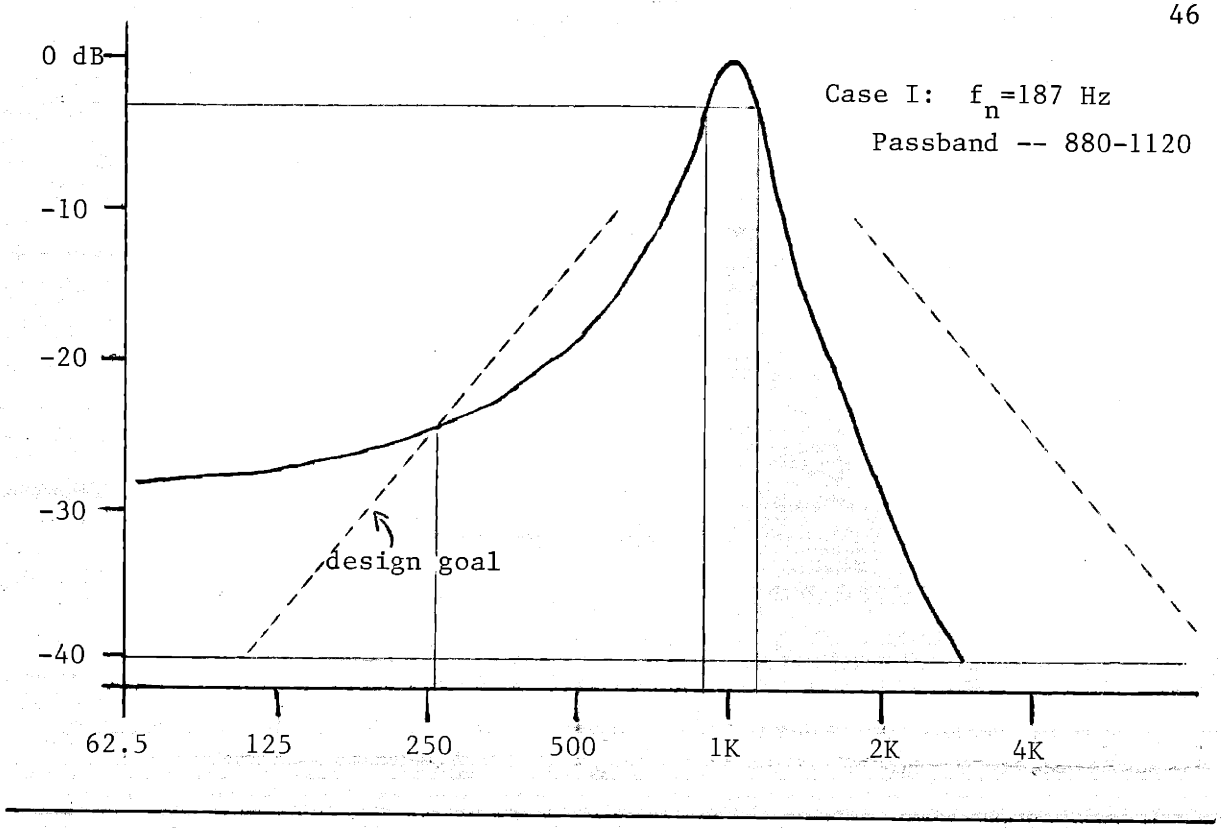

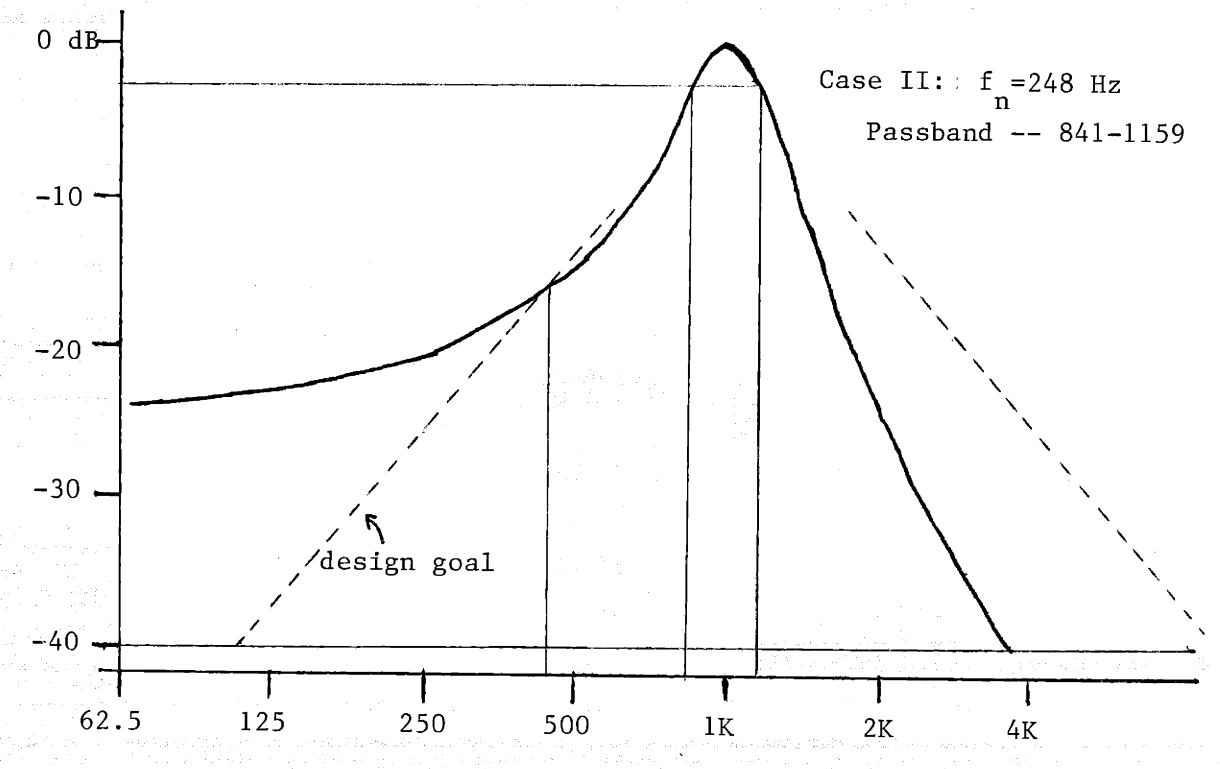

FIGURE III-4 Electrical Response Using Two Cascaded 1st-order Lowpass Sections with Multiplier

multiplier. Since A.N.S.I. specifications call for the measurement to be made acoustically with a narrowband analyzer, a spectral gap around the tone frequency would not be evident. More importantly, though, the masking effectiveness, according to manufacturers but not surprising in light of available research data, is not noticeably changed as a result of a small amount of low frequency energy or a hole a few Hz wide around the tone frequency. In any event, though the latest A.N.S.I S3.6 draft is subject to some interpretation and debate, the intention in this project was to meet or exceed it in terms of masker quality.

In summary, design goals for the pure tones to be produced by this system included: 1) 3% frequency accuracy (100-10KHz); no audible drift or jitter; 2) harmonic distortion not to exceed 1% total and with no concentration at any high harmonics; 3) a signal to noise ratio of 80 dB or greater; and 4) available sweep rates of 1/2, 1, and 2 octaves per minute ±5% for smooth sounding logarithmic sweeping of one of the pure tones. Regarding the masking signal, target specifications were: 1) -3 dB points within limits specified by the A.N.S.I. draft and clarified by figure III-3; 2) attenuation equal to or greater than shown in the solid curve of figure III-3 for frequencies greater than one-half octave from the center, including a stopband attenuation of at least 40 dB; 3) psychoacoustically smooth sweeping of the masker with center frequencies from 100-10,000 Hz along with the associated sweeping pure tone. Though level control was not considered a part of this design, a fixed electrical output level for all signals as they sweep was also intended. The prototype was designed not only to meet these goals but also to answer some questions about available components and electronic

techniques. A large part of the work involved selecting an appropriate system architecture, setting aside some ideas for future work. The result of the effort is a system which proves the utility of the chosen techniques and can be built upon to include the human engineering, level control, subject interface, and paradigm implementation required in a modern clinical audiometer.

IV. CONSIDERATIONS AND CHOICES IN SYSTEM ARCHITECTURE

In order to perform sweep frequency testing with a narrow band masker, an audiometer must be designed with three important control features. First, the attenuator must be automatically controlled and reversible by means of the handswitch. Generally a motor driven attenuator which is mechanically linked to the recording mechanism is employed. Secondly, the frequency must smoothly sweep while the system automatically corrects for reference threshold levels. This task is also usually accomplished with a mechanical linkage, as the non-monotonic nature of the reference level correction greatly complicates solving the problem electronically. Finally, the spectral characteristics of the masker must be controlled as a function of frequency. A method involving a controlled lowpass filter with four quadrant multiplication, as discussed in Chapter III, or an accurately controlled bandpass filter is necessary. A microprocessor can greatly simplify the hardware necessary to ensure overall tracking of the masker and the test tone. Preliminary work indicates that level control can be accomplished entirely under software control through the use of a digital-to-analog converter and a currently available voltage-controlled amplifier with wide dynamic range (DBX, Inc., Newton, MA). The scope of this project, however, involves the generation of three signals, each with fixed level: two independent pure tones and a narrowband masker to accompany one of them. Certainly mechanical linkages ought to be unnecessary in a processor-based design, and the hardware/software tradeoffs need to be thoroughly explored before selecting one of the many architectural options. Several ideas which are somewhat ahead of their

time for commercial application are discussed in this chapter, leading to a presentation of the final system block diagram.

An attractive point of view for signal generation is the intensive use of the system computer in conjunction with digital-to-analog converters to create the waveforms with as little extra hardware support as possible. The ultimate system is way beyond current commercial technology. It would include one very, very fast special purpose digital machine and one digital-to-analog converter multiplexed between the left and right channels. Investigation of a software dominated approach clearly points out the limitations of state-of-the-art microprocessors in synthesis applications.

With reference to figure IV-1, first consider the digital synthesis of a sine wave. There are three basic methods available for determining the sine of an argument: 1) the use of a digital recursion oscillator; 2) direct computation based on some numerical approximation; and 3) direct table lookup [Tierney, in Gorski-Popiel, 1975]. As in any sampled data system, design tradeoffs begin with determining the word length and the sampling rate. Requirements of signal-to-noise ratio and allowable distortion guide these first decisions. Word length directly relates to quantization error. Assume for the moment that the conversion is perfect, and, for simplicity, that numbers are fractional and represented by sign and magnitude. For a word length of b bits, the range of values which can be represented without clipping is from $-(1 - 2^{1-b})$ to $+(1 - 2^{1-b})$ with steps equalling 2^{1-b}. The quantization error, e[n], then satisfies the following inequality: $-(2^{-b}) \leq e[n] \leq +(2^{-b})$. For

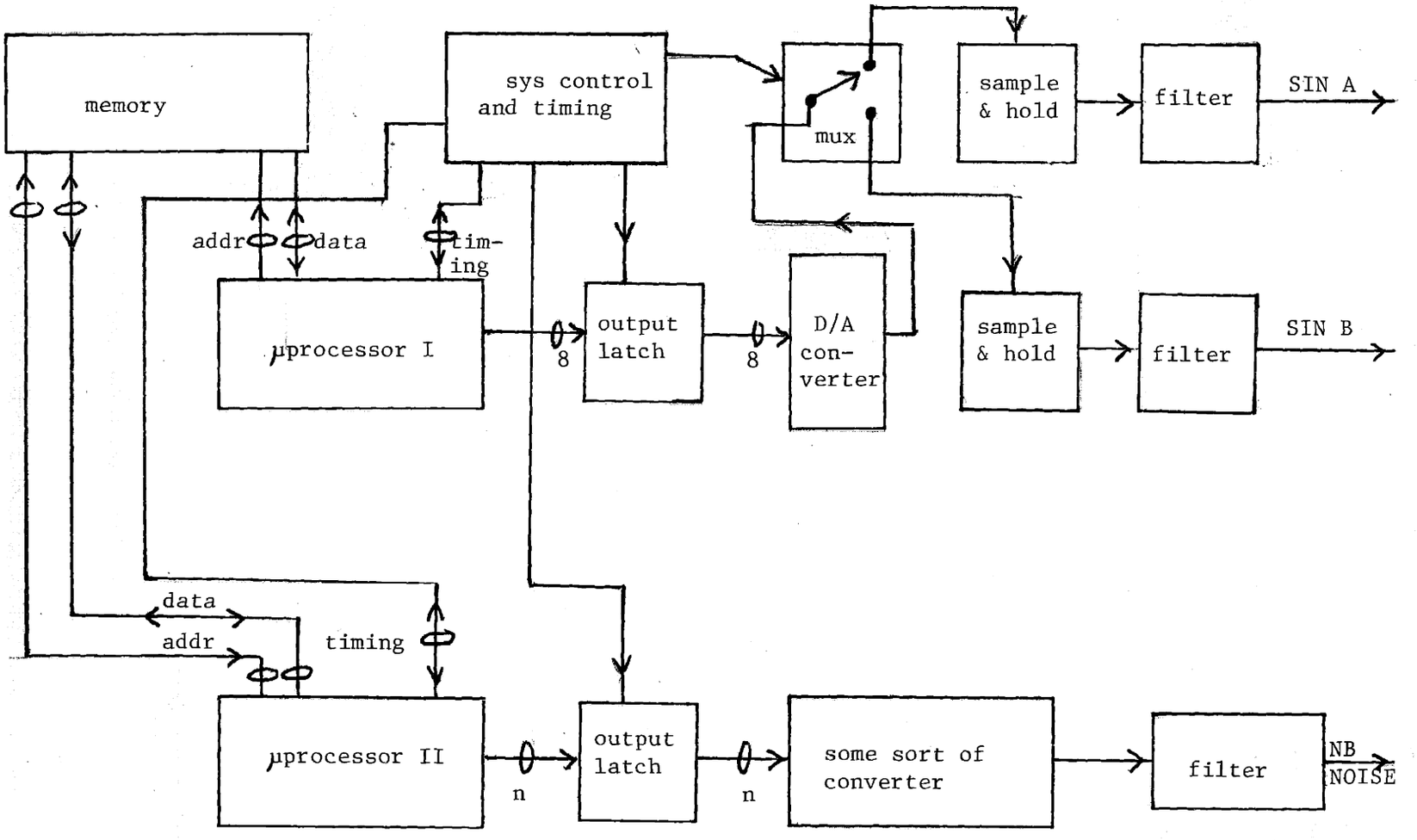

FIGURE IV-1 Direct Synthesis Scheme

example, the range of values representable without clipping for an eight bit system would be from -127/128 to +127/128, with a quantization error never exceeding 1/256 in magnitude. Usually in mathematical derivations involving quantization error, the error is considered to be uncorrelated with the signal. In the special case of sine wave generation, however, the error cannot be represented as a random signal. At any given frequency, the waveform is completely deterministic and therefore there is theoretically no random noise component present in the digital signal. If the number of samples per sine wave cycle is held fixed at some integer value, resultant distortion is independent of frequency. Note that signal-to-noise ratio in such a system depends on the quality of the converter only. The amount of total harmonic distortion (THD) can be estimated in a straightforward and rapid manner. The error signal can have a peak magnitude of 2^{-b}. A rough comparison of this magnitude with the signal, which has a peak of approximately unity, yields an estimated total harmonic distortion of -6b dB. A design goal of 1% THD therefore requires at least seven bits. The use of eight bits would provide a signal with about 1/2% total harmonic distortion. Also, in the ideal system with a sampling frequency f_s equalling a multiple of the signal frequency F, the distortion present is entirely odd harmonic and its level varies little with the number of samples per cycle when that number is greater than about eight.

The finding that eight bits is more than sufficient for pure tone quality indicates possible successful application of digital sine synthesis in an audiometer. There are other major considerations, however. Listening tests show that high order harmonics on low frequency tones are very audible, due in part to the approximate 40 dB difference between the

reference threshold of low frequencies, such as 100 Hz, and that of frequencies in the range of 1,000-3,000 Hz. Care must be taken, therefore, in the choice of sampling rate. Unless high quality tracking filters are included in the system, sampling will have to be accomplished at rates greater than 20 KHz, preferably nearer 40 KHz, a stringent requirement for real time processing. As an example, the microprocessor chosen for this work, the Zilog Z-80, has an output instruction time of about 4.5 microseconds. If a single processor is used to produce two pure tones, operating at 40 KHz means that the sampling period is 25 microseconds, and with the 2 x 4.5 microseconds required for output instructions, this leaves only 16 microseconds for the remainder of the algorithm, certainly insufficient for any sophisticated routine.

The sampling constraint in a direct synthesis system applies regardless of which of the three methods are employed: use of a digital oscillator, computation, or table lookup. The unstable nature of a discrete-time oscillator with quantization error has resulted in little use of this technique. Computation is commonly used in <u>non-real</u> time situations where signals of known duration are to be created. In this case, the generation of a fixed sine wave of frequency F requires the calculation of $s[n] = k \sin(2\pi FnT)$, where T is the sampling period, and k is a necessary scaling constant close to 1. It is interesting to note the complexity of the expression for a smooth logarithmic frequency sweep that starts at $F = F_1$ and progresses upward at a rate of R octaves per second:

$$s[n] = k \sin [(2\pi F_1)(2^{Rt} - 1)/(R \log_e 2)]$$

No microprocessor currently in existence is fast enough to perform even the fixed frequency calculation unless perhaps f_s is harmonically related to F.

With a fixed number of steps per cycle, a modified table lookup routine seems most suitable for direct synthesis.

A possible table oriented design for sine wave synthesis would involve the storage of several different sine waveforms differing in the number of steps per cycle. At various points in a frequency sweep, the number of steps per cycle would change, in order to ease the timing requirements. To illustrate, with 256 steps per cycle at 100 Hz, a sampling rate of 25.6K Hz would satisfy the requirement of eliminating audible high frequencies, but at high signal frequencies such at 10 KHz the sampling rate would have to be 2.56 MHz. Only two steps per cycle are really necessary for the production of "pure tones" above 10 KHz, thus the number of steps per cycle can be reduced at higher frequencies without loss of signal quality. During a sweep through a range in which the number of steps per cycle remains constant, the sampling clock must sweep logarithmically, a requirement which complicates the design; however, limiting the clock's sweep range to one octave may be a practical compromise. If transitions occur once per octave, storage of sine waveforms having 256, 128, 64, 32, 16, 8, 4, and 2 steps per cycle certainly would not tax available memory. Another effect of changing the waveform used for approximation is that the energy in the fundamental would have to be adjusted at each transition. Further complexity arises from the need to perform tests involving two pure tones presented simultaneously. The timing interaction needed to program one processor to produce two digital signals of differing sampling rates would be a major design issue. However, only one of the simultaneous tones needs to sweep during any common testing paradigm. Also note that a high source frequency needs to be employed in the timing circuitry, because to

guarantee a smooth sweep, small frequency steps, accomplished through high resolution in the sampling rate, are required, as explained later.

Two microprocessors are included in figure IV-1, one dedicated to sine synthesis, and a second independent computer for the production of masking sounds. Pseudorandom wideband noise with spectral lines close enough for use in an audiometric system can be generated easily by means of a shift resister and feedback (see chapter VII). It is conceivable then that an algorithm could be derived to form lowpassed or bandpassed pseudorandom noise. One way this could be done is through the implementation of a digital filter having wideband noise as its input. An important feature of digital filtering processes is that the entire frequency axis can be scaled simply by changing the sampling rate. A narrowband filter of one-third octave centered around 1,000 Hz would become a third-octave around 2,000 Hz merely by doubling the clock frequency. In the same way, a lowpass cutoff frequency can be controlled. Also, digital filters are environmentally insensitive and can be programmed with great flexibility.

In considering digital filtering for this application, available design guidelines for determining the complexity of the filter structure required to meet the criteria were investigated. As a starting point, the word length and sampling rate need to be chosen, based on similar considerations as in the discussion of sine synthesis. To maintain a noise floor of -40 dB, at least seven bits are required, and the sampling frequency must be inaudible and always at least an octave greater than the highest frequency at which filtering is required. There are two major classes of digital filters, both diagrammed in figure IV-2. In a finite

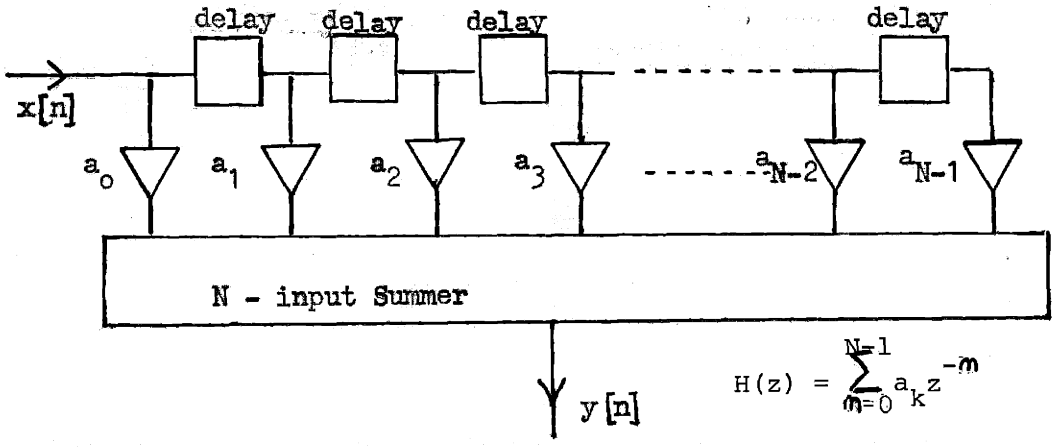

A. Direct Form F. I. R. Filter Structure, order=N

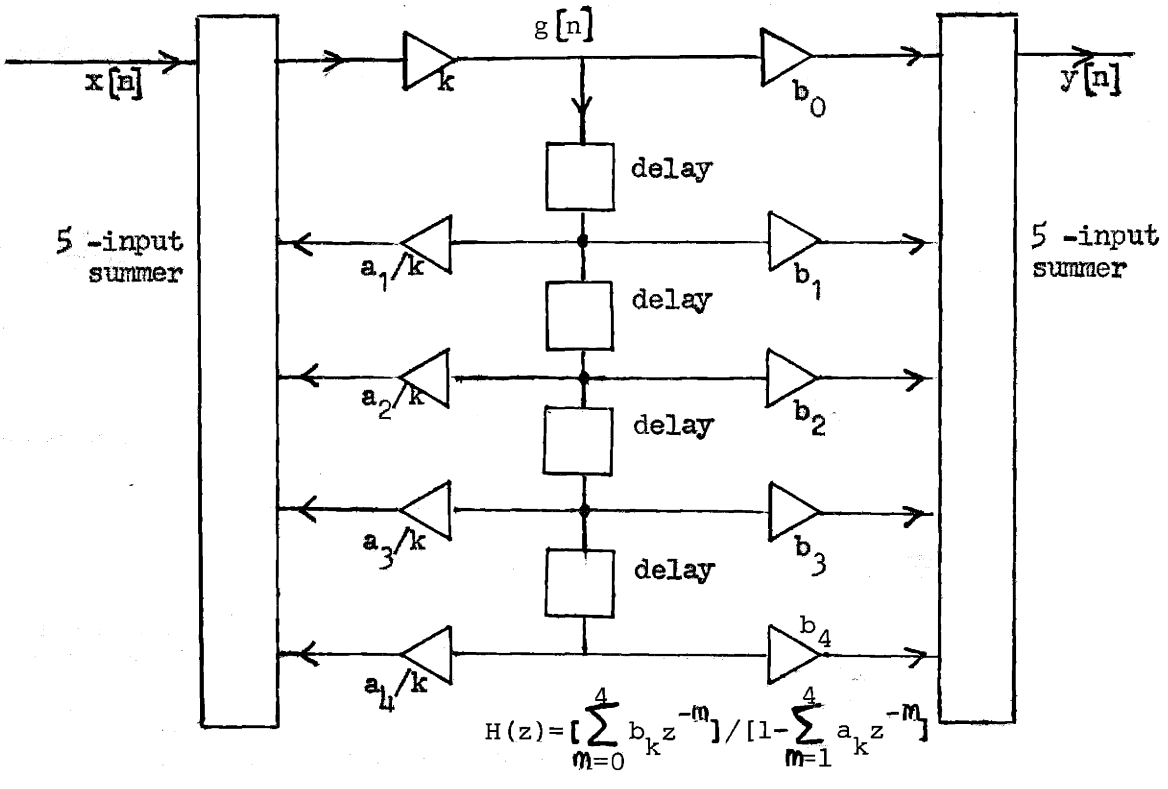

B. Direct Form II I. I. R. Filter Structure, order=4

FIG. IV-2 Two Digital Filter Networks

impulse response digital filter (FIR), the phase relationship can be made linear with frequency, an advantage in many processing applications, but of no concern here. FIR filters also have the advantage that there is no feedback, therefore there are no poles and stability is guaranteed. In contrast, infinite impulse response filters (IIR) require far fewer sections than comparable FIR designs, have complex phase characteristics, and often have stability problems due to quantization and computation noise. The corresponding filter transfer functions for both types are also shown in the figure.

Two techniques for estimating the order of optimal FIR linear phase lowpass filters are given by Rabiner, McClellan, and Parks [1975]. The two formulae are based on specifications of the amplitude of the transfer function, and needless to say are stated in very different terms than used in the standards for audiometers. For this application, a bandpass filter is sought. Though estimation procedures are available for lowpass FIR designs, optimal bandpass design formulae have not yet been presented. Kaiser [1974] is responsible for the simpler of the two design formulae, modified from his results with windowing design techniques. It is fairly easy to design using windows. The impulse response of an ideal filter is multiplied by a window function and then sampled, resulting in the coefficients for an FIR design. A rectangular window, a seemingly obvious choice, leads to poor filter performance due to extreme distortion of the magnitude response, especially at the passband edges (Gibb's phenomenon). To reduce this problem, many other types of windows, with smoother transition characteristics, have been specified. In the frequency domain, windowing results in the circular convolution of the ideal response with

the window's transform. An ideal lowpass filter with bandwidth B can be represented by a rectangle of width 2B centered around 0 in the frequency domain. An "equivalent" bandpass filter will have this rectangle located symmetrically around the center frequency and therefore has a bandwidth of 2B. It is apparent that in designing these two ideal filters using the same window, distortion of the magnitude responses is very similar, differing only in second order aliasing effects. A reasonable assumption, therefore, is that the order of an FIR bandpass filter will be only slightly higher than that necessary for the equivalent lowpass when windowing is employed. Another point of view leads to a similar conclusion. If a lowpass filter impulse response of finite length is multiplied by a similarly windowed sinusoid of frequency F, the resulting function is the impulse response of a bandpass centered around F and with twice the bandwidth of the original lowpass, as desired. For optimized designs, the relationship is not that clear, but still it is expected that the bandpass order will not be much greater than that predicted by the formula for a lowpass, and furthermore, it seems that the order will most nearly be equal for narrowband filters. Another feature of the design formulæ is that they assume linear phase characteristics. Design without this constraint results in at most a two-to-one reduction of filter order, but usually the reduction is not great enough, especially in narrowband filters, to offset the advantage in computing speed attainable with the symmetrical linear phase structure. The conservative estimate that will be used here is that an FIR bandpass filter would require 50% more stages than its optimized lowpass equivalent.

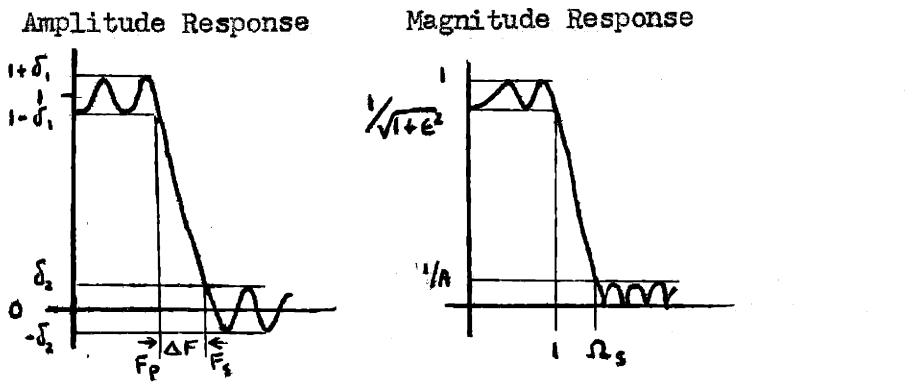

FIG. IV-3 Terminology Used to Describe Lowpass Filters

The variables used in the estimation formulae are shown in figure IV-3. First, the ripple in the passband, δ_1, is defined as the deviation from an average value of unity. Allowing ripple in the passband necessarily eases the filter order requirements and a 2 dB deviation (a slight overdesign) is used here to arrive at a value for δ_1 of 0.115. The stopband attenuation required is -40 dB thereby specifying δ_2 as 0.01. For these estimation procedures, the measure of transition width, ΔF, is normalized with respect to a sampling frequency of one. The narrower curve shown in figure III-3 serves as a model for sharp rolloff characteristics. In an effort to surely avoid a low frequency region which does not meet the A.N.S.I. specification, an attenuation of 40 dB near 125 Hz is desirable. In terms of this estimation procedure, this corresponds to the equivalent lowpass filter having a stopband edge frequency of $875/f_s$. The passband edge frequency for these calculations can be specified by considering the

fact that the resulting filter will have many ripples in the passband, such as shown in the upper right of figure III-3. Using that sketch as a guide, a reasonable value for F_p is $90/f_s$. Assuming a sampling frequency of 40 KHz, the parameter ΔF to be used in the estimation is therefore equal to (875-90)/40000 or $19.6 \cdot 10^{-3}$. The simpler formula for determining the order of the equivalent lowpass filter is:

$$N = (-20 \log_{10}\sqrt{\delta_1\delta_2} - 13)/(14.6\,\Delta F) + 1$$

Applying it and rounding up the result yields $N_{LP} = 59$. The second formula, supposedly more exact was applied as well and gave a value of $N_{LP} = 63$. This second more tedious calculation is shown below:

$$N = [Q(\delta_1,\delta_2) - P(\delta_1,\delta_2)\cdot(\Delta F)^2]/(\Delta F) + 1$$

where,

$$Q(\delta_1,\delta_2) = [.005309\ (\log_{10}\delta_1)^2 + .07114\ (\log_{10}\delta_1) - .4761]\log_{10}\delta_2 - [.00266\ (\log_{10}\delta_1) + .5941\log_{10}\delta_1 + .4278],$$

and $P(\delta_1,\delta_2) = 11.012 + 0.51244\ (\log_{10}\delta_1 - \log_{10}\delta_2)$.

Remembering that a bandpass filter is estimated to have 50% greater order, the final estimate is $N_{BP} \simeq 94$.

The precise determination of IIR filter order for given characteristics can be aided by the use of the charts presented by Rabiner, et al [1974]. IIR filters are generally designed through the use of an optimized analog protofilter and the bilinear transformation, whereas FIR digital filters are usually optimized directly in the digital domain.

Owing to this different point of view, the IIR filter designer has choice as to the filter type desired, as well as an exact procedure for determining N. The design charts can be used for Butterworth, Chebyshev or Cauer elliptic lowpass filter types. As in the case of FIR order estimation, this determination must be modified because we are seeking results for a bandpass filter. However, the fact that IIR designs are based on analog protofilters results in the order for a bandpass being exactly twice that required for the equivalent lowpass. Rabiner's figures for IIR lowpass filters require another set of filter parameters which must be derived from the analog protofilter's magnitude response as shown in figure IV-3. Fortunately, though, he derived the algebraic manipulations necessary to relate the two types of filter specifications. Two numbers need to be calculated for use with the charts:

1) $\eta = (2\delta_2\sqrt{\delta_1})/[(1-\delta_1)\cdot\sqrt{(1+\delta_1)^2 - \delta_2^2}] = \varepsilon/(A^2-1)^{\frac{1}{2}} = .00687$

2) the transition ratio $K = 1/\Omega_s = \tan(\pi F_P)/\tan(\pi F_S) = 0.103$.

Using these parameters, the charts indicate that for a Butterworth filter, $N_{LP} = 3$, and for either a Chebyshev or elliptic design, $N_{LP} = 2$. For an elliptic <u>bandpass</u> design, the most efficient of the three types, the order necessary is $N_{BP} = 4$.

There is no question as to which type of filter network involves less processor calculation, but as pointed out earlier, stability issues often weigh more heavily than filter order. Another interesting aspect of the application of digital filtering is the dynamic considerations during the required sweeping of the masker. Unless the sampling rate is swept along with pure tone frequency, filter coefficients have to be modified continually. Inspection of the design formulae show that for frequencies

above 1,000 Hz, if f_s is fixed, requirements on the FIR filter are such that fewer delays would be necessary; conversely, for lower frequencies, the order would have to be increased. In fact, the order would need to be about a factor of 10 greater for the 100 Hz masking filter than for the 1 KHz filter. The IIR structure, on the other hand, would not need to be modified during the sweep to meet the desired specification. At 1,000 Hz, the specification is easily met for an elliptic 4th-order bandpass. Though quality degrades at lower frequencies for both filter types, the transition ratio is the important parameter in the IIR design and it remains very nearly constant (within a few percent) for the filters centered at frequencies lower than 2,000 Hz. Thus there is no problem anywhere in the range. One more point relative to the scheme outlined in figure IV-1 is that since the sine generator needs to be designed with a log sweepable sampling clock, the dynamics of the masking noise filter can be eased by using that same clock, thereby limiting the number of times during a sweep that the filter coefficients must be changed. No attempt was made to design either of the two digital filters discussed because not even a completely dedicated microprocessor of today could perform the necessary computations fast enough. Real-time digital signal processing of audio can currently be performed only with specially designed and very expensive computing machinery.

Further reflection on the digital processing of signals raised some interesting ideas for future study. Another approach to the problem of creating narrowband noise is to consider the statistical properties of the signal desired. An algorithm that outputs a pseudorandom wideband signal and involves only one simple bit-shift and one exclusive-or operation per

clock period can easily be implemented. The algorithm is extremely simple using only a single-bit word length and could be driven at a sampling rate of 40 KHz for audiometric applications, however the spectral characteristics of the signal are also simple. In further processing with a digital filter, in order to maintain the required 40 dB signal-to-noise ratio, the processor would need at least a seven bit word length, regardless of the sampling rate used. In the digital filters discussed, computation must be performed with the same seven bit length throughout. There is no way to trade off a higher sampling frequency for a shorter word length or a less complex algorithm. It seems that there might be a means for the processing of <u>random</u> signals, however, which could compromise between word length and sampling rate and still be simple enough for practical use. In the extreme case, perhaps a single bit train at a fast enough rate could serve to create pseudorandom narrowband noise directly [Roberts and Davis, 1966]. Were more than one bit involved, a conversion scheme of some type would have to be employed. Another advantage of random signal processing might be the ability to use very simple converters. For instance, if a few output bits are changed at a rapid rate, and the converter is simply a summer, the possibility of "building" a signal with desired stochastic properties might be realizable. Current progress in special purpose signal processing architectures may lead into research on random digital signal generation, but to date, little work seems to have been done on these questions.

The advantages of digital processing in terms of accuracy and control are attractive for many applications. For this reason, techniques of discrete-time analog signal processing (DASP) are currently being rapidly

developed for commercial use. Discrete time analog processing systems are based around devices which delay sampled signals by successive discrete time periods. Quantization of sampled data is not a factor in these systems and neither is computation time, because multiplication and addition are performed in an analog fashion. The advent of tapped analog delay elements, possible with recent advances in charge transfer device technology, makes this an alternative for design. Compared to digital filters, many of the same design choices exist for DASP systems. The same filter structures can be used with identical design procedures. Scaling of the spectral characteristics, of course, can be accomplished through control of the clock frequency.

An investigation into these new techniques revealed that clocking constraints combined with the limited dynamic range of available charge transfer or "bucket brigade" devices showed that their usefulness is restricted to less demanding applications than the one at hand. In order to avoid the complexity of changing the filter coefficients, easy in software but very difficult in hardware, any practical DASP design would involve a sampling rate always outside of the audible range and equal to some fixed multiple of the filter's center frequency. The calculations which follow are based upon the use of a 19.2 KHz clock for generation of the 100 Hz masker. A 192 KHz clock would therefore be used for the 1 KHz masker. The order estimation procedures covered earlier can be applied to this situation also. Results of the FIR estimation formulae, modified as above to reflect a bandpass application, and using $\delta_1 = 0.115$, $\delta_2 = 0.01$, $F_P = 90/192000 = 4.69 \cdot 10^{-4}$, and $F_S = 875/192000 = 4.56 \cdot 10^{-3}$ provide estimates of $N_{BP} = 414$ for the simpler calculation and $N_{BP} = 444$ for the other formula.

FIGURE IV-4 Digital Elliptic Bandpass Filter Design

Filter Parameters:

order = 4

passband ripple = 2.0 dB (±1dB)

lower passband edge = 870.5 Hz (-1dB pt)

upper passband edge = 1155.0 Hz (-1dB pt)

stopband attenuation = 41.0 dB (-42dB re peak)

sampling frequency = 192.0 K Hz

Computer Design Results:

lower stopband edge = 441.4 Hz (-41dB pt)

upper stopband edge = 2277.0 Hz (-41dB pt)

Filter Coefficients (rounded to 6 sig. digits) --

$a_1 = 3.99036$	$b_0 = .00792788$
$a_2 = -5.97331$	$b_1 = -.0316377$
$a_3 = 3.97553$	$b_2 = .0474196$
$a_4 = -.992582$	$b_3 = -.0316377$
	$b_4 = .00792788$

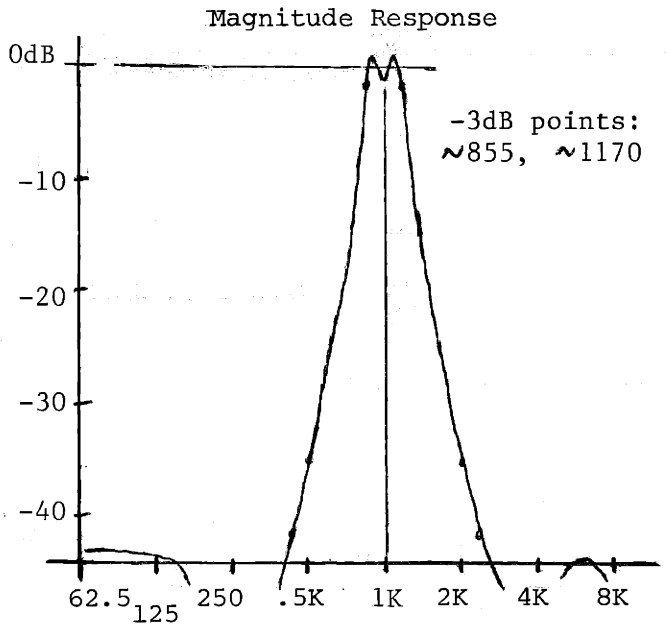

Poles and Zeroes:

pole pair 1 --
.997251 ± .0367023 j

pole pair 2 --
.997930 ± .0291245 j

zero pair 1 --
.995406 ± .0957449 j

zero pair 2 --
.999937 ± .0112218 j

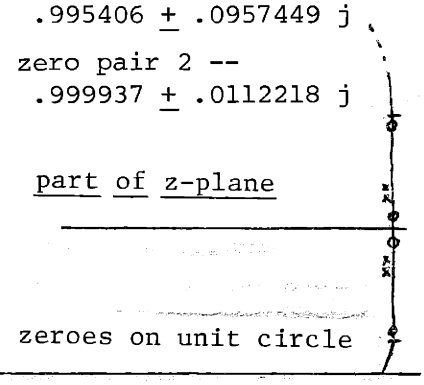

In contrast, the order for an elliptical filter is determined to be $N_{BP} = 4$, agreeing with earlier observations on IIR designs.

With the charge transfer device in mind, a computer program [Gray and Markel, 1976] was used to design an elliptic digital bandpass filter to meet the requirements for generation of the 1 KHz narrowband masker. The results are shown in figure IV-4. Equivalent performance can be attained at any other frequency by simply changing the clock rate. The design program accepts parameters of filter order, dB ripple in the passband, the passband edge frequencies, the attenuation in the stopband, and the sampling frequency. The transition width, then turns out to be as narrow as possible while the other parameters are met. In this case, stated in terminology consistent with the rest of the paper, an order of 4, with 2 dB passband ripple, edge frequencies (-1 dB points) of 870.5 and 1155.0 Hz, a 41 dB stopband attenuation, and a 19.2 KHz sampling rate were specified for the filter design program. This led to a filter of slightly narrower than one-half octave bandwidth which easily meets the A.N.S.I. requirements for rolloff. Though the choice of parameters was somewhat arbitrary, the design results clearly indicate performance expected using the elliptic IIR technique. The -3 dB points in the design are about 855 and 1,170 Hz and greater than 40 dB attenuation is attained at frequencies lower than 450 Hz and higher than 2,250 Hz. The elliptic filter is extremely sharp, however actual implementation with the tapped analog delay element is difficult.

As figure IV-4 illustrates, the poles are located very close to the unit circle in the z-plane, this being a warning as to possible stability problems. The transfer function of the filter is:

$$\frac{0.00792788 - .0316377\, z^{-1} + .0474196\, z^{-2} - .0316377\, z^{-3} + .00792788\, z^{-4}}{1 - 3.99036\, z^{-1} + 5.97331\, z^{-2} - 3.97553\, z^{-3} + .992582\, z^{-4}}$$

where $z = e^{j2\pi f/f_s}$. The poles are due to feedback and the zeroes are due to feedforward of delayed signals in the network. (see figure IV-2). At D.C. the filter gain is seen to depend on a sum of five fairly large numbers. A clear view of the stability problem is obtained by considering the poles only. The transfer function relating the filter input, x[n], and the input to the CTD, g[n], contains only poles. The function, G(z)/X(z) has a gain at zero frequency of $k/(1 - \sum_{m=1}^{4} a_m)$, which for k = 1 is approximately 120 dB. At f = 1 KHz, there is 145 dB gain, and at 2.5 KHz, the gain is 90 dB. Therefore even if the stability were not a problem here, the system's dynamic range would be. It is possible, as indicated in figure IV-2 to scale the function G(z)/X(z) by setting k > 1. A value of k equalling 10 would probably result in a manageable signal at the CTD input, but attempts to actually implement the filter showed its impracticality. The use of more taps in a direct form IIR design, or a less sensitive parallel filter structure would be more appropriate. Unfortunately, no integrated tapped delay line available today has only a few taps, therefore to build a practical structure, clocked sample and hold circuits would have to be designed. Filtering in two stages, with the first being clocked at a lower frequency, might also prove effective.

With the realization that digital or discrete time approaches are not applicable, other means of signal generation must be explored. First, for the generation of pure tones, several tunable sinewave generation techniques are described by figure IV-5. Type A is an example of a currently popular integrated circuit technique. A voltage is used to

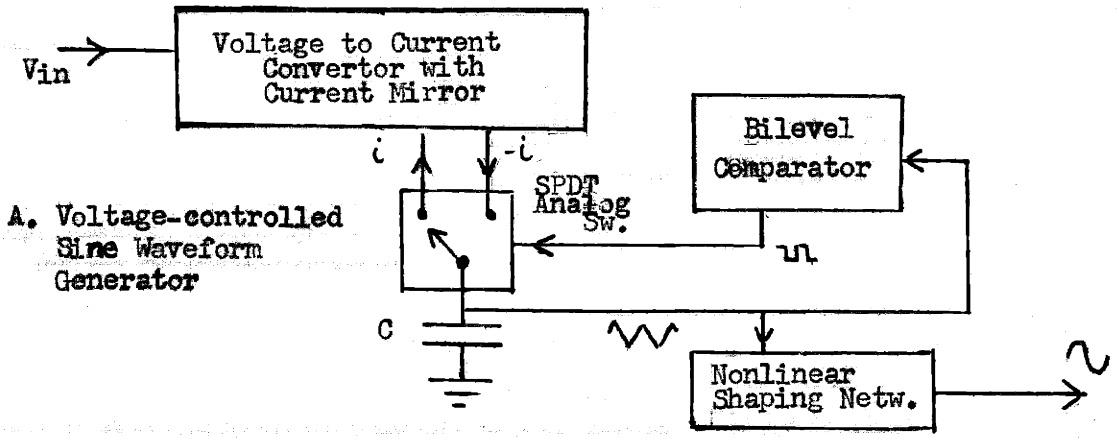

A. Voltage-controlled Sine Waveform Generator

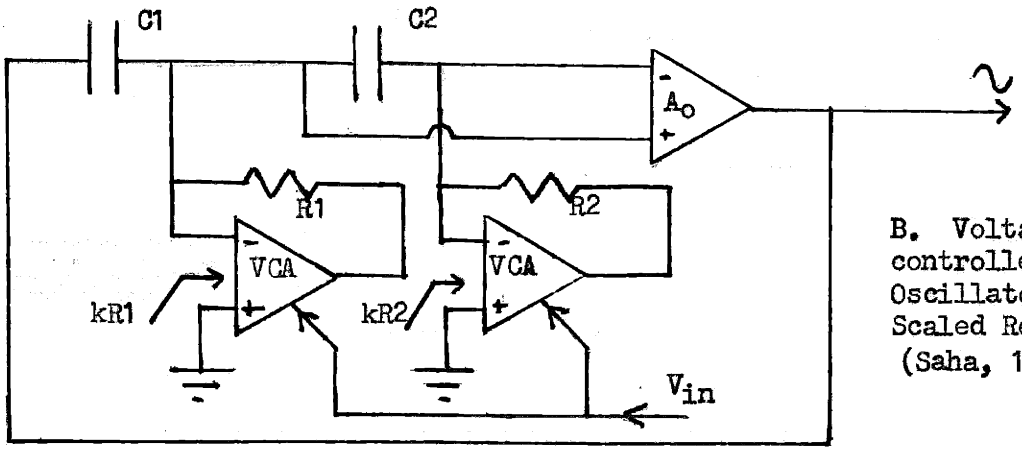

B. Voltage-controlled Oscillator with Scaled Resistors (Saha, 1975)

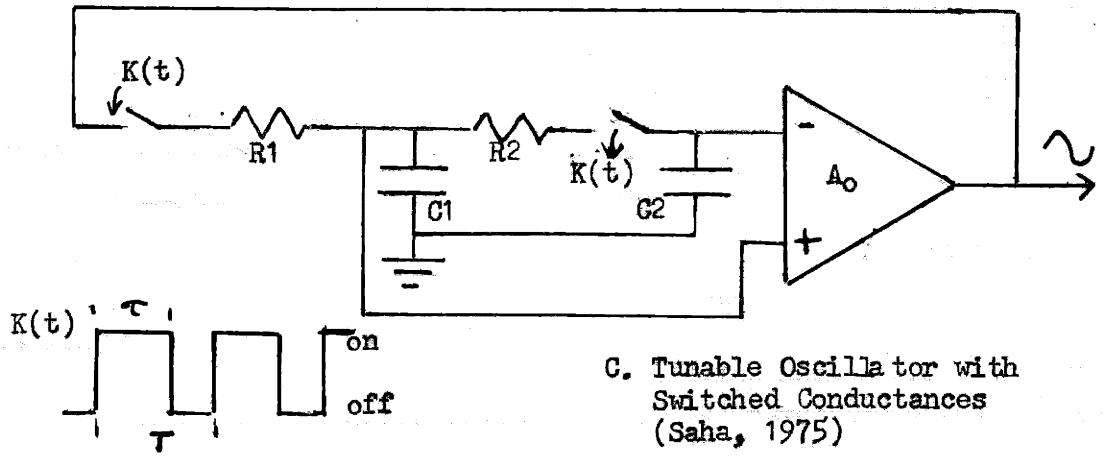

C. Tunable Oscilla tor with Switched Conductances (Saha, 1975)

FIGURE IV-5 Tunable Sine Wave Generation Techniques

control the current charging or discharging the capacitor. A bilevel comparator detects the capacitor voltage, and in turn alternates the charging current direction to maintain a triangle waveform within specified amplitude limits. This triangle output is then shaped with a nonlinear network to approximate a sine wave. Most configurations of this sort require two adjustments, one for the symmetry of the triangle, and the other for optimization of the shaping network. Voltage controlled scaled resistances are the major feature of the type B circuit shown. The example is of a standard analog oscillator design, modified through the use of two voltage controlled amplifiers (VCA) which act like variable resistors. Stability is ensured by careful regulation (not shown) of the amplifier gain, A_o. There are many active oscillator types which can be made tunable using voltage controlled amplifiers or multipliers. In the third example, type C, control is accomplished by switching two conductances, thereby scaling their effect. The circuit configuration is basically quite similar to the one used in the scaled resistor example, but the control here is linearly based on the duty cycle, τ/T, of a rectangular switching control waveform whose frequency must be at least an order of magnitude greater than the highest frequency to be generated. Improvements in the performance of integrated FET analog switches is popularizing switching techniques such as this.

Each of these three techniques has its limitations. A linear control function is desirable, and the wider the tuning range, the more difficult this is, especially in the case of switching techniques. However for low frequency oscillators not requiring a wide tuning range, the linearity and ease of control in switching systems points to wide future application.

The precision necessary for low distortion outputs from the type A design limits its practicality in high fidelity instrumentation. In this application, however, a sine wave with 1% total harmonic distortion is acceptable. Either the sine wave shaper or scaled resistor approach can be used over a wide range, but the availability of inexpensive integrated circuits incorporating astable triangle generation with subsequent shaping, trimmable to the 1% desired distortion, suggests that type A circuits are the most logical choice.

Analogous to circuitry for tunable oscillators, there are techniques for the electronic control of filters. The optical technique mentioned earlier is a clear example of the use of scaled resistances. Figure IV-6 shows three other tunable filters, two of which use switching concepts and another with a voltage controlled amplifier. In the first circuit shown, the VCA scales the capacitor in the configuration thereby moving a single pole. Extensions of this concept can be used for control of higher order filters as well. Cantarno and Pallottino's design [1969] is an example of a stop-go type of filter, similar to the type C oscillator of figure IV-5. The on-time of the switches scales both poles. The author has had experience with second and third order stop-go designs. Invariably the limitations of speed and linearity of analog switches degraded the performance for narrow on-times. Unless very high speed analog switches are used (<100 nsecs transition time) these techniques are impractical for full range audio sweeping. The design presented by Caves et al.[1977] has a more complex switching signal, in that two phases are necessary. However, linear sweeping of the filter is very simply accomplished by changing the clock frequency. The technique is based on using a switched

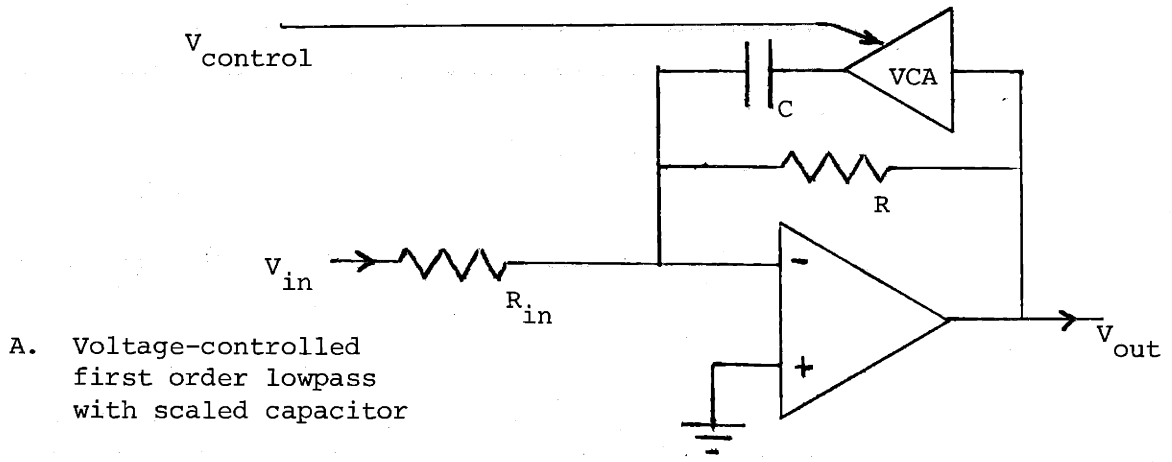

A. Voltage-controlled first order lowpass with scaled capacitor

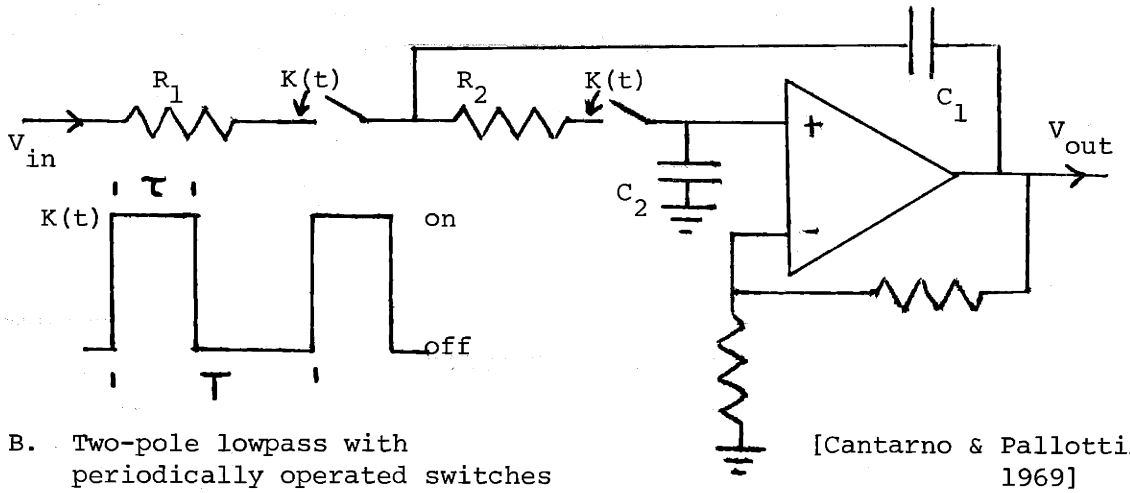

B. Two-pole lowpass with periodically operated switches [Cantarno & Pallottino, 1969]

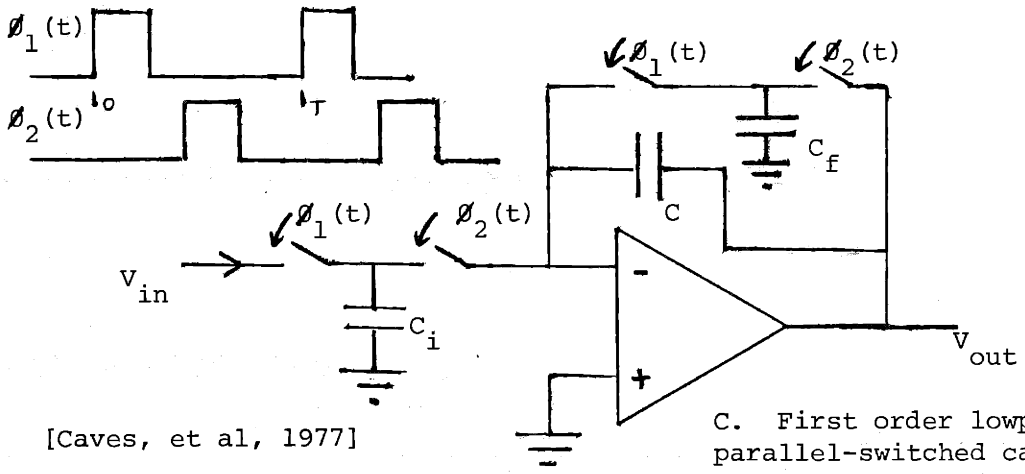

[Caves, et al, 1977]

C. First order lowpass with parallel-switched capacitors as resistor equivalents

FIGURE IV-6 Tunable Filtering Techniques

capacitor as a resistor equivalent. Because the two switches involved with each resistor equivalent are never both closed simultaneously, charge is moved in small packets from one of the switching nodes to the other through the capacitor. More charge moves and therefore the equivalent resistance appears smaller for higher clock rates. Experimental integration of Caves' design has been successful, demonstrating that filters with large time constants can be integrated by using small capacitors and switches. In recent years there has been renewed interest in the development of switching techniques for filtering, including the more complex N-path filters [Patangia and Blostein, 1978] because of the microelectronic hardware now available for their implementation.

Utilization of these concepts for sine wave generation or filtering might require digital-to-analog conversion to create the necessary control voltages or clocked digital circuitry to produce the switching waveforms. For pure tones in sweep frequency audiometry, an important consideration is the system's resolution, since only discrete frequencies can be programmed. An aesthetic requirement is that there be the psychoacoustic perception of smoothness in the sweep; and the human ear can detect very small changes in frequency. Green [1976] has reviewed results of studies having to do with the difference limen of frequency (DLF), that is, the just noticeable pure tone frequency change. The sensitivity of the ear to changes in frequency as a function of frequency and level. It is well established that the DLF remains fairly constant for levels greater than about 40 dB above threshold [Richards, 1976]. However, data from various studies show large differences in the DLF at various frequencies. There is a trend evident in the data that the just noticeable

difference in frequency is linearly proportional to absolute frequency, a concept reminiscent of the observations of Fechner in the nineteenth century. At 1,000 Hz, a 1 Hz change is generally detectable, at 4,000 Hz, about a 5 Hz change is detectable, and at 10 KHz, the DLF is about 20 Hz. In the low frequency region, though, discrimination of frequency is far worse than Fechner's law would predict. Various researchers have reported results ranging from 0.3 Hz to 3.0 Hz for the DLF at 125 Hz. Differences in experimental procedure undoubtedly caused some of this disagreement. Also, there are large intersubject variations in terms of frequency discrimination.

This data points to a necessary resolution in programming the frequency in a Bekesy-type audiometer. If 0.5 Hz resolution is desired (i.e. 0.5% at 100 Hz), which may not be sufficient at low frequencies, then nearly 20,000 steps are required. This implies the need for 15 bit conversion in the linear programming of frequency. A better approach is to use an <u>expanding</u> converter system, that is, one which incorporates antilog calculation. Such a device outputs a change in analog voltage at each digital step which is proportional to the magnitude, in agreement with the general concepts of sensation scaling. Using an expander also simplifies the software required to generate a logarithmic sweep because only a ramp is necessary for control. A 0.1% change in frequency per step, probably acceptable in the entire audible range, results in about 693 steps per octave, and 12 bits could therefore be used to cover the audiometric range appropriately. This approach is shown in the open loop system diagrammed in figure III-7.

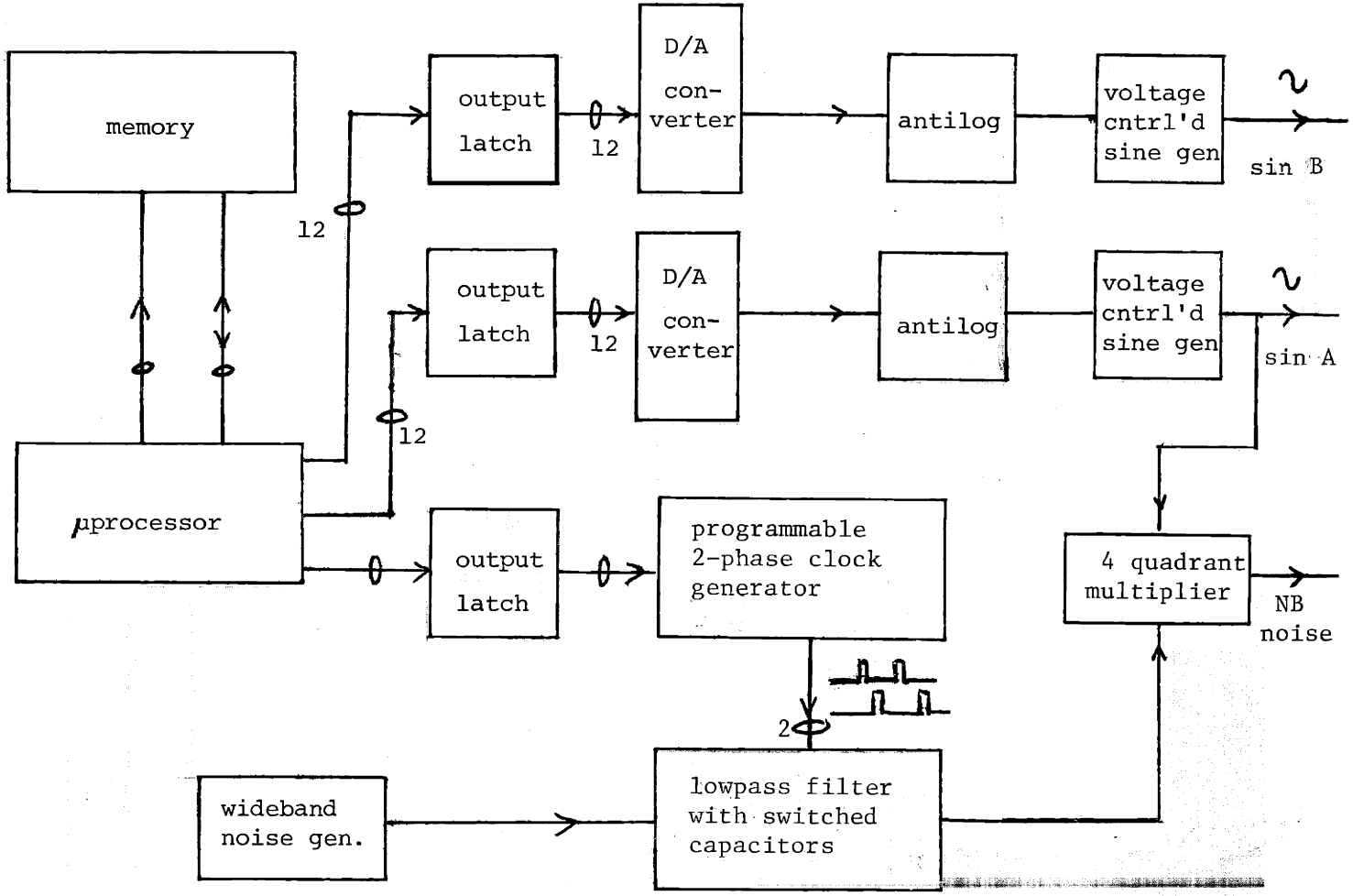

FIGURE IV-7 An Open-loop System

The figure also includes a means for producing masking noise. A controlled switching type lowpass filter is indicated. The wide specification in the A.N.S.I. standard for allowable bandwidths, combined with the lessening of resolution required for smoothness in a swept noise signal, might enable successful application of a custom designed switched filter. The second order elliptic lowpass which served as the analog protofilter for the DASP design earlier could be adapted for use in this system architecture.

In an open loop system, frequency accuracy and tracking of the masker depend entirely upon the precision of the converters and the generators themselves. Therefore it would be difficult to calibrate. This is more important for the pure tones, and since the nonlinearities of the two sine wave channels are independent, matching frequencies or generating known frequency differences throughout the range would probably not be possible with commercial components. Only a closed loop system involving a frequency reference could eliminate this problem of relative accuracy between the sources. A phaselocked loop consists of a phase detector, a filter, and some sort of tuneable frequency source, and can serve the purpose of locking the tunable generator to a frequency reference. Synchronous detection, television raster scan stabilization, and frequency demodulation, are a few of its many applications. These techniques are a special form of parametric feedback where the parameter is phase. Phase difference between the generated signal and the reference signal is held nearly fixed in systems with high loop gain. As in the open loop method discussed above, signal quality in a phase locked system is determined by the tunable generator employed, provided that the system is stable and phase

jitter is minimal. The significant advantage, though, is the relative simplicity of generating an accurate phase reference for lock as compared to the difficulty in attaining accurate linear or logarithmic frequency control in an open loop system. The reference signal for phaselock applications can be as simple as a square wave (or even a pulsed waveform), depending on the type of phase detector used. Applied to the generation of a sweepable pure tone for hearing tests, if the phase detector is a digital type the problem reduces to the synthesis of swept square waves, far simpler than direct synthesis of a sinusoid.

A microprocessor supported by external clocked logic can be used for variable frequency square wave generation having the resolution required for this application. The final system block diagram, figure IV-8, indicates that the two sine wave channels are driven by two different square wave generators. No usual testing paradigm requires the simultaneous sweeping of two pure tone signals, therefore the resolution necessary in the B channel can be guided by considering the test of difference limen of frequency, occasionally performed in clinical settings, and usually currently unavailable in standard commercial equipment. In a DLF test, the signal from the high resolution A channel could vary in frequency around a reference tone produced by the B channel, which would need only to produce reference frequencies with 3% accuracy. In this design, the A square wave generator has about 75 times the resolution of the B generator at 1,000 Hz. Another factor regarding the availability of two pure tone sources has to do with the difficulty in rapidly changing the frequency of a phaselocked sine generator. Loop dynamics slow the response to rapid changes in input frequency, thus in order to smoothly perform ABLB

or MLB paradigms, the use of two generators may be necessary.

In deciding upon the closed loop technique, some basic questions of feasibility had to be reviewed. Voltage controlled sine waveform generators are available with low enough distortion and noise for this application. In phaselocking them, however, it is important that the square wave reference sweeps smoothly, else the pure tone would have transient components. Since the square wave generators can only be programmed to operate at discrete frequencies, the algorithm must compute at each step, unless a lookup table is used. However, regardless of the software technique implemented, there is a timing constraint. For example, if 1,000 steps are desired per octave to ensure smoothness, and the sweep rate is two octaves per minute, the fastest desired, then every 30 milliseconds, a new value for frequency (period) must be available. This constrains the computing or retrieval algorithm to be fast and hopefully faster than 30 milliseconds so that the processor can have time for other functions. Programmable counters are used in the prototype. These counters have internal latching, but still it must be ensured that no changes on the period programming lines can occur during the latching, else falsely timed cycles would result. For this reason, the counters are always updated synchronously, and interrupt response time was another significant consideration in the system design. The calculation algorithm used for the logarithmic sweep is basically a multiplication of the present frequency by 1 + 1/2048, a procedure chosen for its simplicity. About 1,400 calculations per octave are generated, requiring sweep timer interrupts about once every 21 milliseconds for a two octave per minute sweep. The high resolution 18 bit counter in conjunction with this

algorithm produces a discrete frequency sweep which is perceived to be perfectly smooth and continuous. The square wave generators and their programming are discussed in detail in Chapter V.

The use of voltage controlled sine wave generation provides an indirect means of controlling the filter for masking noise generation. The signal which controls the frequency of sine A is a D.C. level which is proportional to frequency. With a first order correction of offset and slope this voltage is used to tune a voltage controlled filter, thereby tracking the masker characteristics. Although switching type filters seemed attractive, the filter order and complexity necessary for any given application is the same whether switches are used for scaling or voltage controlled amplifiers are used. This along with the known difficulties in switching designs with wide tuning range, and the simple derivation of an appropriately linear signal for voltage control led to the final architecture shown. A pseudorandom noise generator is used as the wideband source for the tunable lowpass filter. Multiplication is then employed to translate the spectrum into a band centered around the test tone. The tunable filter is a two pole state variable Chebyshev type with about 2 - 3 dB ripple in its passband. Calculations indicate that a filter such as this has slightly insufficient stopband attenuation (-38dB, see chapter VII) Additional circuitry is necessary to strictly meet the project goals for masker characteristics. The spectral lines in the resulting pseudorandom masking signal are very closely spaced and are related to the frequency of the clock which drives the noise generator and the length of the shift register employed. Since the repetition rate of the pseudorandom sequence is directly proportional to the clock rate, spectral density can be readily

controlled. A frequency multiplier, basically a phaselocked circuit with a frequency divider in the feedback path, is employed to maintain a clock rate proportional to the frequency of the pure tone of channel A. With such an arrangement, the energy in the lowpassed output is kept constant, though its bandwidth changes, and no automatic gain control is required. Note that the entire masking noise generator tracks independently of the system's microprocessor. All that is required to create the narrowband noise is a square wave whose frequency is at the desired center frequency. Four pushbuttons are also illustrate in the block diagram. These were included for ease in testing the design. This operator interface, of course, would have to be modified before incorporating the system into a clinical instrument.

Chapters V through VII discuss the design details and measured performance of the prototype. All of the components necessary in this design architecture are of readily available types. Calibration is simple because there are no adjustments for frequency accuracy, and tracking of the masker is ensured with only two adjustments, one for low frequencies (offset), and the other for high frequencies (slope). Four and two quadrant (VCA) multipliers can be purchased with their internal offsets pretrimmed, eliminating the tedious trimming which was necessary in the prototype due to component choice. Because the software essential to create the three signals only involves the outputting of control words for three devices (two square wave generators and the sweep timer) and the computation of one simple multiply during each stepping period (normally), there is much extra processor time available for interaction with the subject, interfacing with the operator, control of the levels, and control

of a recording mechanism.

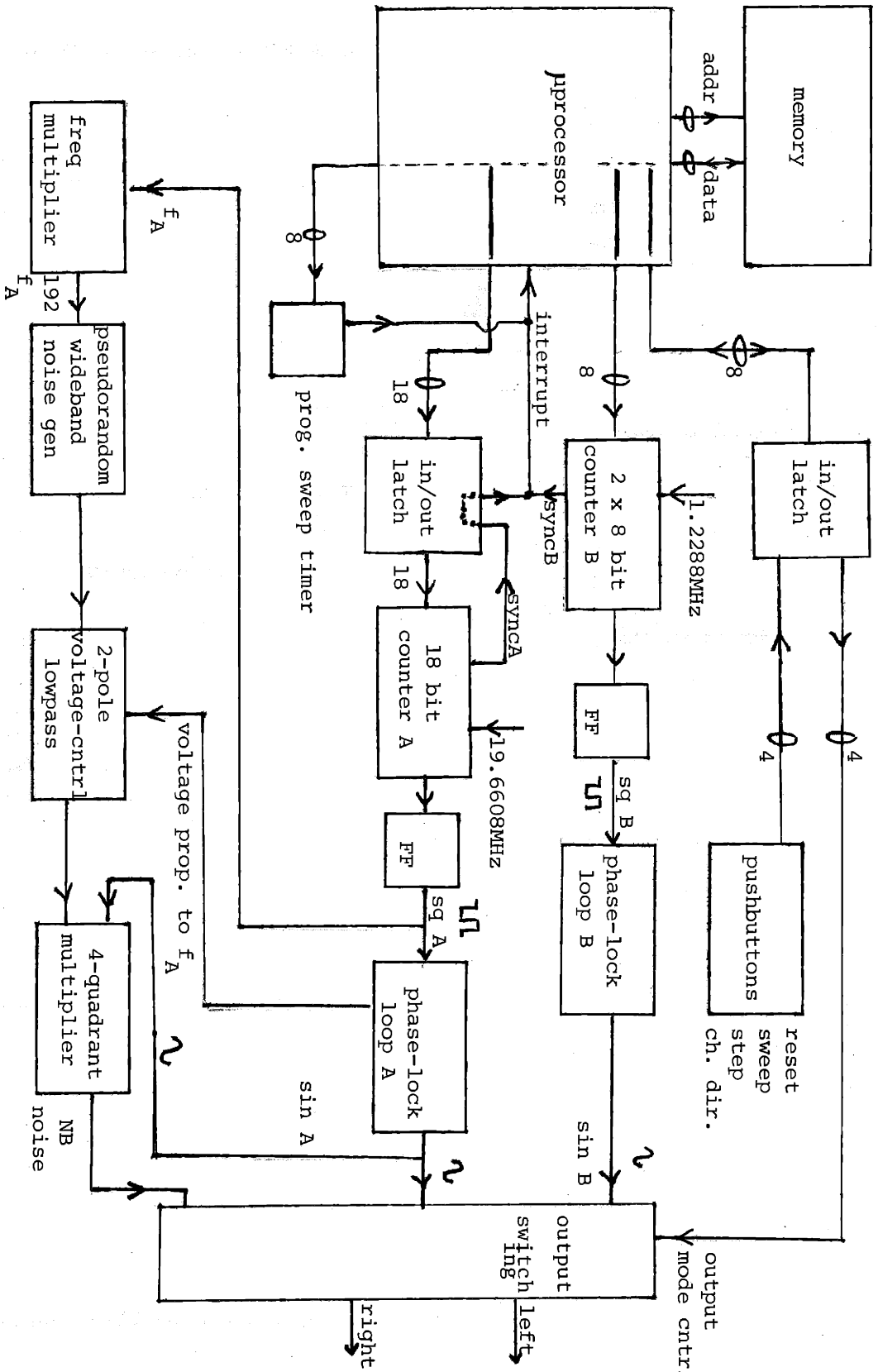

FIGURE IV-8 Final System Block Diagram

V. THE SOFTWARE -- SQUARE WAVE GENERATION

This system of signal generation was designed with the aid of the Zilog PDS Program Development System. The PDS is a floppy disk based microcomputer utilizing a family of cards centered around the Z-80 central processing unit (CPU). Architecturally, the Z-80 is similar to many other microprocessors currently available. It operates with a maximum clock rate of 2.5 MHz (2.4576 MHz is used in the PDS), data is handled in eight-bit bytes, and the address bus is 16 bits wide. There are three boards within the PDS used for this project: the microcomputer board (MCB), the memory disk controller board (MDC), and the input/output board (IOB). The microcomputer system block diagram, which includes only those components relevant to this application, is shown in figure V-1. The MCB contains the Z-80 microprocessor, 4K bytes of dynamic random access memory (RAM), a 3K byte programmable read-only memory (PROM), a serial interface for terminal operation, and buffers for data, address, and control lines. System firmware is located in the PROM and includes the bootstrap loader and floppy disk driver, a terminal handler, the debugger, and the command interpreter. The interface with an RS-232 terminal is provided by means of a USART (universal synchronous/asynchronous receiver transmitter) and a timer element, called the STC, which is also used by the debugger. The first 4K bytes of memory are reserved for the system firmware and an extra 1K user PROM. There is also a parallel interface circuit, not shown in the figure, included on the MCB. With the addition of circuitry to expand its parallel input-output capability, the use of the STC for timing, and a custom PROM, the MCB could probably serve as the entire processing system

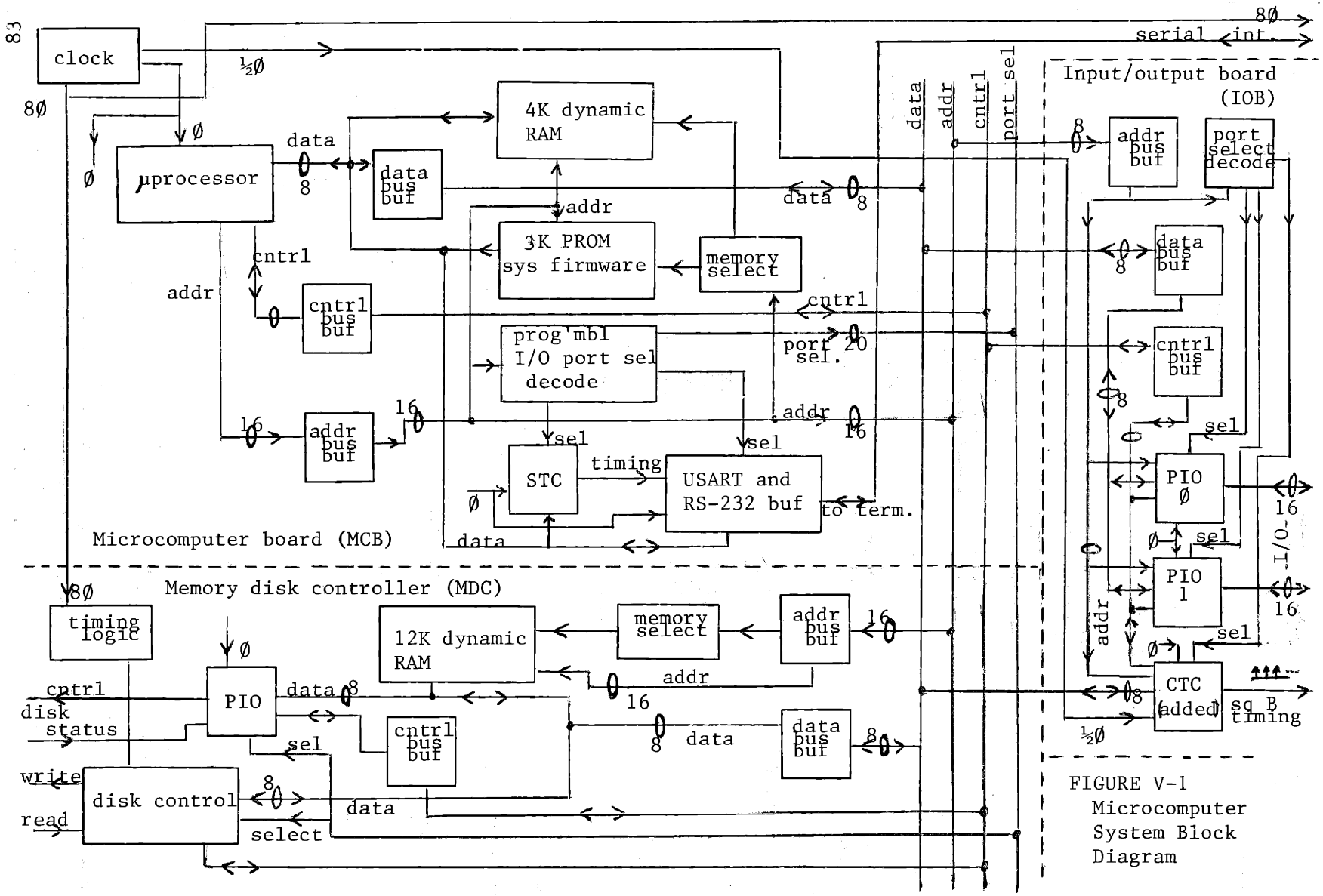

FIGURE V-1
Microcomputer System Block Diagram

for the audiometric application discussed.

The PDS is designed for program development and thus incorporates a disk based operating system with an editor, an assembler, and many utility programs. The MDC interfaces with the floppy disk and contains another 12K bytes of dynamic RAM. Included as well in the microcomputer system is the IOB, which is an optional card within the PDS. There are four parallel interface circuits on this board (only two are shown in figure V-1), and much extra space provided for user circuitry. All interface functions between the CPU and the signal generators are accomplished through two types of Z-80 family integrated circuits, the counter-timer circuit (CTC) and the parallel input-output circuit (PIO). The PIO is a two port device providing a TTL compatible interface between peripheral devices and the CPU. Counting and timing operations in a Z-80 system can be conveniently performed with the CTC, a device with four independent programmable channels. The STC on the microcomputer board is actually a CTC package. The entire interface necessary for this project is accomplished with three channels of a CTC and 27 bits of input-output from two PIOs. The CTC for this application was added to the IOB, as shown in the block diagram. The schematic of figure AII-1 details the interconnections of the interface elements used.

The two ports of a PIO can be operated independently to input or output data, and in the bit control mode, the only one used for this work, each line is individually assigned as either an input or an output. It is possible to generate an interrupt based on a logical and/or combination of inputs. An internal mask register in the PIO specifies which of the eight

lines are to be monitored for the interrupt and a two bit control register defines whether those lines are active high or active low and whether they are combined in logical AND or logical OR fashion. For instance, if it is desired to generate an interrupt when any one of four lines goes low, the mask must be programmed to monitor only those four lines, and the control register must be set up for the active low, OR combination. There are handshake signals within the PIO package, but they are not utilized in the bit control mode.

The four independent channels of a CTC each contain a programmable eight bit down counter. Every channel has, in addition to timing, triggering, and control logic, an eight bit time constant register which buffers the down counters from the CPU bus. Communication with external hardware is accomplished through clock-trigger input lines and zero count-timeout (ZC-TO) output lines. Each of the four channels has an input line which is used either to trigger the timing action, or as an external clock input to the counter. Three of the four channels (there were not enough pins in the package) have ZC-TO lines which, by pulsing high for about one clock period, indicate when the down counter is at zero. In the counter mode, either positive or negative transitions of the clock-trigger line decrement the channel's down counter, preprogrammed by the CPU. The maximum input frequency is one-half of the system clock rate, or 1.2288 MHz in this case. At zero count, the ZC-TO line outputs a pulse; the down counter is then reloaded with the current contents of the time constant register, independent of the CPU, and the channel continues to count without interruption. The time constant can be altered at any time under program control, and if changed during a counting period, the current cycle

will continue until the next zero count, at which point the new time constant is loaded. In the timer mode, the CTC generates timing intervals that are integral multiples of the system clock period. A prescaler is employed to divide the clock rate by either 16 or 256. Depending on the channel control word, timing either commences immediately after the time constant is loaded or when triggered externally. At any time, the CPU can read the current contents of the down counter without disturbing operation. Also, each channel can generate an interrupt at zero count if so enabled.

The Z-80 microprocessor has an elaborate interrupt structure. It honors three types of external events, in the following order of priority: 1) bus request, used for direct memory access; 2) nonmaskable interrupt; and 3) maskable interrupt. Only the maskable type is used in interfacing with this hardware for signal generation. The most powerful and fastest maskable interrupt mode, and the only one of three used for this application, is the vectored interrupt mode. In this mode, the CPU responds to an interrupt by reading a vector from the interrupting device. These eight bits in conjunction with the I register, a special purpose eight bit register in the CPU, form an indirect pointer to the starting address of the service routine. Both the CTC and the PIO contain interrupt vector registers. In either case, by convention, the least significant bit of the vectors supplied by these devices is always 0. This does not reduce flexibility because two memory locations must be used to store each 16 bit starting address. Each PIO port has an independent interrupt vector register, but in the case of the CTC, the vectors supplied by the four channels are sequential. The lower three bits of the vector supplied by a CTC depend on which channel is requesting service. When channel 0

interrupts, the lower three bits are 000 and when channel 1 interrupts, these bits are 010, and so on. The most significant five bits of the CTC vector and 7 bits of the two PIO vectors must be preprogrammed by the processor during setup.

There is a hardware priority scheme included in Z-80 interface circuits such as the CTC and PIO. Referring to figure AII-1, a partial schematic of the IOB, the three devices used are hooked into a daisy chain in an order determined by the IEI and IEO lines. The highest priority device has its IEI line tied high. While the highest priority device is being serviced its IEO line is low, disabling the recognition of lower priority interrupts until the ongoing routine is completed. The STC, which is used for establishing the baud rate and for timing during debugging, is first in the daisy chain. Following it are the three circuits used in the signal generator, connected in the following order: CTC, PIO0 and PIO1. Note in the schematic that the IEO line of the CTC connects to the IEI line of PIO0, and similarly the IEO line of the first PIO connects to the IEI line of the second. The program for swept square wave generation is written such that normally there is no interrupt nesting, therefore the order of these three circuits in the daisy chain is of no concern. Within the interface circuits, the A byte of a PIO has priority over the B byte, and the interrupt priority of the CTC channels is organized sequentially with channel 0 first and channel 3 last.

The primary purpose of the microcomputer in this system of audiometric signal generation is the control of two square waves. Figure V-2 is a block diagram of the two square wave generators. As pointed out earlier,

these two circuits have different resolutions, as only the A channel is smooth enough for sweep frequency audiometry. The program which controls them, however, can sweep either one, because it was unclear before the entire system was completed whether or not the B generator, based around the inexpensive CTC element, would have sufficient resolution for the application. Because of phaselocked loop dynamics, it was thought that perhaps the smoothing effect of the loop filter could enable the use of a swept square which by itself does not sound smooth. (Results of these listening tests are discussed later in Chapter VI.) The block diagram indicates that an 18-bit programmable up-counter is used for the A channel, and two sections of the CTC are used for the B channel frequency reference. Both of these square wave sources must sweep without producing any false cycles and therefore both of them generate interrupts for synchronization. When the sweep timer informs the CPU that the frequency must step, the system waits until the appropriate interrupt (SYNCA or SYNCB) occurs, and in that way "glitches" during sweeping are prevented (see later discussion). The channel A generator is driven by a 19.6608 MHz clock, which is eight times the clock frequency which drives the CPU. This high frequency is available in the system because it is also used to time disk access. Channels 1 and 2 of the CTC (CTC1 and CTC2) are cascaded such that the output of CTC1 drives the input of CTC2. The base frequency for countdown in channel B is 1.2288 MHz, the highest frequency which the CTC can count. The software is designed such that the postdivider, CTC2, is programmed to divide by 1, 2, 4, 8, 16, 32, or 64 only. Because of this, the algorithm for determination of the time constants for the two CTC channels is simple and rapid. To maintain high resolution, CTC1 is always

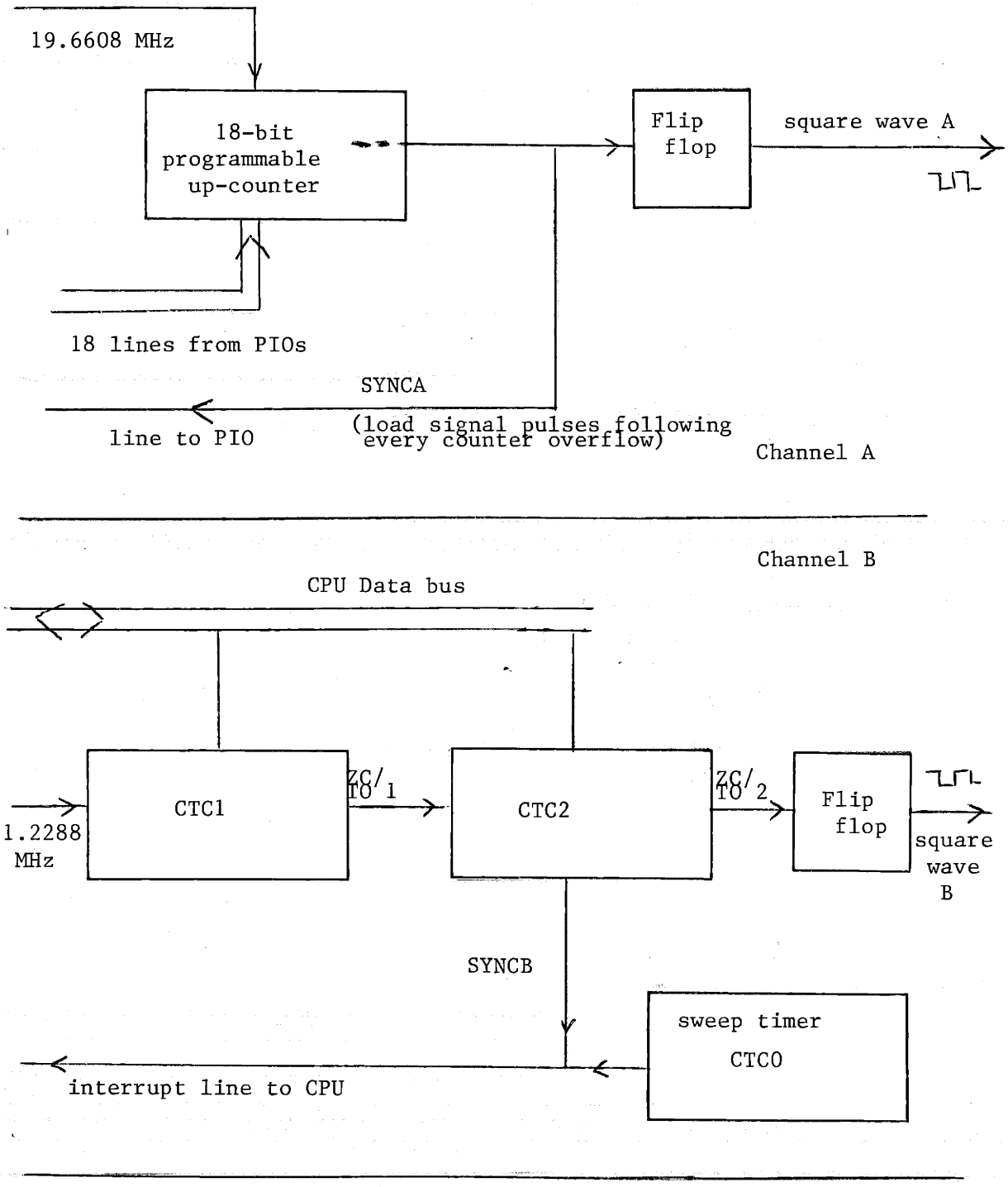

FIGURE V-2 Block Diagram of Square Wave Generators

programmed to divide by a number between 128 and 255, except at the highest frequencies, where resolution in the B channel is poor. The sweep timing is controlled by CTC0. Figure AII-2 is a detailed schematic showing the A square wave generator circuitry, the flip flop used to divide the CTC output for the B channel reference, and the four pushbuttons which interface with the software. This schematic along with figure AII-1 can be used to clarify the interconnection of the microprocessor system and the hardware used for signal generation.

The process taking place in the A channel counting circuitry can be thought of as dividing a frequency of 9.8304 MHz by some number not greater than 2^{18} or 262,144. The 18-bit up-counter of channel A reloads at the next clock pulse following overflow. Therefore, to divide by N, the counter has to be programmed with the number 2^{18}-N. Many of the audiometric frequencies can be exactly derived. Those that cannot be produced precisely can best be approximated by dividing by $9.8304 \cdot 10^6/F_A$, rounded to the nearest integer value, where F_A is the desired A square wave frequency. By considering the next higher possible programmable frequency, a measure of the resolution can be derived. Let N equal the number which divides the clock for the best approximation to the desired frequency. Then $9.8304 \cdot 10^6 \cdot [1/(N-1) - 1/N]$ or $9.8304 \cdot 10^6 \cdot [1/(N^2 - N)]$ equals the difference in Hertz between any two closest programmable frequencies. Since N is approximately proportional to $1/F_A$, this implies that the resolution, defined in the above manner, is roughly proportional to F_A^2 for large N. In figure V-3, results of this determination of resolution, also expressed in percent relative to the desired frequency, are summarized at various frequencies within the range, along with theoretical frequency

Figure V-3

Theoretical Performance of Square Wave Generator A.

Desired freq, Hz	Best possible approximation	N for 18-bit divider	%error	Resolution Hz	Resolution %
75	75.0000	131072	0	.00057	.00076
100	100.0000	98304	0	.00102	.00102
125	125.0003	78643	+.00025	.00159	.00127
150	150.0000	65536	0	.00229	.00153
200	200.0000	49152	0	.00407	.00203
250	249.9975	39322	-.00102	.00636	.00254
375	375.0057	26214	+.00153	.0143	.00381
500	499.9949	19661	-.00102	.0254	.00509
750	750.0114	13107	+.00153	.0572	.00763
1000	1000.041	9830	+.00407	.1017	.0102
1500	1499.908	6554	-.00610	.2289	.0153
2000	2000.081	4915	+.00407	.4070	.0203
2400	2400.000	4096	0	.5861	.0244
3000	2999.817	3277	-.00610	.9157	.0305
4000	3999.349	2458	-.0163	1.628	.0407
6000	6001.465	1638	+.0244	3.666	.0611
8000	7998.698	1229	-.0163	6.514	.0814
10000	10000.41	983	+.00407	10.18	.1018
12000	12002.93	819	+.0344	14.67	.1222
12010	12002.93	819	+.0589	14.67	.1222

accuracy.

The B square wave generator has significantly less accuracy and poorer resolution than the A generator. For this channel, the output square wave has a frequency of $614.4 \cdot 10^3/(TC1 \cdot TC2)$, where TC1 and TC2 are the time constants programmed into CTC1 and CTC2, respectively. As in the other channel, many of the audiometric frequencies can be precisely generated. Because of the two stage dividing scheme, the difference between neighboring steps does not monotonically increase with frequency as in the A generator. The time constant of CTC2 is changed once per octave throughout most of the range. In terms of resolution measured in percent, the B generator performance repeats in the first six octaves. It would be possible to more accurately program the square B hardware, but restricting CTC2 to divide by powers of two is not only adequate for the application, but also very simple to implement. The lowest frequency produced for the audiometric application is 75 Hz, and only for that frequency is CTC2 programmed to postdivide by 64. For frequencies greater than 75 Hz up to and including 150 Hz, CTC2 divides by 32. Similarly each subsequent octave is traversed, through the octave ranging between 2400 Hz and 4800 Hz, during which CTC2 divides by 1. For higher frequencies, accuracy and resolution are sacrificed, as CTC1 must be programmed to divide by numbers less than 128. In the extreme case, at 12.8 KHz, the highest frequency produced by the channel, CTC1 divides by 48. Thus the limitations of using a CTC in an audio square wave generator are apparent. Figure V-4 indicates the accuracy and resolution at various points in the sweep. As in the preceding figure, resolution is defined to be the difference in Hertz between a given frequency and its next higher programmable neighbor. The

Figure V-4

Theoretical Performance of Square Wave Generator B

Desired freq, Hz	Best possible approximation	Time constant CTC1	Time constant CTC2	%error	Resolution Hz	Resolution %
75	75.0000	128	64	0	.2941	.392
100	100.0000	192	32	0	.5236	.524
125	124.6753	154	32	-.260	.8149	.652
*148.8372	148.8372	129	32	0	1.163	.781
150	150.0000	128	32	0	.5882	.392
200	200.0000	192	16	0	1.047	.524
250	249.3506	154	16	-.260	1.630	.652
*297.6744	297.6744	129	16	0	2.326	.781
375	374.6341	205	8	-.0976	1.836	.490
500	498.7013	154	8	-.260	3.259	.652
*595.3488	595.3488	129	8	0	4.651	.781
750	749.2683	205	4	-.0976	3.673	.490
1000	997.4026	154	4	-.260	6.519	.652
*1190.698	1190.698	129	4	0	9.302	.781
1500	1498.537	205	2	-.0976	7.346	.490
2000	1994.805	154	2	-.260	13.04	.652
*2382.395	2382.395	129	2	0	18.60	.782
2400	2400.000	128	2	0	9.412	.392
3000	2997.073	205	1	-.0976	14.69	.490
4000	3989.610	154	1	-.260	26.08	.652
6000	6023.529	102	1	+.392	59.64	.990
8000	7979.221	77	1	-.260	105.0	1.316
10000	10072.13	61	1	+.721	167.9	1.667
12000	12047.06	51	1	+.392	240.9	2.000

non-monotonic nature is clear for frequencies below 4800 Hz. The poorest resolution, as defined here, is attained at frequencies for which CTC1 is programmed to divide by 129 and several of these are also included in the table, marked with asterisks, for comparison. These large jumps in resolution are most apparent in figure V-4 around 150 Hz and 2400 Hz.

The software for control of the two square wave generators is highly flexible and is part of a package designed to demonstrate the utility of the system for sweep frequency audiometry and also to test the associated hardware design. Almost immediately after the program begins execution, the startup message appears: "4 CHARACTERS: 0-9, A-I ONLY". The system then waits for these four characters to be inputted from the terminal. They specify the frequencies for both pure tone sources, one of which (the A channel) is also the center frequency of the masker; the signals to be presented to the left and right earphones; and the nature of the sweep. No signals are audible until the four input characters have been analyzed and the square wave generators are initialized. Then the requested signals are connected to the earphones and the system starts to "play". The four input characters are referred to as FREQA, FREQB, SWEEPMODE, and OPMODE. Since characters 0-9 and A-I are all recognized by the software, there are 19 choices for each. The two pure tone generators can be programmed initially at any of the 11 standard audiometric frequencies plus eight others ranging from 75 Hz to 12 KHz. The A generator, whose initial frequency is determined by the FREQA character, is the primary pure tone source; the B generator's initial frequency is determined by the FREQB character. The rate of sweeping and the resolution of the frequency steps employed are determined by the third character, SWEEPMODE. Lastly, the

choice of signals presented to the two earphones is determined by the OPMODE character, which also programs the initial sweep direction up or down and determines which of the two generators will sweep. Note that for many of the OPMODE choices, either the FREQA or FREQB character is insignificant. Only for the options involving the simultaneous presentation of two pure tones are both of the frequency characters relevant to the signals outputted. Figure V-5 describes the many options. Note that few of these would be incorporated without alteration in a clinical system.

After the four characters are entered via the terminal, the system responds by presenting the desired signals, and the four pushbuttons become active. They are labelled RESET, SWEEP, STEP, and CHDIR. Unless the OPMODE choice is 0, which causes the system to quietly wait, a signal that is sweepable is presented to one or both of the earphones. At any time after initialization, the system can be RESET. Depressing the SWEEP pushbutton (pb) will start the signal(s) sweeping. The sweep continues only while the pushbutton is depressed. When the SWEEP pb is released, the STEP pb can be used to cause "arithmetic steps" to take place. Each time the STEP pb is depressed, the computational algorithm proceeds to multiply a number of times specified by the SWEEPMODE character. Depending on the hardware capabilities of the particular channel being stepped, and the sensitivity of the listener to small changes in frequency, the step may or may not be audible. Like many other features of the design, the STEP pb is included only as an aid in testing the hardware. The CHDIR pb is used to reverse sweep direction. If the direction of the sweep is not changed manually, it will change automatically whenever the frequency of the

Figure V-5

Summary of Program Options

FREQA and FREQB determine the initial frequencies of both generators:

0 -- 75	5 -- 250	A -- 1500	E -- 4000
1 -- 100	6 -- 375	B -- 2000	F -- 6000
2 -- 125	7 -- 500	C -- 2400	G -- 8000
3 -- 150	8 -- 750	D -- 3000	H -- 10000
4 -- 200	9 -- 1000		I -- 12000

SWEEPMODE sets up the sweep and step parameters:

	Rate in oct/min	Arithmetic step size		Rate in oct/min	Arithmetic step size
0 --	.5	1	A --	1	8
1 --	1	1	B --	2	8
2 --	2	1	C --	8	8
3 --	.5	2	D --	32	8
4 --	1	2	E --	.5	16
5 --	2	2	F --	1	16
6 --	.5	4	G --	2	16
7 --	1	4	H --	8	16
8 --	2	4	I --	32	16
9 --	.5	8			

(Figure V-5 continued)

OPMODE determines left and right earphone signals, which generator sweeps, and sweep direction:

```
0 -- WAIT,     Both phones disconnected
1 -- left=A right=A, A sweeps up
2 -- left=B right=B, B sweeps up
3 -- left=N right=N, A sweeps up
4 -- left=A right=N, A sweeps up
5 -- left=N right=A, A sweeps up
6 -- left=A right=B, A sweeps up, forced to OPMODE 1 if FREQA=FREQB
7 -- left=B right=A, A sweeps up, forced to OPMODE 1 if FREQA=FREQB
8 -- left=A right=B, A sweeps up
9 -- left=A right=B, B sweeps up
A -- left=A right=A, A sweeps down unless FREQA=0
B -- left=B right=B, B sweeps down unless FREQB=0
C -- left=N right=N, A sweeps down unless FREQA=0
D -- left=A right=N, A sweeps down unless FREQA=0
E -- left=N right=A, A sweeps down unless FREQA=0
F -- left=A right=B, A sweeps down unless FREQA=0, forced to OPMODE A if
                                                   FREQA=FREQB
G -- left=B right=A, A sweeps down unless FREQA=0, forced to OPMODE A if
                                                   FREQA=FREQB
H -- left=A right=B, A sweeps down unless FREQA=0
I -- left=A right=B, B sweeps down unless FREQB=0
```

sweeping generator reaches either the 75 Hz lower limit or the 12.8 KHz upper limit.

The software flow chart is shown in figure V-9. It is quite detailed so that the description below can be understood without referral to the detailed program listing in Appendix I. The listing contains numerous comments, and location of routines mentioned in the flow chart is aided by the inclusion of address notations throughout.

The first 1000H locations in memory are reserved for the firmware and user PROMs, and therefore the program begins at 2000H, a convenient starting address which cannot interfere with the firmware or stack. (All numbers followed by "H" in this paper are in hexadecimal notation.) There are a few minor constraints on user programs within the PDS. In order to utilize the power of the system debugger, the STC cannot be programmed for use without taking special precautions. This is the major reason why a separate CTC was added for this project development. Zilog documentation recommends that the stack pointer be located at 10C0H and states that the I register must be set to 13H before debugging begins, and the program is written with these precaustions in mind. Vectored interrupts are used throughout, and with the restriction on the I register value, it is necessary to store the starting addresses for the service routines in the appropriate memory region. The first program statement is labelled BEGIN, and whenever the RESET pushbutton is depressed, the program restarts there. A restart can occur during interrupt servicing and for this reason the first instruction of the program disables interrupts, including any that may be pending. Then "housekeeping functions", including setting up the

vectored interrupt mode, placing the stack pointer, and loading the service routine addresses are performed.

Initialization of the four PIO ports and three CTC channels follows. Only three bits of PIOOA are used. Bit 3 is the SYNCA input line, used for synchronizing the programming of the A generator, and bits 0 and 1 are the two most significant of 18 bits used to program the period of square wave A. The remaining 16 bits are supplied by ports PIOOB and PIO1B, whose lines are all defined as outputs. Four lines of PIO1A are inputs used to interface the pushbuttons and the other four lines of the port are outputs used for control of the signal routing to the earphones (labelled MODE0 - MODE3 in the schematics). During initialization, the mode lines are set for the WAIT condition, with both left and right earphones disconnected. Also, the A generator is preset to 1000 Hz. Only the RESET pb is actively monitored for interrupts during these first program sections. Various pushbuttons are enabled and disabled during the program in order to avoid the complications of nested interrupt structures, however this is not generally evident in the use of the program. The SYNCA interrupt capability is active only when the A channel frequency is about to be uptdated.

CTC channel 0 is used for sweep timing and is initialized in the timer mode with a prescaler of 256 and its interrupt capability disabled. The down counter of CTC0 is thus set to count pulses of a 9600 Hz reference. Later, the time constant is loaded into this CTC channel and during sweeping its interrupts are enabled. For square wave B generation, CTC1 and CTC2 are both initialized in the counter mode. They are preset such

that the square wave B frequency, like the square wave A frequency, is 1000 Hz until later programmed according to the input control characters. CTC1 never interrupts and CTC2 only interrupts (SYNCB) immediately before the square wave frequency is stepped.

For clarification, before proceeding with the discussion of program flow, major aspects having to do with the hardware/software interface will be reviewed. The representation of frequency within the software is an important first consideration. The accuracy of computation for sweeping and the precision available for programming desired frequencies are both related to this internal representation. A 24-bit number proportional to period was chosen to specify the frequencies within this system's software. This 3-byte number allows full use of the 18-bit accuracy of the A square wave generator, and its triple precision reduces computational errors to insignificant levels. Internally, the current desired period, T, of either channel's square wave is approximated as $157.2864 \cdot 10^6/F$, an integer (see figure V-6). The scaling factor relating this value to the desired period was chosen for ease of implementation and simplicity in hardware programming. Since 157.2864 MHz is equal 64 times the CPU clock frequency, ϕ, and both channels are driven at rates simply related to ϕ (8ϕ for the A channel and $\frac{1}{2}\phi$ for the B channel), transformation of the software value into the appropriate hardware values for either channel involves only shifting, complementing and rounding. In the A channel, to generate a frequency F_A, the 18-bit number programmed into the up-counter is $2^{18} - 9.8304 \cdot 10^6/F_A$. The 3-byte software representation, therefore, needs only to be divided by 16 (shifted 4 bits right), subtracted from 2^{18} (complemented and incremented), and rounded before being outputted to the A

Figure V-6

Software Representation of Period at Various Frequencies

Note: Rounded hexadecimal versions are derived from exact decimal values which equal 157,286,400/F

Freq	Rounded hex	Exact decimal
75	20 00 00	2097152.00
100	18 00 00	1572864.00
125	13 33 33	1258291.20
150	10 00 00	1048576.00
200	0C 00 00	786432.00
250	09 99 9A	629145.60
375	06 66 66	419430.40
500	04 CC CD	324572.80
750	03 33 33	209715.20
1000	02 66 66	157286.40
1500	01 19 9A	104857.60
2000	01 33 33	78643.20
2400	01 00 00	65536.00
3000	00 CC CD	52428.80
4000	00 99 9A	39321.60
6000	00 66 66	26214.40
8000	00 4C CD	19660.80
10000	00 3D 71	15728.64
12000	00 33 33	13107.20

channel hardware. In the case of the B channel, preparing the output words from the 24-bit internal representation is only slightly more complex. The B channel's square wave period equals $614.4 \cdot 10^3/(TC1 \cdot TC2)$; therefore, because $157.2864 \cdot 10^6$ equals $614.4 \cdot 10^3 \cdot 256$, TC1 and TC2 must be programmed such that their product approximately equals the internal period representation divided by 256. In preparing the B channel output words, first the 24 bits are shifted right until the most significant 8 bits are zero. This operation indirectly specifies TC2. If no shifting is necessary, CTC2 divides by 1 and if the maximum of 6 bit-shifts are necessary, CTC2 divides by 64. The remaining 16 bits equal an approximation for $256 \cdot TC1$, and therefore the computation of TC1 merely involves rounding the most significant byte. Subroutines PREPA and PREPB perform these arithmetic manipulations for A and B hardware programming, respectively.

Another important apsect in the system is the algorithm employed for sweeping. The smallest possible frequency step is attained by multiplication of the present period by $(1 \pm 1/2048)$. The resulting product is then prepared for output to one of the two channels, and upon receipt of the proper timer interrupt, the hardware is synchronously updated with the new value. Note that after the new period is prepared for outputting, it may not appear any different than the old period. Low resolution hardware cannot be programmed with the precision necessary to exhibit a change of 0.05% as is produced at each of these computational steps. This is quite evident in the B channel hardware and at high frequencies, even the 18-bit A channel hardware is insensitive to single steps. For frequencies less that 4800 Hz, the A channel hardware can

produce each single step change, and at 9600 Hz, approximately every other hardware update, during a high resolution sweep, is not evident in the output signal; nonetheless, when the primary A source sweeps it is perceived as continuous.

As many of the SWEEPMODE operations are included for ease in testing the hardware, only those that could be used for audiometric testing will be discussed in detail. These are the first three options, which provide the finest resolution steps at rates of 1/2, 1 and 2 octaves per minute. In these cases, while the SWEEP pb is depressed, the sweep timer, CTC0, interrupts the CPU every 21.15 milliseconds. For 2 octave per minute sweeping, the hardware is updated once per timer period. The calculation involved at each setp is repetitive, thus for an initial frequency of F and an upward sweep direction, after 30 seconds the frequency equals $F \cdot (1 + 1/2048)^{30/(21.15 \cdot 10^{-3})}$ or $1.9988 \cdot F$, assuming no timing or calculation errors. For downward sweeps, theoretical performance is similarly precise. After thirty seconds, the frequency equals $F \cdot (1 - 1/2048)^{30/(21.15 \cdot 10^{-3})} =$ .50012 F. Note that the downward and upward sweep speeds are almost identical because $(1 + 1/2048)$ very nearly equals $(1 - 1/2048)^{-1}$. To sweep at slower rates, steps are taken once every two or four timer interrupts. There are other sweeping options involving larger steps and/or higher sweep rates. In all cases, the process is interrupt-driven with interrupts occuring once every 21.15 milliseconds except for the fastest sweep, 32 octaves per minute, which is interrupt-driven at 5.31 millisecond intervals. Larger step sizes are taken by repeating the basic multiply routine a number of times before preparing and outputting the result. Refer to the listing (Appendix I) and flow chart (figure V-9) for details.

In an audiometric system, the pure tones must sweep smoothly. A synchronous loading procedure is employed in the design of these two generators to ensure their transient-free operation. As the A channel is the primary frequency source, the hardware and software interaction involved with its "glitch-free" sweeping will be outlined. While the A channel steadily produces any given frequency, the lines which program the 18-bit counter do not change. At every counter overflow, the data on these lines is reloaded and the next count cycle begins. To alter the frequency, this data is modified, but it must be ensured, as mentioned earlier, that the data is stable at the time it is loaded. Therefore, all frequency changes are outputted to the hardware during the period between counter overflows, such that at the next load new data is stable. When the microprocessor is ready to output new data, it halts and waits until the SYNCA interrupt occurs, because its response to the interrupt is fastest when halted. This interrupt is simultaneous with the counter load, and when it occurs, the old data is still present. The new data is then outputted as quickly as possible to be sure that it is stable for loading at the next counter overflow.

At the highest frequency which is produced by the hardware, 12.8 KHz, counter loads occur about every 39 microseconds. The SYNCA interrupt service routine is thus constrained to complete the outputting of new data within a 39 microsecond window. Analysis of the routine (ISERVA, see Appendix I) shows that it requires about 36 microseconds to execute. This length of time includes 20 CPU clock periods maximum (407 nanoseconds each) for the vectored interrupt response time, 12 for the disabling of the SYNCA

interrupt capability (the next load pulse therefore cannot interrupt), and 19 x 3 or 57 for the retrieval and outputting of the 18 bits of new data. Before the routine is called all arithmetic operations and other necessary details are completed; the ISERVA routine is as rapid as possible. There is very little extra time available, but smooth counter reloads could be accomplished when the A channel is generating frequencies as high as 13.8 KHz. Figure V-7 illustrates this high frequency limitation of the system.

A different sort of timing problem, also shown in figure V-7, is present at low frequencies when sweeping. Because the timer interrups occur once every 21.15 milliseconds, the entire multiply and update procedure must be accomplished in less than that amount of time, else frequency transitions could not occur once per interrupt period. The entire set of instructions performed between counter updates during sweeping only requires about 0.5 milliseconds, but the amount of time that the processor is halted waiting of the SYNCA interrupt can be quite long, expecially for low frequencies. When the A square wave frequency is 75 Hz, that wait time can be as great as 6.67 milliseconds. An inherent limitation on sweep speed for low frequency signals is apparent. For high resolution steps (i.e. one step per timer interrupt) the fastest sweep speed attainable for a signal near this low frequency limit is about 6 octaves per minute. Conversely at the 2 octave per minute sweep rate, the lowest frequency which can be swept (19-bit counter is needed) is 25Hz. This frequency limitation is the primary reason why the faster sweep rates must involve larger frequency steps. Note that the channel A hardware cannot output square waves of frequencies lower than 37.5 Hz.

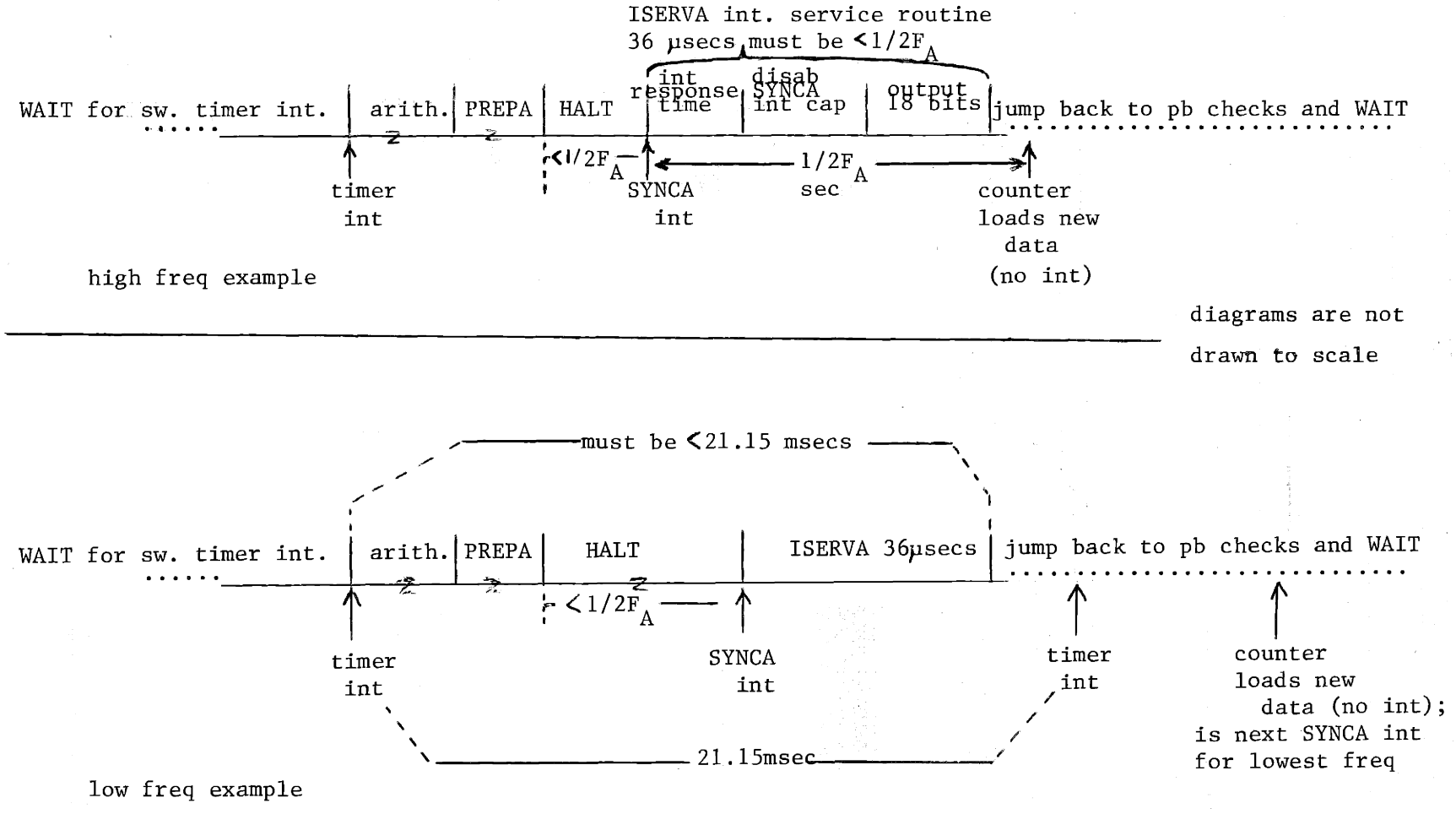

FIGURE V-7 High Frequency and Low Frequency Timing Limitations

In summary, there are two major factors which limit the system's capabilities in generating square waves. First, the hardware and software both are involved with available frequency resolution and accuracy. Second, timing constraints limit sweep rate and frequency range. In this design, these limitations differ for the two channels. As explained above, for a 2 octave per minute sweep, the A channel frequency range is approximately 37.5 Hz to 13.8 KHz, and if no frequencies lower than 75 Hz are desired, the maximum sweep rate is about 6 octaves per minute. B channel considerations are similar and are summarized here. Detailed analysis can be aided by careful consideration of the SYNCB interrupt service routine (ISERVB). The frequency range in the B channel is about from 50 Hz to 15.3 KHz for the two octave per minute sweep rate. As for the A channel, limiting the lowest frequency enables higher sweep rates. In this case, a rate of 3 octaves per minute is attainable for a 75 Hz lower limit. Accuracy in both channels is sufficient for audiometric work, however, only the primary A channel is resolute enough for swept frequency testing.

With these clarifying comments on the hardware/software interface in mind, the software flow chart can be more easily understood. Following the housekeeping and interface circuit initialization, the PROM firmware debugger is called twice to output the startup message and input the four control characters. Each of these four characters is analyzed by the software to set up the proper program parameters and flags. There are six tables, located after the program instructions, which are referenced by the control characters. The first three of these tables associate the FREQA and FREQB characters with three bytes each to supply the necessary initial internal representations for frequency. The SWEEPMODE character

specifies two values to the algorithm, the number of miltiplies per step, i.e. the step size (NCTR), and the number of interrupts per step (NICTR). These parameters are listed in the two tables following those used for the initial frequencies. The last table is referenced by the OPMODE character choice. These words control the output signal routing to the earphones and set up certain program flags, as will be explained.

Following the table lookup there is further processing based on the options selected by the user. First, note with reference to figure V-5 that for OPMODE choices 6, 7, F, and G, if the FREQA and FREQB characters are identical, the same pure tone signal (channel A) will be presented to both earphones, overriding the OPMODE choice and causing a default to OPMODE 1 or A depending on whether the original choice was a number or a letter. The reason for this is that usually when equal frequencies are selected for both chanels, the intent is to present the same signal binaurally. In this system, the channels are not identical, and even if programmed for the same frequency they will be slightly different. OPMODES 8, 9, H, and I do not provide the default feature and thus could be adopted for use in procedures such as the test for difference limen of frequency (which would also require additional software to ensure accurate programmability of frequency differences). This special feature is incorporated in the section labelled PATCH1. There are in addition two other PATCH routines. PATCH2 determines which generator will sweep and is also based on the OPMODE choice. The routine sets up an index register with the address of either the A frequency or B frequency representation. The same flag used in the PATCH2 routine is tested again after computation; thus the proper generator is updated. Finally PATCH3 loads the sweep timer

CTC0, with a time constant based on the SWEEPMODE choice, but note that its interrupts are still not enabled.

Having performed these analyses on the input characters, the system is ready to output the initial frequency choices and connect the phones as directed by the OPMODE character. The PREPA and PREPB routines are first called in this section to transform the two 24-bit internal representations into words for programming both hardware channels. At this point, the system can either sweep, step, or wait.

If none of the pushbuttons is depressed, the system merely waits, outputting fixed frequency signals. To determine whether or not sweeping is desired, or already in progress, the processor inputs the data from the four pushbuttons. Based on whether or not the SWEEP pb is depressed (no interrupt involved here) the program branches. If sweeping is desired (pb depressed), the sweep timer interrupts are enabled, and after receipt of a specified number of interrupts (NICTR), each serviced by the routine ISERVT, the program continues with the computation and subsequent updating of frequency. If the input data indicates that the SWEEP pb is not depressed, the interrupts from the SWEEP and STEP pbs are then enabled, and only if one or the other pb is depressed can the program progress.

The program sections which follow this step/sweep branching decision first determine the sweep direction by checking whether the current direction was changed by the CHDIR pb, and whether either the upper or lower frequency limit has been reached; and then the step computation is performed. As division by 2048 is simply an 11 bit shift right, the multiply routine is either a shift and add (sweep down) or a shift and

Figure V-8

Measured Performance of Square Wave Generators.

A. Frequency Accuracy (measured with ITRON Model 650-0 counter timer, #1152)

Desired Frequency	Channel A	%error	Channel B	%error
75	75.022	+.029	75.022	+.029
100	100.029	+.029	100.029	+.029
125	125.042	+.034	124.712	-.230
150	150.044	+.029	150.044	+.029
200	200.058	+.029	200.058	+.029
250	250.075	+.030	249.426	-.230
375	375.122	+.033	374.742	-.069
500	500.140	+.028	498.853	-.229
750	750.227	+.030	749.485	-.069
1000	1000.330	+.033	997.695	-.231
1500	1500.350	+.023	1498.980	-.068
2000	2000.680	+.034	1995.410	-.230
2400	2400.730	+.030	2400.730	+.030
3000	3000.750	+.025	2997.960	-.068
4000	4000.640	+.016	3990.900	-.228
6000	6003.190	+.053	6025.260	+.421
8000	8001.020	+.013	7981.550	-.231
10000	10003.300	+.033	10075.100	+.751
12000	12006.400	+.053	12050.500	+.421

B. Sweep Timing Accuracy (see text for description of indirect measurement method)

Sweep up at 1 octave per minute desired:
1 octave traversed in 59.995 seconds.

Sweep down at 1 octave per minute desired:
1 octave traversed in 60.037 seconds.

Note: Crystal accuracy -- 19.6608 MHz ideal, measured to be 19.6663 MHz, in error by +.028%.

subtract (sweep up). The newly computed period is then outputted to the appropriate generator synchronously as described above, and after the ISERVA (or ISERVB) routine is completed the program jumps back to the section which checks the pushbuttons to again determine whether sweeping, stepping, or simply waiting is desired.

The overall performance of the square wave generators controlled by this software is detailed in figure V-8. Frequency accuracy of the crystal reference is noted and is a minor source of error. Sweep timing could not be measured directly, but in order to determine the effects of roundoff in the repetitive multiply computation, the number of steps traversed per octave was determined by measuring the frequency and using an internal software register to count the steps. It was observed that for any octave traversed upward, 1419 (nearest integer value) steps are taken, and that for any octave traversed downward, 1420 steps are taken. The approximate one step difference is clearly insignificant in this application. Surprisingly, the computational roundoff noise was not, on the average, noticeably different at low frequencies compared to high frequencies, verified by the fact that the same number of steps are present from 75-150 Hz and from 4.8-9.6KHz. Frequency and sweep timing accuracy far exceed the project's goals.

FIGURE V-9 SOFTWARE FLOW CHART

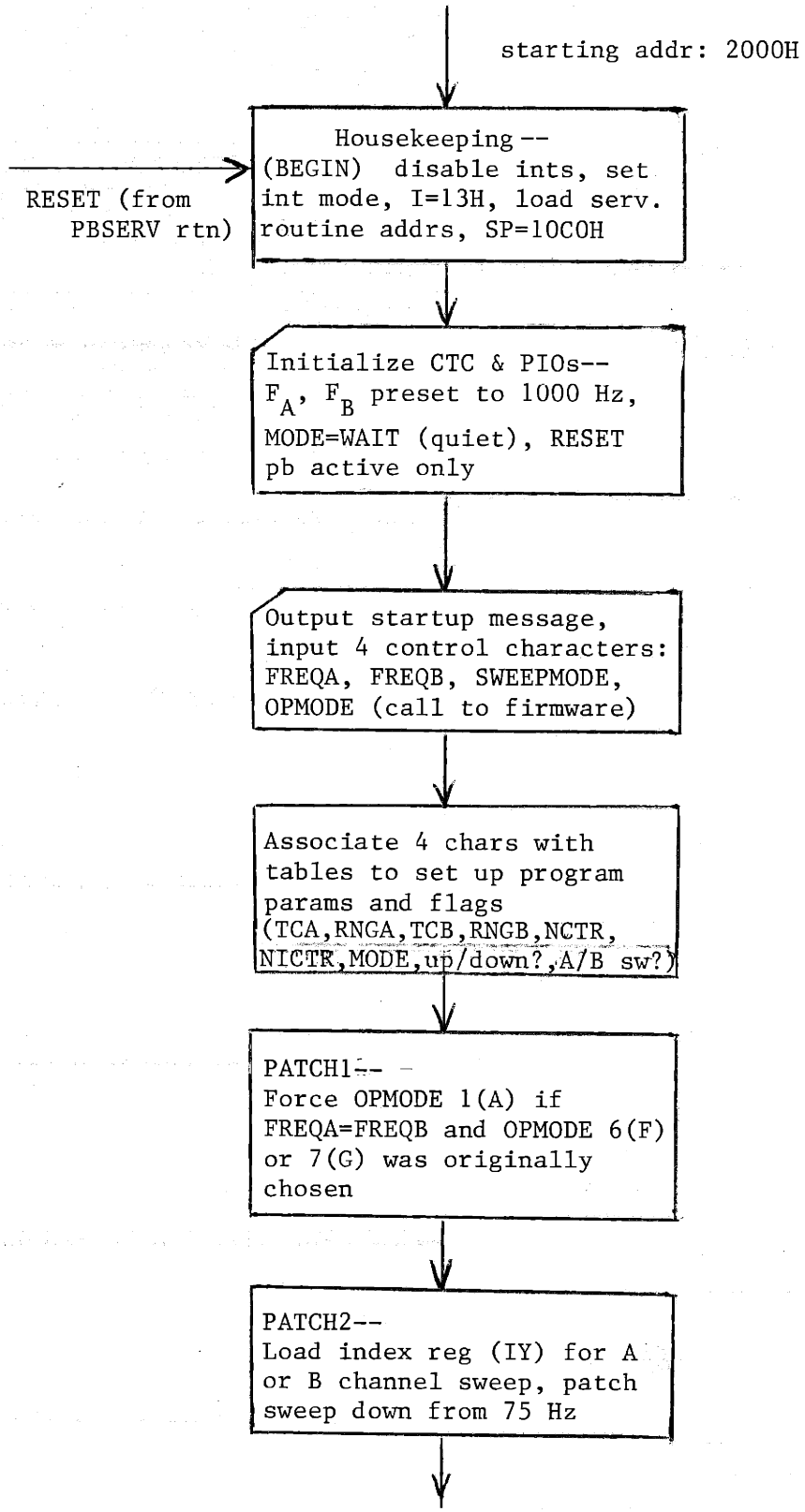

(Flow Chart, continued)

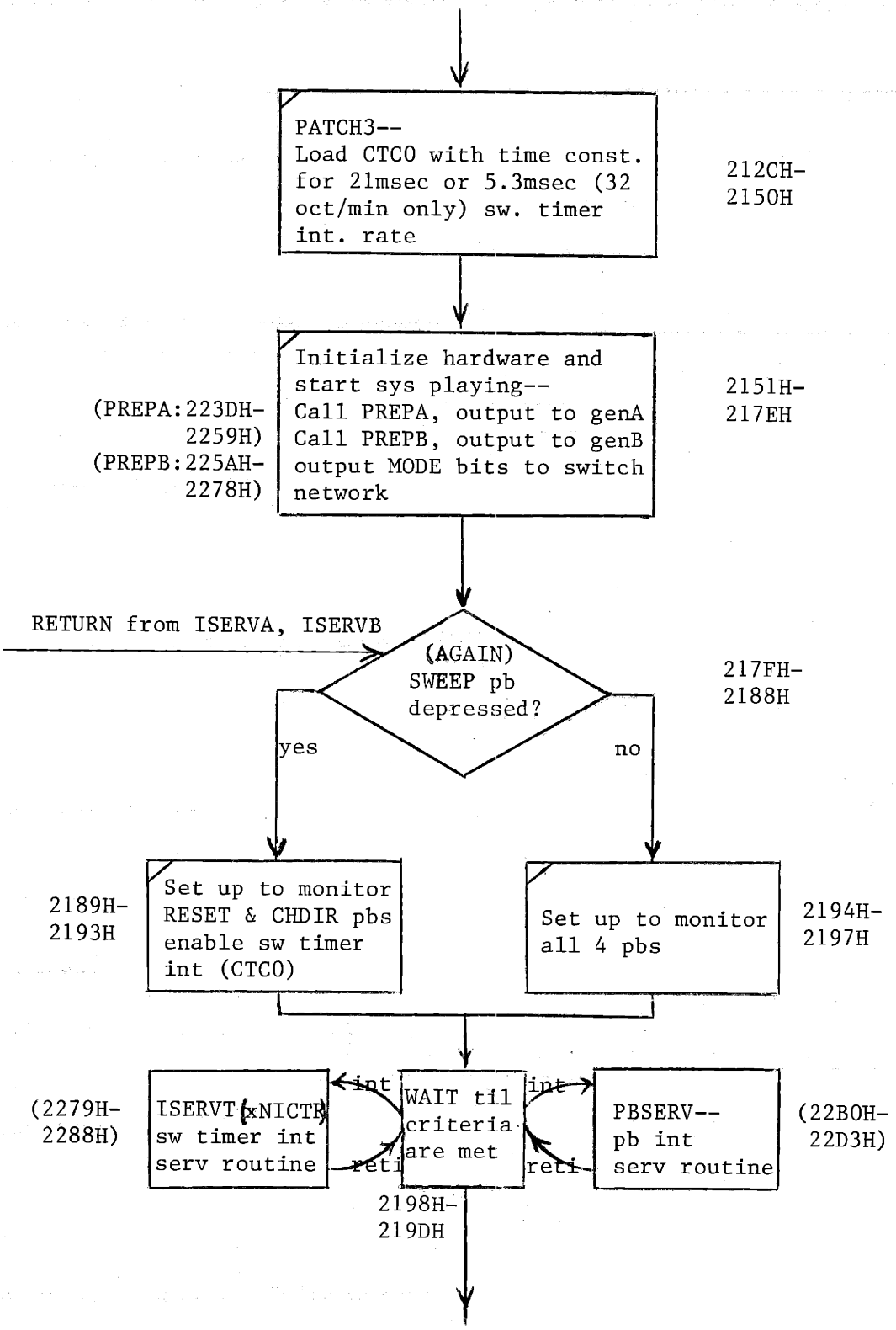

(Flow Chart, continued)

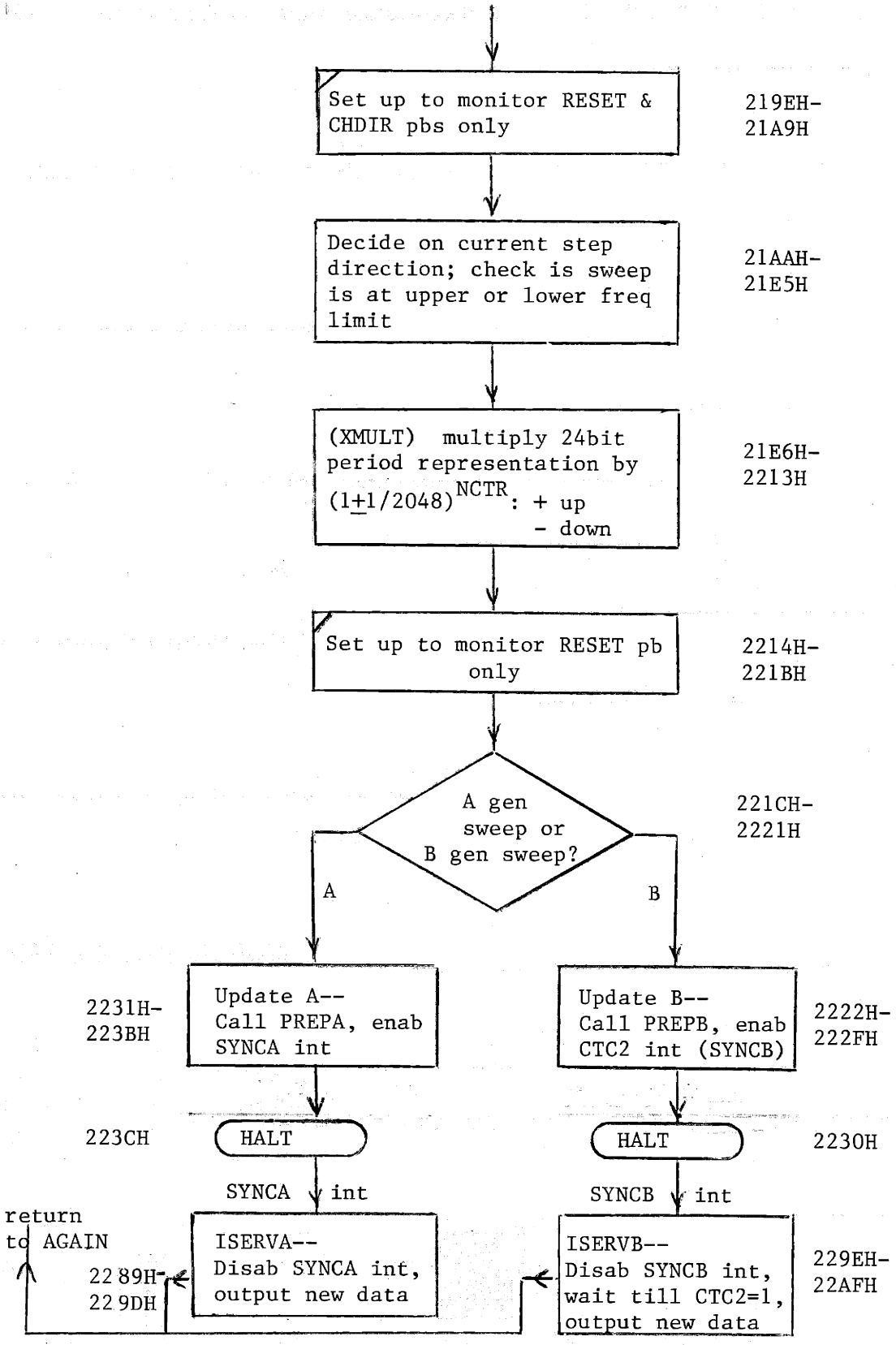

VI. PURE TONE GENERATION

In this system, two independent pure tones are generated. Based on the utilization of phaselock techniques, the frequency of each tone is equal to that of a square wave reference controlled by the software. The components and capabilities of phaselocked circuits were briefly mentioned in Chapter IV, where the concepts were introduced along with the final architectural choice. The requirements for the loops used in this project are very particular to their application. They do not operate in the presence of any appreciable input noise as the reference square wave signal is produced locally, but these phaselocked loops (PLL) must not loose lock over a very wide range (the hold-in range must exceed 7 octaves) and also must be able to pull into lock after large steps in frequency (the pull-in range must also be greater than 7 octaves). In addition, at 2 octaves per minute sweeping, the loop must not loose lock, and finally, phase jitter must not be audible at any frequency within the range. The primary feature which distinguishes this phaselocked design from classical loops is the inclusion of a nonlinearity between the filter output and the voltage controlled generator (VCG) input. The antilog (or exponentiator) circuit used alters the control of the VCG from the usual linear function, expressed in Hz per volt, to an exponential function which can be expressed in octaves per volt. The important areas of performance that were affected by the addition of the nonlinear element for compensation are sweep tracking and the reduction of jitter caused by internal noise. Both of these issues will be treated in detail.

As a starting point in the mathematical analysis of PLLs, the quasi-linear relationships of a loop in lock will be discussed. There are some assumptions which must be made before a linear analysis can be carried out. It is of primary importance to recognize that the analysis is concerned with the variables of phase in the input reference and VCG output signals. Unless the loop is in lock, meaning that the frequency of the output signal equals that of the input signal, the linear point of view is not valid. Even in lock, especially for compensated designs, the system is somewhat nonlinear, however, the operation of a well-behaved system can be considered linear in a region, and that is the approach which will be taken here. It is useful to think of the phase detector (PD) as a device which converts phase information into voltage information and conversely to think of the VCG as a voltage to phase converter. Actually, the VCG linearly converts voltage to frequency, but the relationship between frequency and phase is easily described. Thus the conditions for valid linear analysis are: 1) the loop is in lock, 2) the phase detector is linear in its conversion of phase difference to voltage, and 3) the VCG is a linear system in its conversion of voltage back to phase.

Conceptually it is reasonable that the phase detector output could change the VCG frequency (phase) in a direction that reduces the phase difference present, thereby ensuring stability. Figure VI-1 shows the block diagram of a compensated phaselocked loop. The active filter illustrated is typical and commonly used because of its simplicity and effectiveness. It is of the same type as used in the system prototype and its characteristics will be included in the following derivations. The

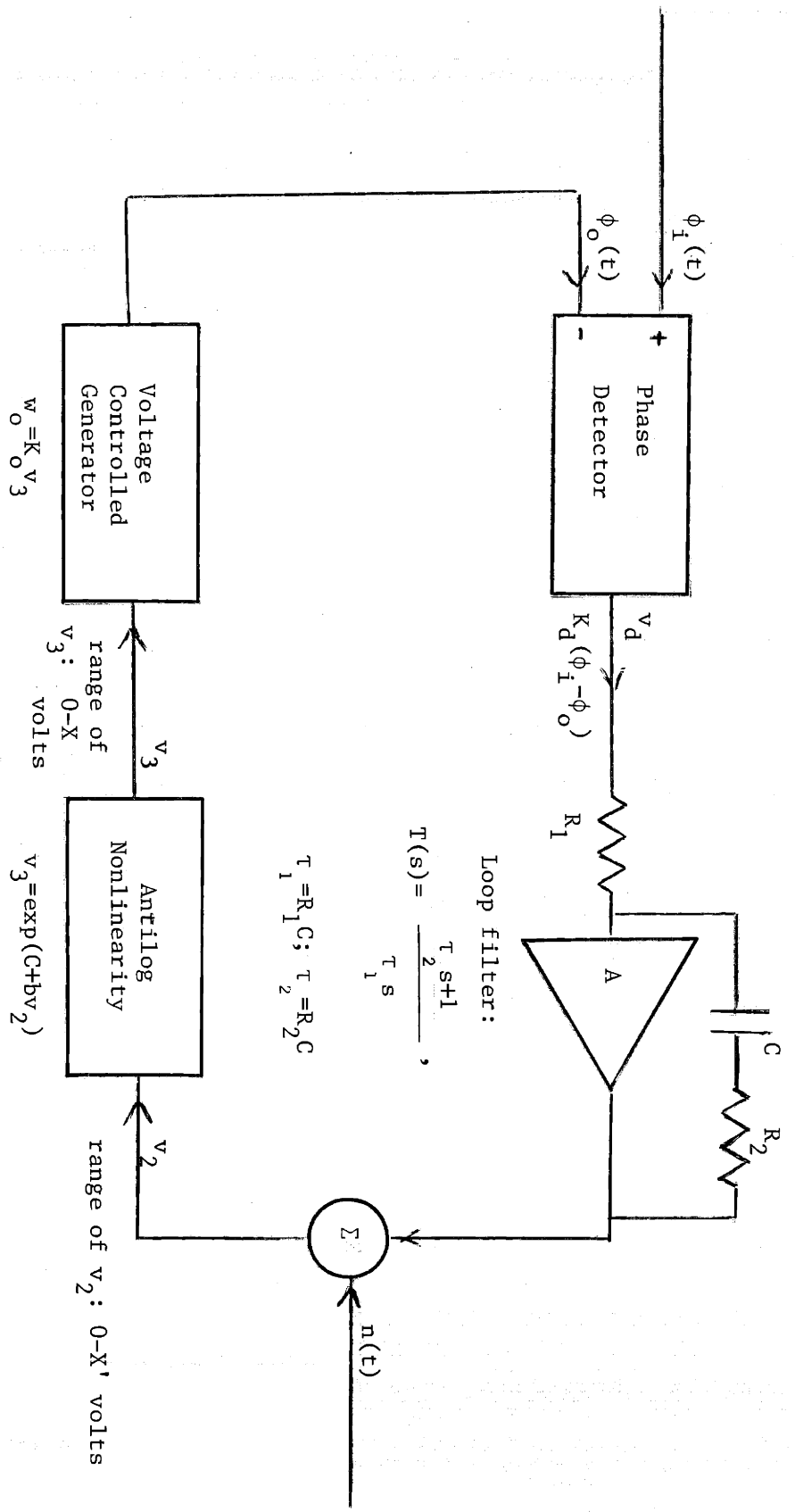

FIGURE VI-1 Block Diagram of Compensated Phaselocked Loop

diagram also shows an internal noise source, n(t), which will be discussed later in connection with the phase jitter problem. (Detailed schematics of the two PLLs are in appendix II, figures AII-3 and AII-4).

The variables that are of concern are ϕ_i and ϕ_o, the reference and VCG signal phases. A major result of the following analysis is the frequency domain relationship $H(s) = \Phi_o(s)/\Phi_i(s)$, from which the natural frequency and damping factor can be derived, as the result is second order. Because we are dealing with phase, the variable 's' present in the loop equations is definitely distinct from both the reference and output frequencies. To illustrate this, note that the waveforms that are being locked are square waves. The phase as a function of time of these square waves is a ramp, which in the frequency domain is proportional to s^{-2}, quite different than the transform representation of the square wave signal itself. Equations will first be expressed in general terms without numerical values for the various parameters. Then discussion and calculations comparing the classical PLL with the final designs in this system will be presented, emphasizing the primary channel (A), as the two are similar. Remember that linear analysis is based on a locked condition. The behavior of PLLs out of lock will also be treated.

It is assumed that the phase detector outputs a voltage proportional to the difference in phase between its two input signals, $\phi_i(t)$ and $\phi_o(t)$. Depending on the type of detector used [see Gardner, 1966], the relation $v_d = K_d(\phi_i - \phi_o)$ is more or less accurate. It is generally most valid for small phase differences. When a loop loses lock, phase error climbs rapidly and invariably the PD cannot operate linearly. The

constant K_d is referred to as the detector's gain, expressed in volts per radian.

Generally, descriptions of voltage controlled signal generators relate the control input voltage (or current) to the frequency of the output signal. For linear analysis, a relation is necessary which specifies the output <u>phase</u> in terms of the input voltage. Based on the fact that frequency is the derivative of phase, a useful form can be stated. The usual VCG characterization is $w_o=K_o v_3$, which, expressed in the frequency domain in terms of phase, is equivalent to $s\Phi_o(s)=K_o V_3(s)$. This description is adequate for a classic PLL; however for compensated loops such as in this design, the nonlinearity must also be specified. For the moment, though, consider the effect of the antilog circuit to be incorporated within the value of K_o. This point of view then requires the inclusion of the operating frequency w in the linear equations because the "gain" of the nonlinearity is dependent upon its operating point. The VCG gain term in the basic PLL equations will therefore be expressed as $K_o'(w)$, with dimensions of radians per second per volt.

Figure VI-2 shows the basic loop equations. Four different forms are presented for reference. The first transfer function expresses $H(s)=\Phi_o/\Phi_i$ in terms of the general loop filter T(s). Next, specifying T(s) as an active lag-lead network gives a more exact form. The third entry in the figure uses standard servo terminology and provides more insight with less complexity. Note that the loop performs lowpass filtering on phase inputs. The final function shown is $H_e(s)$ which relates the phase error, $\Phi_e=\Phi_i-\Phi_o$, to the input phase signal. The PLL error response has a highpass character.

1) $$H(s) = \Phi_o(s)/\Phi_i(s) = \frac{K_o'(w) \cdot K_d \cdot T(s)}{s + K_o'(w) \cdot K_d \cdot T(s)}$$

2) for lag-lead filter shown in fig. VI-1: $$H(s) = \frac{K_o'(w) \cdot K_d \cdot (s\tau_2 + 1)/\tau_1}{s^2 + s\{K_o'(w) \cdot K_d \tau_2/\tau_1\} + K_o'(w) \cdot K_d/\tau_1}$$

3) using servo terminology: $$H(s) = \frac{2\xi w_n s + w_n^2}{s^2 + 2\xi w_n s + w_n^2},$$

where $$w_n = \{K_o'(w) \cdot K_d/\tau_1\}^{\frac{1}{2}}$$

and $$\xi = (\tau_2/2)\{K_o'(w) \cdot K_d/\tau_1\}^{\frac{1}{2}}$$

4) $$H_e(s) = \Phi_e(s)/\Phi_i(s) = \{\Phi_i(s) - \Phi_o(s)\}/\Phi_i(s) =$$

$$\frac{s}{s + K_o'(w) \cdot K_d \cdot T(s)} = \frac{s^2}{s^2 + 2\xi w_n s + w_n^2}$$

FIGURE VI-2 Basic Phaselocked Loop Equations

Linear analysis can be used to derive the dynamic tracking error and qualitatively describe loop jitter in the presence of internal noise. In both cases, the use of an antilogarithmic nonlinearity is suggested. Before the comparison between the classic and antilog-compensated loops can be made, however, the parameters that are available to the designer must be defined. In the classic case, the constants K_d, K_o, τ_1, and τ_2 are all present in the basic linear loop equations. Only three of these four are independent, however. In the antilog design, there are five parameters. Two of them are based on the function relating the VCG output frequency to v_2. Referring to figure VI-1, the general antilog element has the characteristic $v_3=\exp(C+bv_2)$; combining this with the VCG relation, $w_o=K_o v_3$, gives the dependence $w_o=K_o\exp(C+bv_2)$. Since K_o and C are not independent, this relation can be more simply stated as $w_o=\exp(a+bv_2)$. For linear analysis, the slope of the function $w_o(v_2)$ is the desired $K_o'(w)$ (the antilog is being considered linear within a region): $dw_o/dv_2=b\exp(a+bv_2)=bw$, where for a loop in lock $w_i=w_o=w$. Thus, b, K_d, τ_1, and τ_2 all appear in the linear equations for the antilog-compensated PLL, with only three of these parameters being independent. The remaining parameter, 'a', must be chosen by considering the saturation of the VCG and does not enter directly into the linear derivations. Figure VI-3 is compilation describing all major loop parameters and variables used throughout this chapter.

An obvious effect of incorporating an exponentiator in a PLL is the resulting dependence of w_n and ξ on the operating frequency w. Because K_o' is proportional to w, both the natural frequency and damping factor are proportional to $w^{\frac{1}{2}}$ in the compensated loop design. Figure VI-4

$\phi_i(t) \leftrightarrow \Phi_i(s)$	phase of input reference signal
$\phi_o(t) \leftrightarrow \Phi_o(s)$	phase of VCG output signal
$\phi_e(t) \leftrightarrow \Phi_e(s)$	phase error, $\phi_i - \phi_o$
$n(t) \leftrightarrow N(s)$	model of loop noise signal
ϕ_a	steady-state acceleration (tracking) error for frequency ramp input
$\phi_a(\max)$	worst case tracking error (2 oct/min sweep) in classic loop
w_i	frequency of input reference signal
w_o	frequency of VCG output signal
w	operating frequency of PLL in lock ($w=w_i=w_o$)
K_d	gain of phase detector, volts/rad
K_o	gain of VCG, rad/sec per volt
$K_o'(w)$	gain of VCG in general compensated loops, rad/sec per volt
$T(s)$	loop filter transfer function
$v_d(t) \leftrightarrow V_d(s)$	output voltage of PD (high freqs attenuated by filter)
$v_2(t) \leftrightarrow V_2(s)$	input voltage to nonlinearity in compensated loops
$v_3(t) \leftrightarrow V_3(s)$	control input voltage to VCG ($v_3=v_2$ in classic PLL)
X'	upper limit on v_2 (range 0-X' volts)
X	upper limit on v_3 (range 0-X volts)
τ_1, τ_2	loop filter time constants, $T(s)=(s\tau_2+1)/\tau_1$
a, b	describe control function of antilog-VCG combination: $w_o=\exp(a+bv_2)$
w_n	natural frequency of PLL
ξ	damping factor of PLL
w_l	lowest frequency for lock
w_h	highest frequency for lock
S	saturated output voltage of PD ($\pm S$)
R	rate of exponential frequency sweep, oct/sec.

FIGURE VI-3 Summary of PLL Parameters and Variables

presents this and other major results of the comparison between the classic and antilog-compensated PLL types. Whenever possible, features of both loops are expressed in terms of the basic design parameters described above.

The first major area of linear investigation is the consideration of phase error during frequency sweeps. Note that in this particular application, when the test frequency is changed abruptly, loss of lock in the PLL does not hamper the design's utility, provided that lock is regained within some reasonable length of time (a few seconds). In fact, to build a PLL that does not loose lock when the reference is changed quickly from one audiometric frequency to another would be nearly impossible. The pull-in phenomenon is covered in later sections dealing with out-of-lock nonlinear behavior. The primary tracking constraint for these PLLs is that they must not loose lock during an exponential frequency sweep. (Audiometric sweeping will henceforth be described as exponential rather than "logarithmic" because the more commonly used term is actually a misnomer in that the instantaneous frequency is an exponential function of time.) Linear techniques can be used to describe loop behavior for frequency ramp inputs [Gardner, 1966], and these results can be generalized to predict behavior for exponentially sweeping inputs.

A frequency ramp input is described in terms of phase as $\Phi_i(s) = r/s^3$, where r is the ramp's slope in radians/second^2. Consideration of the transfer function $H_e(s)$ with this input leads to a steady-state value of tracking error which is called the acceleration error, ϕ_a. For a second-order high-gain loop such as these being discussed, $\phi_a = r/w_n^2$. In

order for the loop to remain in lock, ϕ_a must be within the linear range of the PD throughout the entire sweep. An exponential frequency sweep has an instantaneous rate easily shown to be $w_i R \cdot \log_e 2$ Hz per second, where R is the sweep rate in octaves per second. For a classic PLL, in which w_n is a constant, the worst case dynamic tracking error for an exponentially sweeping reference is at the highest frequency, denoted here as w_h. The maximum dynamic tracking error in the standard PLL then equals $w_h R \cdot \log_e 2 / w_n^2$, and expressing w_n in terms of basic loop parameters, $\phi_a(\max) = (w_h R \cdot \log_e 2)\tau_1 / K_o K_d$.

For the compensated loop, w_n as well as the instantaneous frequency are functions of w. Substituting bw for K_o (assuming the loop is locked) results in $\phi_a = \tau_1 R \log_e 2 / (bK_d)$, which is a constant. In light of the fact that for an uncompensated (linear) loop, a linear ramp produces a constant acceleration error, it is not surprising that for an exponential frequency sweep a loop containing an exponential nonlinearity exhibits a constant tracking error. Note that the damping term ξ does not enter into the relation for steady-state acceleration error. Graphs of L.A. Hoffman [in Gardner, 1966] show the effect of the damping term on transient behavior. Provided that the transient does not cause the loop to loose lock at the onset of the sweep, the damping term is only of secondary importance.

The other major area of linear analysis for the PLLs in this design has to do with internal noise and resulting phase jitter. External noise is not considered here because the reference square wave is transient-free by design. The injection of n(t), shown in figure V-1, models the actual noise source present within the loop. The author feels that this model is

justified for two reasons. First, listening tests on the VCG-antilog combination (run open-loop) reveal that their internal noise is not great enough to audibly affect pure tone quality, and secondly, since the PD is a digital circuit operating at high voltage levels, it is unlikely that its output noise significantly contributes. The true source of noise was not precisely determined experimentally, but evidence points toward the output noise of the active filter as the major source. The addition of noise to the normaly quasistatic control of a VCG cannot be rigorously described in linear terms, but if the noise is bandlimited so as not to contain energy near the signal frequency, and if the noise level is low enough, linear analysis can provide results relating jitter to loop parameters.

The psychoacoustic perception of jitter is not a question to be delved into here, however it is reasonable to surmise that the sensitivity to <u>frequency</u> jitter correlates with data on the difference limen of frequency. Were the threshold of perception of jitter directly related to the just noticeable difference in frequency, this threshold would be approximately proportional to operating frequency w. Carrying the development further, we can express the frequency jitter transfer function J(s) as $sH_N(s)$ (frequency is the derivative of phase), where $H_N(s) = \Phi_e(s)/N(s)$. Figure IV-4 shows the result of this mathematical point of view. Observe that J(s) is a highpass function scaled by K_o in the classic case and scaled by bw in the antilog-compensated case.

Several features of the function J(s) are relevant to a comparison of output jitter in linear and antilog PLL circuitry. If the signal n(t) is

ideally bandlimited white noise (bandwidth=B Hz) the R.M.S. jitter in the output signal is proportional to

$$\int_{j\emptyset}^{2\pi Bj} |J(s)|^2 \, ds$$

Recognize that this measure has only limited quantitative significance and extensive experimentation would be necessary to fully relate the signal character with the perception. In addition, the spectral nature of N(s) was never empirically determined. In accordance with earlier remarks on the ear's sensitivity to changes in frequency, it will be assumed here that for a fixed amount of RMS jitter, the sensation will be stronger at lower frequencies. Note that in a classic PLL this integral is constant at all operating frequencies and thus the low frequency problem observed in the classic design first attempted for this project agrees with the present mathematical development.

A PLL with an exponentiator shows dependence of K_o, w_n, and ξ on the operating frequency w, as described earlier. The form of J(s) is such that the predominant factor in the resulting integral is the variation of K_o. This can be made clear by first comparing the bandwidth B for the integration to the natural frequency w_n. Because the cutoff of the Highpass function is at a small frequency compared to B, the variation of w_n (it increases with w) is of only secondary importance. Similarly, unless the damping factor is very small it is also of little significance to the resultant output signal jitter. Conceptually, it seems clear that since the noise source is positioned directly before the VCG, the VCG gain would be the primary factor in determining the amount of jitter at the output.

FIGURE VI-4 Comparison of Classic and Antilog Compensated PLL Types

Feature	Classic case	Compensated case	Comments
1) natural frequency, w_n	$w_n=(K_oK_d/\tau_1)^{\frac{1}{2}}$	$w_n=(bK_d/\tau_1)^{\frac{1}{2}}\ w^{\frac{1}{2}}$	w_n and ξ both proportional to $w^{\frac{1}{2}}$ in compensated PLL
2) damping factor, ξ	$\xi=(\tau_2/2)\cdot(K_oK_d/\tau_1)^{\frac{1}{2}}$	$\xi=(\tau_2/2)\cdot(bK_d/\tau_1)^{\frac{1}{2}}\ w^{\frac{1}{2}}$	
3) acceleration error during exponential sweep	$\phi_a(max)=w_h\tau_1\cdot R\log_e 2/(K_oK_d)$	$\phi_a=\tau_1\cdot R\log_e 2/(bK_d)$	constant for compensated case, worst at highest freq in classic case
4) output jitter (see text for assumptions) $=\int_{s=j\emptyset}^{2\pi Bj}\lvert J(s)\rvert^2\,ds$	$J(s)=\dfrac{-K_o s^2}{s^2+2\xi w_n s+w_n^2}$	$J(s)=\dfrac{-bw\,s^2}{s^2+2\xi(w)w_n(w)s+w_n^2(w)}$	J(s) proportional to w in compensated case; approx. constant perceived jitter for compensated case; jitter worst at low freqs for classic PLL; equiv jitter when $K_o \approx bw$
5) <u>minimum</u> value for to filter high freqs from PD output	$\tau_1 \geq 10/w_1$	$\tau_1 \geq 10/w_1$	constraint common to both types
6) <u>minimum</u> values for K_o and b to ensure full range VCG operation	$K_o \geq w_h/X$	$b \geq \dfrac{\log_e(w_h/w_1)}{X'}$	also in compensated type, e^a must be $\leq w_1$
7) pull-in, hold-in	ranges limited only by VCG tuning characteristics in both PLL types		
8) sweep rate during pull-in	$\pm SK_o/\tau_1$ rad/sec^2	$\pm bS/(\tau_1\log_e 2)$ octaves/sec	

One conclusion that can be drawn from the preceding observations is that at the frequency where bw in the antilog PLL equals K_o in the classic PLL, their performance in terms of jitter will be roughly the same. At lower frequencies the classic loop performance degrades due to psychoacoustic considerations, but the compensated loop's jitter decreases approximately in proportion to the operating frequency because $K_o'(w)$ is proportional to w. Thus, another result of this investigation is that for an antilog-compensated loop operating under these conditions of internally generated noise, the perceived jitter is about constant at all operating frequencies. (For noise at filter input, analysis yields similar conclusions)

Analysis of the effects of internal noise and acceleration error during exponential sweeping both indicate that an antilogarithmic nonlinearity is well-suited for this particular application. However, the nonideal behavior of loop components must also be considered in comparing the two designs. First, in order for the phase detector to function linearly, the loop filter must significantly attenuate the "high" frequencies present in the PD output signal. Referring to figure VI-5, which illustrates input and output waveforms for the PD used in this project under various conditions, note that when the loop is in lock the detector compares the two leading edges of the input waveform producing a complex rectangular signal at its output. A linear treatment of the situation requires that K_d be defined as the average value of the outputted PD waveform. (Because there is 7.5 volt level-shifting designed into the loop filter, the PD output can be considered to have two states: +7.5 volts and -7.5 volts.) The necessary averaging cannot take place unless $1/\tau_1$ is at least an order of magnitude below the lowest operating

frequency of the loop, w_1. This guideline is the same for both the classic and compensated PLL types.

Next, the saturation of the VCG input is considered. In the classic case, in order to cover the full frequency range from w_1 to w_h, there is a lower limit on K_o. Given a VCG with a control range of from 0 to X volts, where 0 corresponds to DC output, and X corresponds to the maximum outputted frequency, this design constraint can be stated as $K_o \geq w_h/X$. The situation is quite different for the compensated PLL. As mentioned before, the control function relative to the output of the loop filter can be written as $w_o = \exp(a+bv_2)$. If b is positive, in order for the system to function at the lower frequency limit, e^a must be less than or equal to w_1. In any practical realization, v_3 will have a limited dynamic range of say, X' volts, and for simplicity assume that v_3 is always positive. Given a value for 'a' that meets the low frequency criterion, b is then restricted to be greater than $(\log_e w_h - \log_e w_1)/X'$ in order for the nonlinear PLL to cover the full desired range.

The hold-in and pull-in ranges of the two different PLL types are the next points of comparison. The operation of the phase detector is the primary control on the phenomenon of acquisition. Note with reference to figure VI-5 that when the loop is out of lock, the output of the phase detector is essentially saturated at either the positive or negative limit ($\pm$7.5 volts). Even in saturation, this PD behaves monotonically. In other words, there are no frequency differences other than zero, which can reduce the output of the phase detector from near saturation. This is not true of all PDs as many that are constructed for high noise immunity have

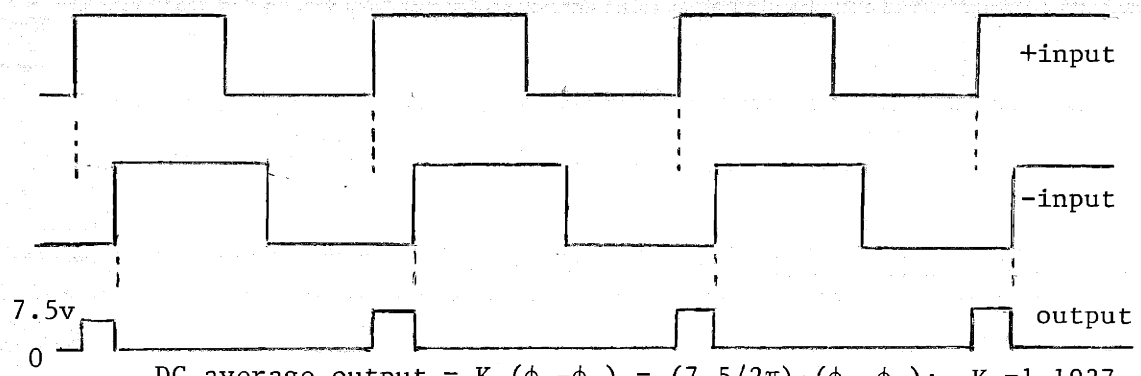

DC average output = $K_d(\phi_i - \phi_o) = (7.5/2\pi)\cdot(\phi_i - \phi_o)$; $K_d = 1.1937$

In-lock: Phase at + input leads phase at - input

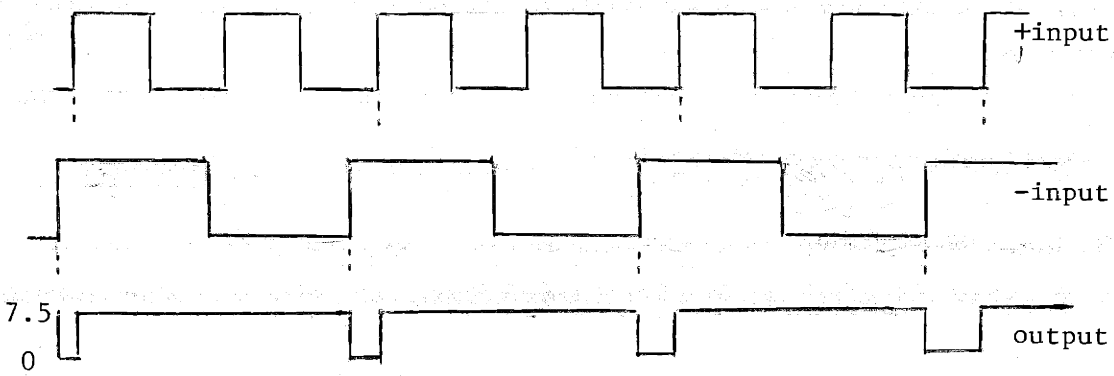

output essentially saturated at +7.5 volts

Out-of-lock: Freq at + input greater than freq at - input

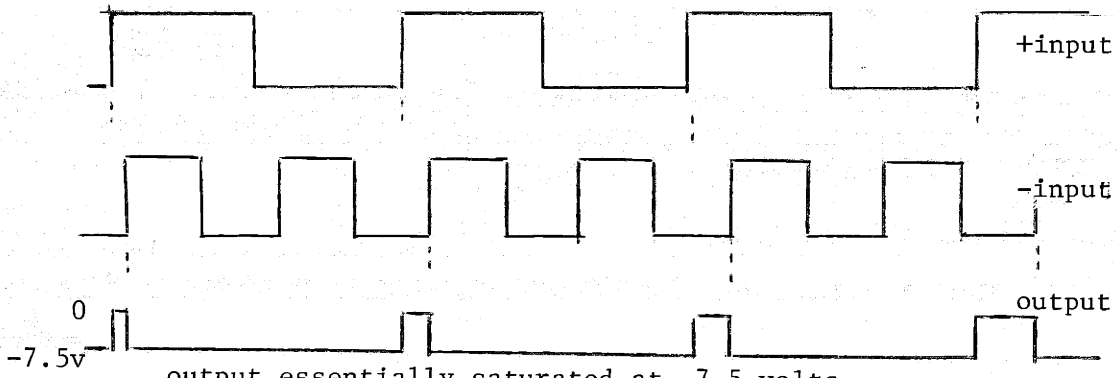

output essentially saturated at -7.5 volts

Out-of-lock: Freq at + input less than freq at - input

FIGURE VI-5 Phase Detector Operation

the disadvantage that the PLL can lock onto harmonics of the reference frequency. However, for the loops in this project, the pull-in range is limited only by the tuning range of the VCG. Furthermore, the hold-in range, that being the range of frequencies over which the loop can maintain lock (without regard for how it got there), is also only limited by the VCG tuning range. The presence of the exponentiator does not effect these ranges.

In considering the amount of time necessary to require lock after a large step in frequency, the classic and compensated loops behave much differently, however. Let $\pm S$ equal the saturated output voltage of the phase detector. While out of lock, this saturated level is integrated by the loop filter as the VCG sweeps towards the reference frequency. With an input voltage of S, the filter output approximates a ramp of slope S/τ_1 volts/second. In the classic loop, this ramp sweeps the VCG linearly at a rate of SK_o/τ_1 rad/sec per second. But in the compensated loop, this ramp at the filter output sweeps the VCG exponentially at a rate of $bS/(\tau_1 \log_e 2)$ octaves per second. An estimate of lock-in time can be derived by calculating the length of time that the ramp would need to be present to sweep the VCG frequency the required amount. In the classic loop, pull-in time following a step from w_l to w_h (or vice versa) would be approximately $(w_h - w_l)\tau_1/SK_o$ seconds, and in the compensated case the pull-in time would be about $\tau_1 \log_e(w_h/w_l)/bS$. Exact calculation of pull-in time is extremely difficult and generally computer simulation methods are necessary for more accurate prediction.

Now that all major formulae for comparison have been presented, the practical design tradeoffs will be illustrated by first designing a hypothetical classic PLL and then comparing its performance with that of the actual antilog-compensated PLL present in the prototype's A channel. The procedure employed in optimizing the prototype PLLs was largely empirical, and a better compromise might therefore be possible. However the prototype is more than adequate to meet design goals in this project and its performance is presented along with the hypothetical design results for comparison in figure VI-7.

For the classic design, first K_o will be selected. The VCG gain term is of primary importance to the jitter problem encountered in these loops. Smaller values for K_o result in less jitter, but contrary to this is the lower limit on K_o set by the necessity of having the tuning range be wide enough to cover 75 Hz to 12.8 KHz. The voltage range, X, of the control input of the VCG will be equal to 6 in this hypothetical design. This value is chosen simply because it is the maximum range for the actual VCG used in the A channel and is reasonable for use here. With X=6 and $w_h = 80.4 \cdot 10^3$ (12.8 KHz), the minimum value for K_o is found to be $13.4\ 10^3$ which is the best possible value for the reduction of jitter. Note that K_d = 1.1937 volts per radian and S = 7.5 volts for the particular PD used in the prototype (see figure VI-5); therefore these values will also be used.

The loop filter in the hypothetical design remains to be specified. Choosing the lower limit for τ_1, which is $10/(2\pi \cdot 75)$, results in a very small worst-case acceleration error, and a correspondingly rapid pull-in

rate. Note that selecting a larger value for τ_1 does not adversely affect jitter performance and is probably better in terms of the filtering of high frequency PD output components. Therefore τ_1=.20 sec is chosen for the hypothetical design. Using this value, ϕ_a (max)=$23 \cdot 10^{-3}$ rad. (2 octave per minute sweep) and a calculation of pull-in time for the maximum frequency step gives 0.16 second. Finally, τ_2 is selected for ξ =1, a commonly used value. Observe, once again, that ξ does not directly affect any of the important performance measures in this application. The significant problem with the classic design is that there is no way to compromise pull-in rate or acceleration error to decrease jitter. This is due to the constraint on the lower limit of K_O, which was chosen at the start to be a minimal value.

Now the details of the compensated PLL used in Channel A of the prototype will be presented. To arrive at values of a and b, necessary for an analytical description of the circuit, the relationship between the exponentiator input voltage and the VCG output frequency was measured and tabulated (figure VI-6). This data is reasonably fit with values a = 12.300 and b = 1.0532, as shown in the last column of the figure. The formula was derived by curve-fitting at 250 and 4000 Hz and is accurate to better than 10% throughout the range. The entire tuning range is covered in a span of about 5 volts. Actually, the best fit formula requires a negative value for b, but because our analysis does not include the inversions actually present in the prototype PLL, this fact will be ignored, as final results are identical. The loop filter specifications, τ_1=0.47 sec and τ_2=0.033 sec, complete the description of the antilog PLL components.

Figure VI-6

Relation between VCG output frequency and Exponentiator input voltage

w rad/sec	(Hz)	v	exp (12.300-1.0532 v)
471	(75)	5.758	511
628	(106)	5.511	662
785	(125)	5.316	813
942	(150)	5.157	962
1260	(200)	4.897	1265
1570	(250)	4.692	1570
2360	(375)	4.317	2330
3140	(500)	4.048	3090
4710	(750)	3.665	4630
6280	(1000)	3.392	6170
9420	(1500)	3.004	9290
12600	(2000)	2.727	12400
15100	(2400)	2.554	14900
18800	(3000)	2.338	18700
25100	(4000)	2.059	25100
37700	(6000)	1.663	38100
50300	(8000)	1.381	51300
62800	(10000)	1.160	64700
75400	(12000)	.9777	78500

Figure VI-7 shows results of calculations based on the above parameters for the compensated PLL. First note the range of values for ξ and w_n. The large damping at high frequencies did not cause any problem. The constant acceleration error for a 2 octave per minute sweep is $8.64 \cdot 10^{-3}$ rad, somewhat better than the worst case tracking error in the classic loop. Although the tracking error is less, the pull-in time is greater. In this case theoretical calculation gives 0.31 second for lock-in after a step between the limits of the frequency range. The important feature, of course, is the amount of jitter. Previous discussion pointed out that equal jitter in the two designs occurs approximately at the frequency where bw=K . Comparing the two designs, jitter is then about equal at $w=12.7 \cdot 10^{3}$ rad/sec or about 2000 Hz. For frequencies lower than this, performance of the classic loop degrades. At 200 Hz, a frequency at which DLF data still generally follows Fechner's law, analysis shows that the classic design would have about 10 times (20 dB) greater jitter than the compensated design.

Experimental results with antilog-compensated PLLs verify the trends observed mathematically and there was a dramatic improvement in performance when the initial classical breadboard design was modified by the addition of the nonlear element. Both PLLs in the prototype sweep at rates up to 32 octaves per minute without loosing lock, and there is no audible jitter at any frequency.

Phaselock loop dynamics smooth the small frequency steps present in the computer controlled sweeping square wave reference. Listening tests were conducted to estimate the psychoacoustic significance of this

	Classic	Compensated
I. Design parameters	$K_o = 13.4\ 10^3$ rad/sec per volt	a = 12.300
		b = 1.0532
	$K_d = 1.1937$ volts/rad	$K_d = 1.1937$ volts/rad
	$\tau_1 = 0.20$ sec	$\tau_1 = 0.47$ sec
	$\tau_2 = 7.07\ 10^{-3}$ sec	$\tau_2 = 33.0\ 10^{-3}$ sec
II. Performance		
a. natural freq	$w_n = 283$ rad/sec	35.5 rad/sec $\leq w_n \leq$ 464 rad/sec
b. damping factor	$\xi = 1$	$0.586 \leq \xi \leq 7.65$
c. tracking error	ϕ_a(max)$=23.2\ 10^{-3}$ rad	$\phi_a = 8.64\ 10^{-3}$ rad
d. pull-in time, largest freq step	0.159 sec	0.306 sec
e. jitter	performance equal at about 2000 Hz, classic loop degrades for freqs 2000 Hz	

FIGURE VI-7 Performance of Hyptothetical Classic Design and Channel A Compensated Design

smoothing effect and to determine whether a lower resolution square wave source (such as the CTC design in the B channel) would be adequate for the audiometric application. The first test was to determine how small steps had to be in order to be undetectable, basically another DLF investigation, though in this case the steps are smoothed. A base frequency of 2000 Hz was chosen, as research data indicate that this is a point of high sensitivity to small percent changes in frequency. The A channel pure tone was presented binaurally and single steps were taken by using the STEP pb. Step sizes of 1, 2, 4, and 8 were used corresponding to changes of .05%, .1%, .2%, and .4%, respectively. None of the listeners could detect steps of the two smallest sizes. DLF data predicts that .1% changes would be audible if there was no smoothing of the transitions as in these signals. However, 0.2% steps were barely audible in these listening tests at 2000 Hz and not audible at all to most listeners below 1000 Hz or above 6000 Hz. Thus it seems that loop dynamics are a factor and step sizes larger than the smallest that the system can provide can probably be used successfully for audiometric application.

Psychoacoustically, listening for smoothness in a frequency sweep is not directly related to discrimination of isolated step changes in frequency, especially at high sweep rates. This was verified by another set of listening tests which concentrated on sweeping rather than stepping. At the fastest sweep rate, 32 octaves per minute, step changes of 0.4% are inaudible throughout the range. Even changes of 0.8% are generally inaudible for this rapid sweep, except at frequencies around 3000 Hz. For the slower sweeps, the same phenomenon is apparent. Step

changes of 0.2% are small enough to ensure a smooth sounding sweep at 2 octaves per minute; however for a 1/2 octave per minute sweep, these listening tests indicate that 0.1% changes ought to be used. Thus it appears that resolution in the A channel is at lease twice as good as it need be for the application. Another clear conclusion is that the B channel, whose low resolution results in steps that are 0.4% changes minimum (see figure V-4), is not appropriate for audiometric sweeps.

Harmonic distortion, signal-to-noise ratio and sine wave output level are not related to the PLL characteristics, as only the quality of the VCG affects these characteristics. Figure VI-8 tabulates measured distortion of the primary channel and figure VI-9 graphically compares total harmonic distortion for the two channels of the prototype. Both voltage-controlled generators were chosen to meet project goals of distortion and signal-to-noise ratio; however the VCG in the primary channel is definitely superior. For the A channel, the output level did not measurably change throughout the frequency range, and the B channel level varied < 0.1 dB(constant temp.) A rough measurement of S/N ratio in the A channel gave 80 dB (about 70 dB in B channel). The A channel meets all project goals and, in conjunction with antilog-compensated phaselocked loops, accurate jitter-free frequency control is attained in both channels.

FIGURE VI-8

PRIMARY CHANNEL PURE TONE DISTORTION

FREQ	2ND HARM	3RD HARM	4TH HARM	5TH HARM	T.H.D.
75	-51.1	-60.9	-56.1	-61.2	-48.6
100	-51.6	-60.5	-56.2	-61.2	-49.4
125	-51.8	-60.0	-56.3	-61.2	-49.4
250	-52.5	-59.6	-56.2	-61.0	-50.1
500	-53.2	-59.9	-56.0	-60.7	-50.5
750	-54.1	-60.4	-55.9	-60.3	-51.1
1000	-54.9	-60.9	-56.1	-60.1	-51.2
1500	-57.3	-62.0	-56.0	-59.7	-52.2
2000	-60.2	-62.6	-56.0	-59.3	-52.5
3000	-61.8	-63.9	-55.9	-58.4	-52.5
4000	-63.7	-63.8	-55.8	-57.6	-52.5
6000	-63.5	-61.7	-55.8	-56.2	-51.7
8000	-61.9	-59.1	-55.8	-55.2	-50.2
10000	-60.4	-56.8	-55.8	-54.2	-47.8
12000	-59.7	-55.3	-56.2	-56.3	-46.1

Note: Measurements are in dB referred to the level of the fundamental and were made using a Hewlett-Packard Model 330B Distortion Analyzer (serial # 32046) for the THD levels, and a General Radio Model 1900A Wave Analyzer (serial # 649) for the individual harmonic levels.

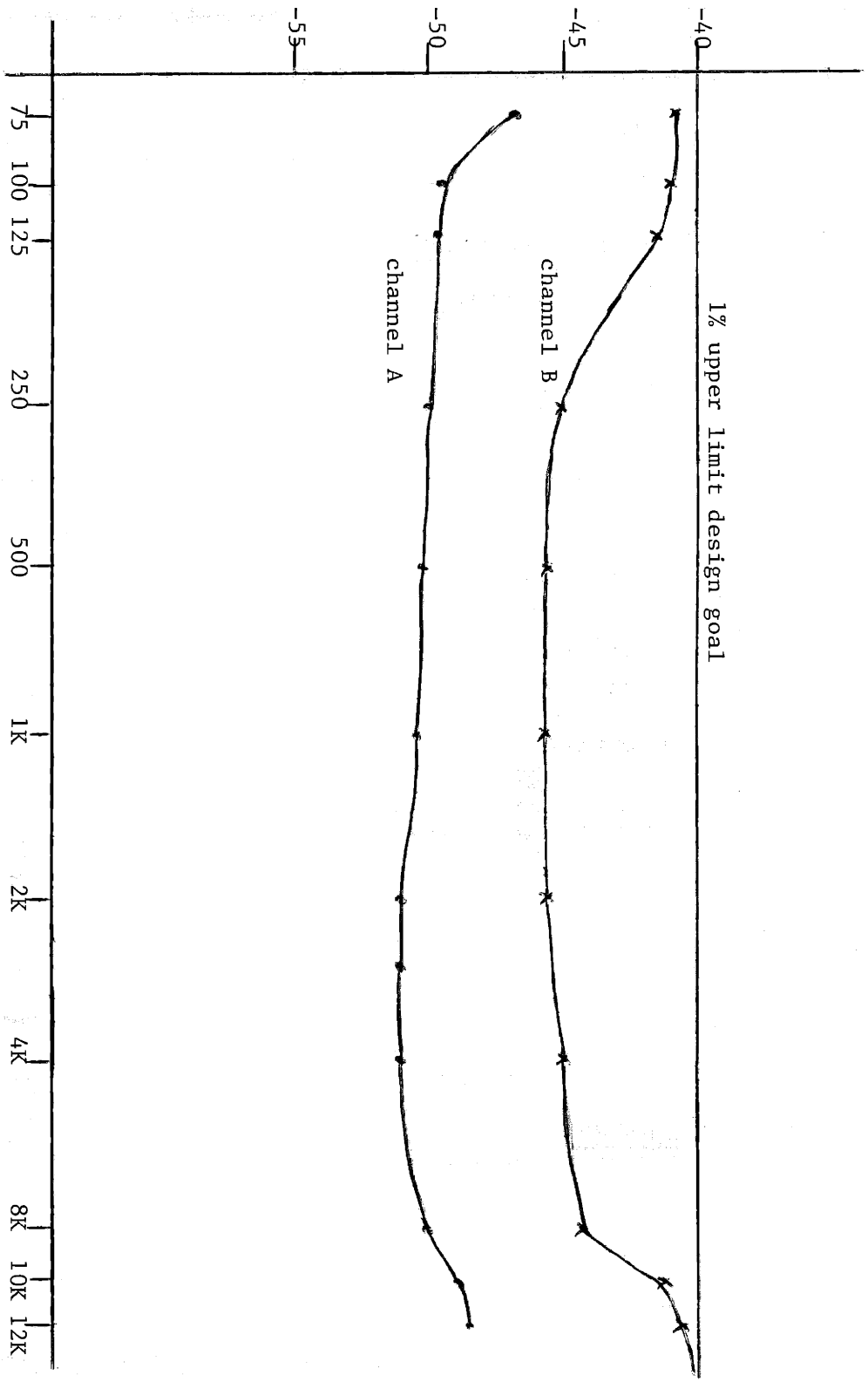

FIGURE VI-9 Graph of Total Harmonic Distortion Versus Frequency for Both Channels

VII. MASKING NOISE GENERATION

The final subsystem to be described for the audiometric signal generator produces masking noise. There are three major blocks within this system: the wideband noise generator with its automatically controlled spectral density; the two-pole voltage controlled lowpass Chebyshev filter; and the four-quadrant multiplier for translation of the lowpassed noise to a band around the test tone frequency. The narrowband masker is generated without the use of additional software and, as pointed out earlier, all control is derived from the A channel circuitry.

Wideband noise for subsequent lowpass filtering is created by clocked shift register logic which generates a pseudorandom binary sequence. The bit-train produced is maximally long, due to the form of feedback used [personal communication, J.M. Steele]. Figure VII-1 shows the block diagram of the noise source. Note that a single XOR gate is used to compare the 18th and 31st bits of the register. The important features of the wideband signal thus produced are the bandwidth and the density of spectral lines. Several authors have shown that the level of the power density function of this sort of pseudorandom signal exhibits a $[\sin(\pi f/f_c) / (\pi f/f_c)]^2$ dependence, where f_c is the clock frequency [Roberts and Davis, 1966; Cumming, 1967]. The bandwidth (-3 dB) is therefore approximately 0.32 f_c. There are $2^{31}-1$ unique shift register states resulting in a sequence which repeats after $(2^{31}-1)/f_c$ seconds. Spectral lines thus occur in the pseudorandom signal at intervals of $f_c/(2^{31}-1)$ Hz.

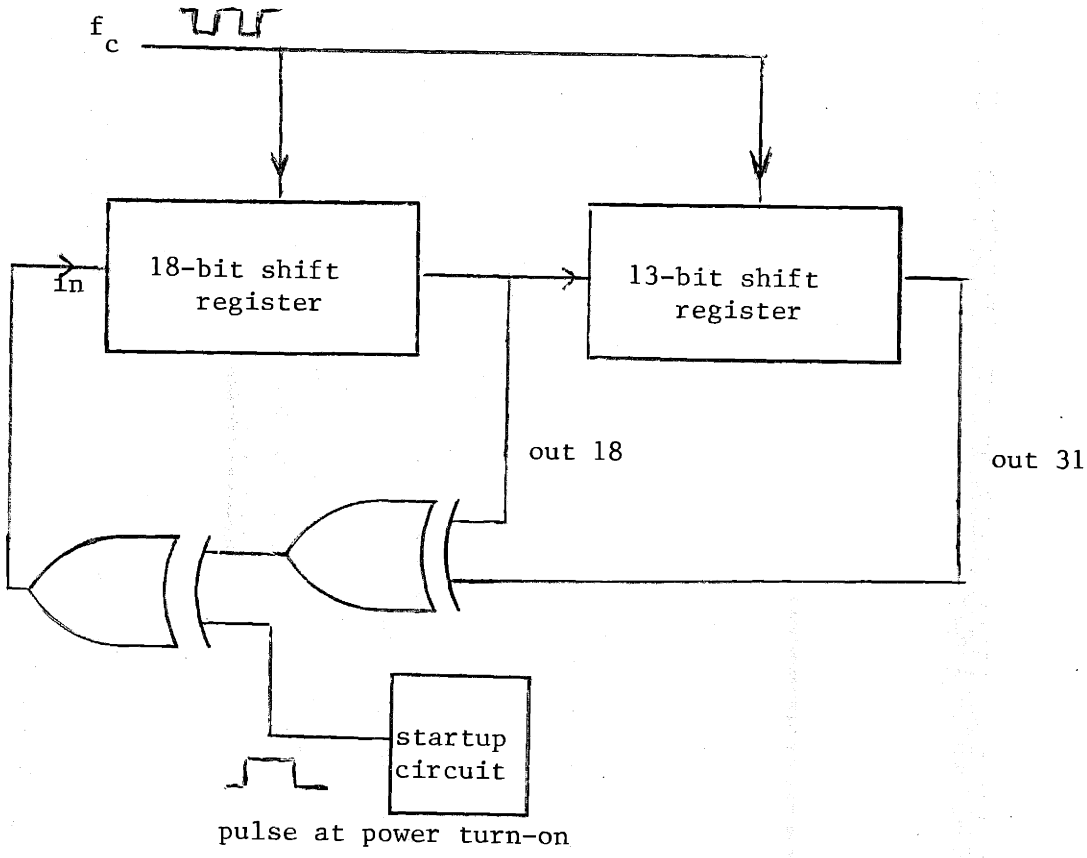

FIGURE VII-1 Block Diagram of Wideband Noise Generator

The only shift register state which is not followed by a different state when clocked occurs when the register contains all 0's. A practical design requires that some sort of antilatching arrangement or start-up procedure be employed. For the particular circuitry used in the prototype noise start-up is ensured by forcing a series of 1's into the register when the system is turned on (see schematic, figure AII-5).

In this design, the clock frequency driving the shift register is derived from the A channel by frequency multiplication (x192), performed with a phaselock technique. Figure VII-2 diagrams the clock frequency generation. The PLL incorporates within its VCG a high frequency tunable square wave source which is divided by digital logic for comparison with the reference square wave. The generator itself (see schematic, figure AII-6 for details) contains a voltage-controlled (2 biased PNPs) current source, a timing capacitor, a comparator, and a switch for discharging the capacitor. In many ways, this technique is similar to that employed for triangle generation in ICs that use nonlinear shaping for sine waves, with the major difference being that the capacitor's charging and discharging times are unequal. Because the current characteristics of a transistor are used for conversion of input voltage to charging current, the control function of this generator is highly nonlinear. Quantitative analysis of PLL performance with this specific nonlinearity was not attempted and the resulting clock signal has obvious jitter, especially when set to low frequencies. The effect of this jitter on the (filtered) masking signal is not apparent in the prototype as no idiosyncracies in the narrowband noise can be detected.

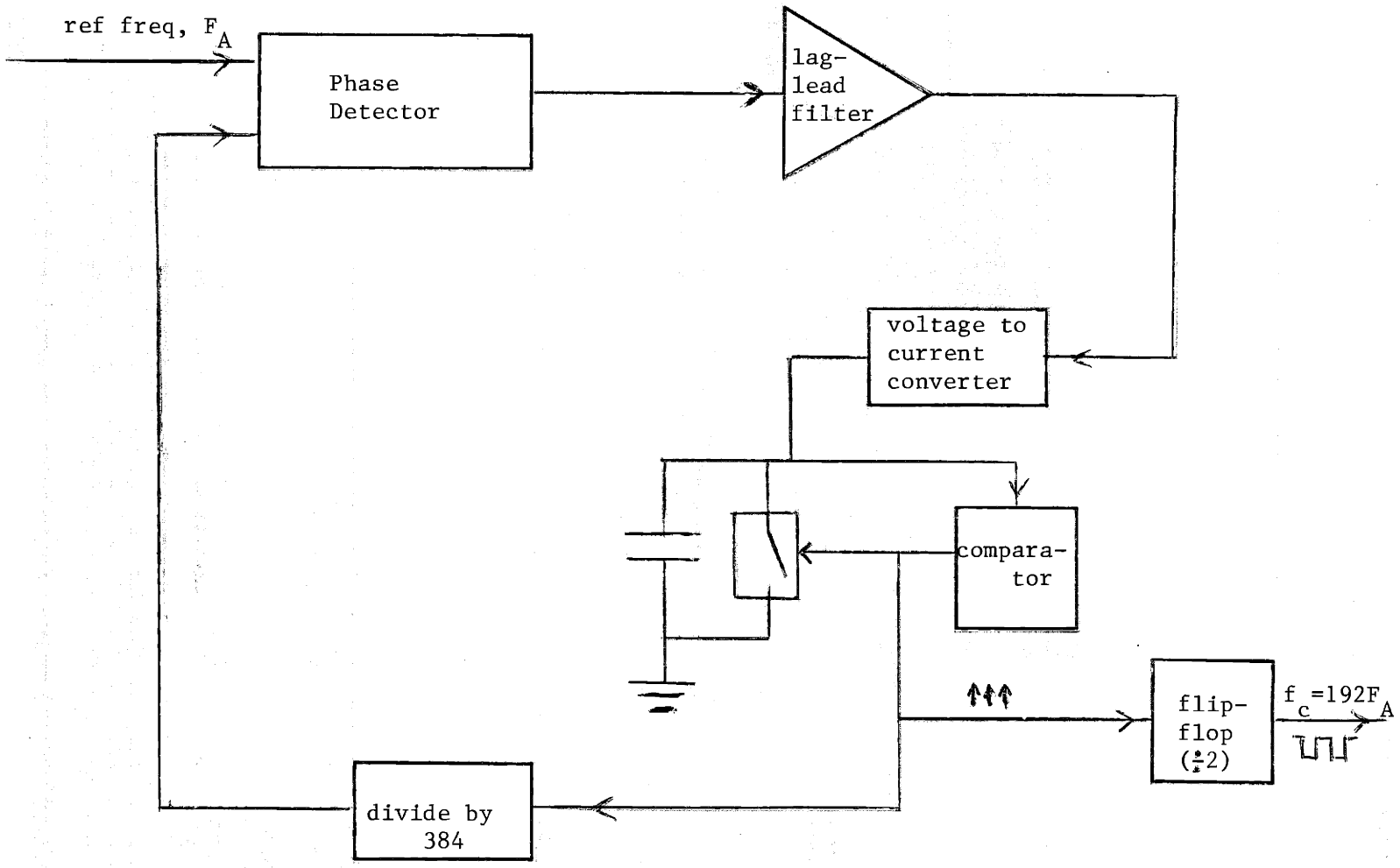

FIGURE VII-2 Block Diagram of Clock Frequency Generator

The clock frequency ranges from 14.4 KHz to 2.46 MHz. As the range is traversed the spacing of spectral lines varies from 6.71 microHertz (75 Hz masker) to 1.14 milliHertz (12.8 KHz masker). Even at the widest spacing, the ear cannot distinguish the pseudorandom signal from a genuinely random signal because the periodicity is so slow (about one cycle every fifteen minutes). Note also that the bandwidth of the pseudorandom noise varies from 4.61 KHz to 768 KHz over the tuning range.

The lowpass filtering scheme used in the prototype system shows performance slightly inferior to that desired for maskers centered below about 1500 Hz. Before discussion of the measured filter characteristics, though, the requirements for the lowpass filter implied by the standard, interpreted earlier and summarized in figure III-3, must be understood. Consider again the generation of the 1000 Hz masker. To satisfy the standard in terms of bandwidth, the lowpass filter must have its -3 dB point between 120 Hz and 159 Hz. (Recall that 0 dB is referenced to the average level in the passband.) Another clear constraint is that the ripple cannot exceed 3 dB. Finally, and most importantly, the rolloff desired is such that at 106 Hz in the masker's spectrum, the noise level is equal to or less than -40 dB. In terms of the lowpass spectrum at the multiplier input, components at 894 Hz and 1106 Hz both contribute to the resulting output energy at 106 Hz. Because the two signals are not correlated, the level of their summation can be calculated as $(a^2+b^2)^{\frac{1}{2}}$ where a and b are the levels of the two individual components.

The tunable filter section is a 2-pole Chebyshev type. Its transfer function can be expressed as $1/[(s^2/w_n^2)+(2\xi s/w_n)+1]$, where as usual, w_n

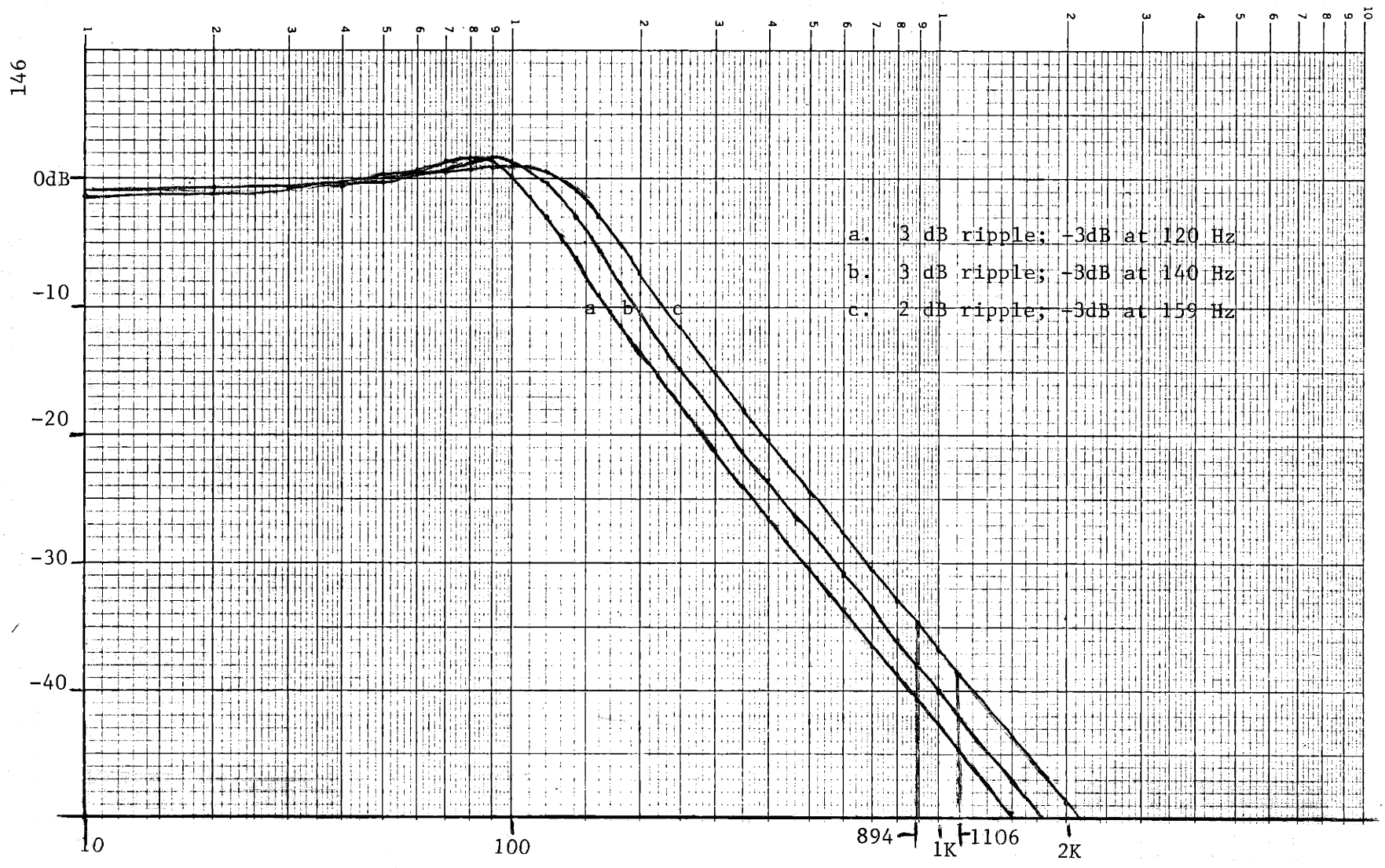

FIGURE VII-3 Two-pole Chebyshev Lowpass Magnitude Functions

and ξ are the natural frequency and damping factor. A common definition of Q for this type of function is $1/(2\xi)$. Examples of the two-pole lowpass magnitude function are presented in figure VII-3. Continuing to use the 1000 Hz masker as an example, three different filters are shown. Energy levels which are significant to meeting the design goal for low frequency rolloff are noted in the figure. Unfortunately, there is no flexibility in selecting the filter parameters, as calculation shows that a tunable 2-pole lowpass by itself cannot meet the desired specification, though only by a slight amount if optimized. Consider the Chebyshev design with 3 dB passband ripple and 120 Hz bandwidth, the best case (in terms of rolloff) for masking at 1000 Hz. Given these parameters, calculations yield a natural frequency of 93.11 Hz and a damping factor of .3832. The noise level at the desired stopband edge in the resulting narrowband spectrum produced after multiplication by the test tone, is the summation of energy at 894 Hz (-40.73 dB) and energy at 1106 Hz (-44.45 dB) in the lowpassed signal. Combining these two levels as described above, gives a level of -39.4 dB at 106 Hz in the masker, insufficient by only 0.6 dB. If a similar calculation is performed for the 2 dB ripple lowpass with the maximum bandwidth of 159 Hz (the worst case shown in the figure), the level at the stopband edge in the masker is in excess by about 6 dB.

Because the Chebyshev filter deviates from the design goal only very slightly under optimal conditions, and because this bit of extra energy at low frequencies does not alter the masker's effectiveness in any significant way, it was decided to use a Chebyshev two-pole design in the prototype. Better rolloff can be attained by using three poles or by

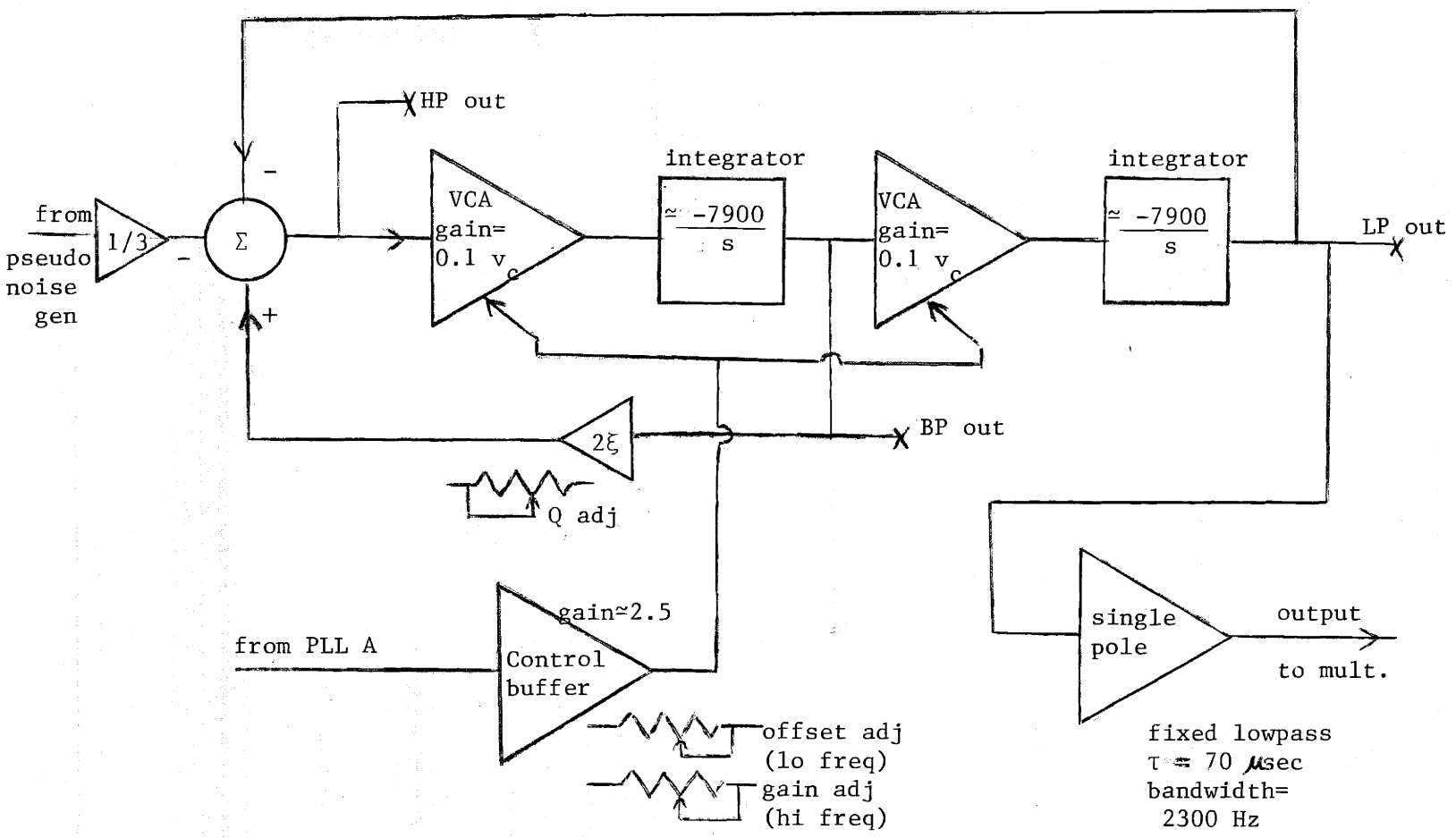

FIGURE VII-4 Block Diagram of Lowpass Filter

adding zeros to the tunable filter. A fixed single pole (bandwidth = 2300 Hz) in the filtering path helps meet the goal for rolloff in high frequency maskers. This filter provides little benefit for low frequency masking, but for masking pure tones above about 1000 Hz its effect is beneficial as the measured data indicates. A block diagram of the lowpass filter is shown in figure VII-4.

Measured values of lowpass filter ripple, bandwidth, and attenuation at the two frequencies (.894 f and 1.106 f) relevant to meeting the low end masker rolloff specification are tabulated in figure VII-5. A prediction of minimum stopband attenuation, based on the summation of the two lowpass noise components, is also shown in the figure, as are calculated values for the natural frequency and damping in the Chebyshev section. Nonideality in the voltage-controlled amplifiers used in tuning the filter and nonlinearity of the control signal derived from channel A contribute to the tracking errors. The passband ripple varies from 2.1 dB at 75 Hz to 3.1 dB at 12 KHz, and stopband attenuation is slightly less than 40 dB (38 dB worst case) for maskers below 1000 Hz. For low sensitivity and better tracking accuracy, the tunable filter employs a state-variable structure. In a state-variable design (see figure VII-4) there are two integrators and a summer. Lowpass, bandpass, and highpass outputs are all available. To tune the filter, voltage controlled amplifiers adjust the gain of the two integrators, simultaneously scaling both filter time constants. Tracking filter performance is calibrated by adjusting the offset and gain in a simple network that buffers the control signal from PLL A (see schematic, figure AII-7 for details). Under ideal conditions, the bandwidth varies linearly with control voltage and the Q remains

channel A freq, f (center freq of masker)	measured BW (-3dB) Hz	measured ripple dB	measured attenuation @.894f dB	@1.106f dB	predicted stopband atten in masker	calculated LP param's nat freq, Hz	ξ
75	9.2	2.1	39.5	43.3	38.0	7.287	.4364
125	15.3	2.4	39.9	43.6	38.4	12.02	.4174
250	30.1	2.5	40.3	44.0	38.8	23.59	.4114
500	60.0	2.7	40.6	44.4	39.1	46.82	.3997
1000	120	2.7	41.1	45.2	39.7	93.64	.3997
2000	241	2.8	42.5	44.2	40.3	187.7	.3941
4000	484	2.8	45.8	50.8	44.6	376.9	.3941
8000	975	3.0	50.8	56.1	49.7	756.5	.3832
10000	1220	3.0	52.0	57.3	50.9	946.6	.3832
12000	1482	3.1	53.7	59.4	52.7	1148	.3780

Note: Equipment used in making these measurements was 1) Data Precision Model 585 Frequency Counter (serial 1615); 2) Ballantine Model 320 RMS Voltmeter (serial 2886); and 3) Krohn-Hite Model 2000 Signal Generator (serial 142).

FIGURE VII-5 Lowpass Tracking Filter Performance

fixed. For low frequency maskers, however, offset in the VCAs become more significant and their mismatch is evident in the data as ξ increases for filter settings with narrower bandwidth. A better optimization of the prototype filter's performance can be attained, however due to theoretical limitations, even the most perfect trimming would not give characteristics that strictly meet the design goal.

The final narrowband signal for masking is degraded by the four-quadrant multiplier because of intermodulation distortion products. In the measured spectral data shown in figure VII-6, this "feedthrough" is evident at the second harmonic of the test tone. Fortunately at the second harmonic the level is still within the specified limits, however the artifact can be lessoned by the choice of a more accurate multiplier. In this prototype, the design goals are met for maskers centered at from 1200 Hz to 10 KHz. Much trimming is necessary to optimize the masking noise generator's performance. This is mostly due to offset adjustments in the VCAs and output multiplier. (Actually, the same IC type 4-quadrant multiplier is used for the tunable filter as well as to translate the lowpassed noise into a band around the pure tone.) Pretrimmed ICs are recommended.

Other than using higher quality components or a more complex tracking filter, there is a way in which a small modification in the design could improve low frequency performance. Currently, the clock frequency driving the wideband noise generator is 192 times the center frequency of the masking noise. With this high frequency, the wideband spectrum is essentially white over the region of interest. The $[(\sin x)/x]^2$ dependence

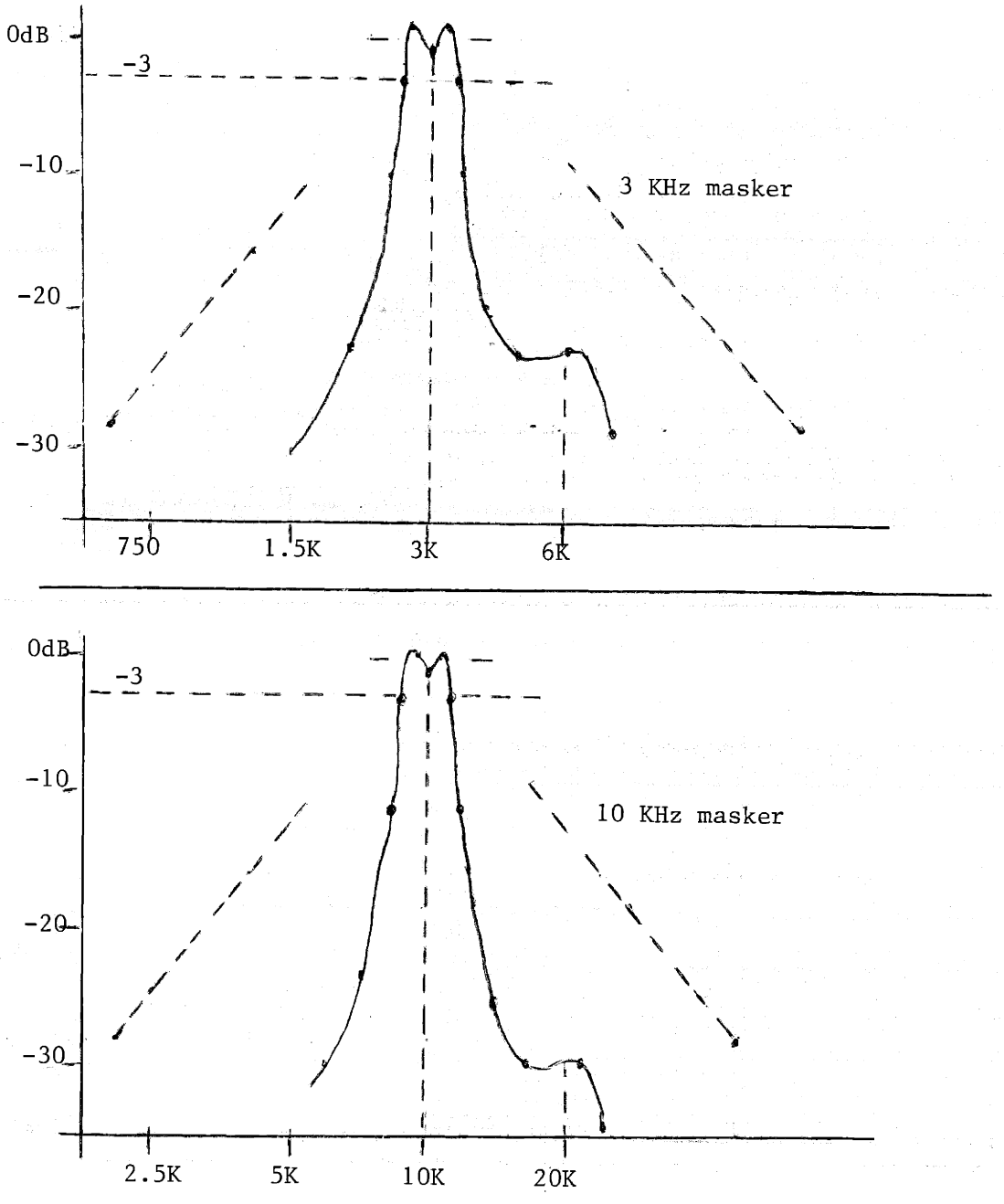

Note: Measurments referenced to -3dB points chosen to conform with known lowpass response. (see fig. VII-5). Measurement method judged to be accurate to ±3 dB, worse at lower levels; used General Radio Model 1900A Wave Analyzer (serial # 649). Dashed curve shows design goal for rolloff--

FIGURE VII-6 Measured Narrowband Noise Spectral Data

can be used to show that at the -3 dB point of the lowpass filter, wideband noise level is down by only 0.004 dB. If the frequency multiplication is such that the noise generator is clocked at only four times the pure tone frequency, attenuation near the lowpass -3 dB point would be only 0.03 dB, but in the region of interest for meeting the rolloff criterion (.894f,1.106f) the attenuation would be about 2 dB. This extra rolloff, which tracks perfectly with filter tuning, would greatly ease the difficulty in meeting the desired goal. In employing this modification, care must be taken to ensure that the clock frequency is not audible in the resultant masking signal. Inspection of the dependence of the pseudorandom noise level on frequency shows that there are nulls at frequencies $n\pi f_c$ and maximum at $3\pi nf_c/2$ where n = 1, 2, 3, etc. The height of the first maximum is -27 dB and with a two-pole tracking filter, its level would be further reduced another 70 dB; therefore this approach seems applicable. Careful measurements with this modification have not been made, but listening tests showed no undesirable effects.

In summary, the masking noise spectral shape is adequately controlled throughout its practical range for audiometric testing. The RMS output level is essentially constant. Examination of the narrowband waveforms with an oscilloscope indicate a high crest factor in the output noise signal. The crest factor is a measure relating the peak to the average in a noise waveform, thus signals with large crest factors (close to 20 dB in this case) are difficult to amplify and transduce. Inclusion of a soft limiter could probably reduce the large peaks by 10 dB without degrading masker quality. More precise and flexible digital processing techniques

must, for practical reasons, be reserved for use in future designs; however, the voltage-controlled analog filtering scheme described here can be tailored to exceed the requirements of masking signal generation for swept-frequency audiometry.

VIII. CONCLUSIONS

The system which has been described is a high quality signal generator designed for audiometric applications. As such it is subject to detailed standard specifications. In every way, the prototype system is adequate, though low frequency energy in the masking signal for tones below 1500 Hz is slightly in excess of the standard (2 dB worst case). It should be pointed out that this draft standard (May, 1978) is the first to include discussion of the spectral characteristics of narrowband masking noise, and interpretations vary. If the minimum acceptable stopband attenuation in the masker spectrum were decreased by 2 dB, or if the allowable passband ripple were increased by 1 dB, the prototype filtering system would not have to be modified to meet the specification. It is not clear to this writer whether or not the drafted standard on narrowband noise ought to be more or less strict, but further details are indeed necessary to eliminate the confusion in various interpretations. In terms of the present project, however, minor adjustment of either the standard or the prototype circuit would be necessary for strict adherence.

With the system architecture chosen, the use of higher quality voltage-controlled sine wave generators could decrease pure tone distortion and/or increase signal-to-noise ratio. A better VCG can be easily substituted in the phaselocked loop, but both types selected for this prototype development are adequate (Interdesign 1511, Exar 2206). Further investigation into nonlinear PLL compensation may provide an even simpler means of reducing jitter to acceptable levels; or perhaps with a more complex filter design, nonlinear compensation may not be necessary.

Some simple digital alterations can increase the flexibility of the software/hardware scheme for generation of the reference signal for phaselock. The frequency range can be extended in a number of ways. Slowing the master clock which drives the 18-bit counter would allow it to produce very low frequencies, although further degrading the resolution at high frequencies. By using postdivision instead, that is adding flip-flops after the counter while still using its load signal for synchronization, the low frequency limit can be extended without increasing microprocessor HALT time. Also, since the resolution is about twice as great as necessary (see chapter VI) the sweep timer can be slowed, or if desired the sweep rate could be increased. The calculation algorithm could then be easily modified to produce frequency steps twice as large as in the present design (i.e. 0.1% rather than 0.05%). The theoretical high frequency limit arises because of interrupt service timing. By using the pulse output of the counter directly as a phaselock reference, rather than dividing by 2 with a flip-flop, the upper limit can be doubled. The phase detectors employed can function adequately with a simple pulse frequency reference. Incorporating ranging by having selectable postdivision (high frequencies: no postdivision; low frequencies: postdivision by 4), would enable the entire audio range of frequencies to be generated. Designing the range change to be transient-free would probably be unnecessary as the present two-decade wide smooth sweep is sufficient for audiometric work.

Extending the square wave frequency range or increasing the sweep rate are not of importance for usual direct pure-tone testing. However, there are applications which could take advantage of the extensions, such

as accurate timing and low frequency modulation. Free-field testing with pure tones requires very elaborate acoustic environments, and for this reason signals that are modulated or are random are generally used. The purpose is to eliminate intensity maxima and minima in the acoustic space, which are due to the reflections from objects and surfaces. Noise signals would be ideal for this as they are incoherent, but they are difficult to measure and calibrate. Either frequency modulation or amplitude modulation of the test tone in free-field reduces the standing wave pattern. Frequency modulation ($<10\%$) by a 5 Hz sine wave or triangle wave has been used in some audiometer designs. A newer idea is to use two modulation signals rather than only one. For instance, one manufacturer (Dyn-Aura, San Diego, CA) modulates the test tone with the sum of two lower frequencies selected such that there can be no harmonically related signal components.

Precise acoustic results obtained with various modulations of a tone are complex and beyond the scope of these remarks. However, many different sorts of frequency modulations for testing and research could be programmed and produced by the audiometric system described. Furthermore, the addition of an analog switch would allow the use of the output multiplier as either an amplitude modulator (2-quadrant) or "balanced" modulator (4-quadrant). A low fixed frequency for amplitude modulation could be produced by the secondary channel while the software frequency modulates the primary channel's tone.

The system design project undertaken has been very successful. The characteristics and minor limitations of all subsystems have been

described, and theoretical constraints on several different hypothetical system architectures have been reviewed. New electronic techniques can greatly change audiometric practice, as did the first use of electricity. Though some computerized systems already exist, none commercially available today offers full-range automatic swept pure-tone testing. Nor are there any systems in use that can generate a variety of modulated signals for free field use. The microprocessor was first marketed less than ten years ago, and commercial use of it is rapidly increasing. A microprocessor-based audiometric system can provide many features of great utility to the clinician. A brief list includes:

1. data record keeping and updating;
2. record searches for studies involving large numbers of subjects;
3. self-calibration of frequency and level;
4. calculation of norms for diagnostic or comparative purposes;
5. complex paradigm implementation;
6. teaching students by the use of software which emulates patient responses;
7. automatic presentation of the proper masker level based on previous results on the non-test ear;
8. interfacing with other clinical instrumentation, e.g. evoked response systems.

It is hoped that this project can act as an impetus to the further application of new technology to the old problem of hearing measurement.

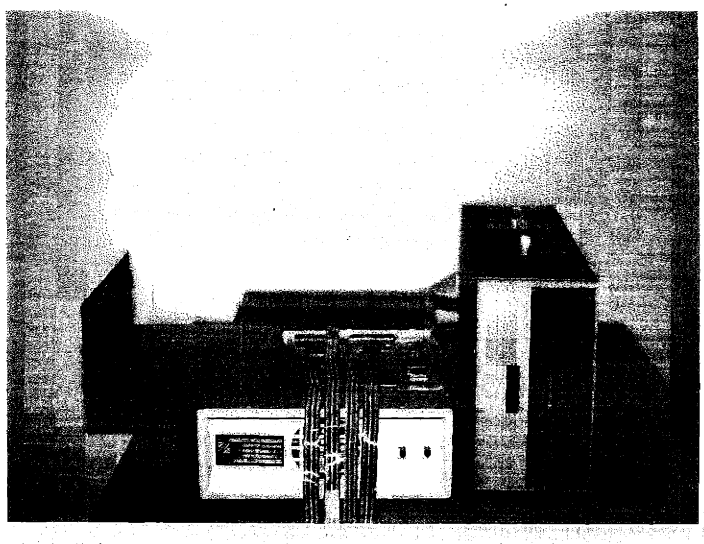

Microcomputer System

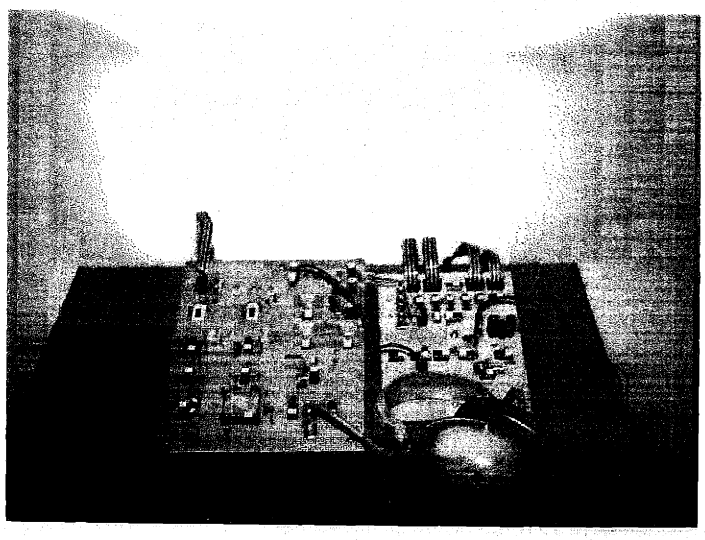

Additional Hardware for Signal Generation

FIGURE VIII-1 Photographs of Completed Prototype
(Mark C. Annis, photographer)

FIGURE VIII-2 Summary of Overall Prototype Performance

A. Primary Pure Tone

1. Frequency range: 75 Hz - 12.8 KHz
2. Frequency accuracy: better than 0.1% throughout range
3. Smoothly sweepable through entire range
4. Sweep speeds: up or down at ½, 1, 2 octaves/minute ±0.1%
5. Fixed level: varies less than 0.1 dB throughout range
6. Signal to noise ratio: ≥80 dB at all frequencies
7. Total Harmonic Distortion: < ½% (-46 dB) throughout range
8. Second Harmonic Distortion: <.3% (-50 dB) throughout range
9. Third Harmonic Distortion: <.2% (-54 dB) throughout range

B. Secondary Pure Tone

1. Frequency range: 75 Hz - 12.8 KHz
2. Frequency accuracy: better than 1.5% throughout range
3. Nonsmoothly sweepable through entire range
4. Sweep speeds: up or down at ½, 1, 2 octaves/minute ±0.1%
5. Fixed level: varies less than 1 dB with frequency and temperature
6. Signal to noise ratio: ≥70 dB at all frequencies
7. Total Harmonic Distortion: < 1% (-40 dB) throughout range

(Performance summary continued, figure VIII-2)

C. Masking Noise Generator

1. Nominal bandwidth of narrowband noise (re ANSI interpretation fig. III-3):

   0.88 F_A to 1.12 F_A, where F_A if primary frequency; primary freq arithmetically centered (approx 0.35 octave wide)

2. Variation of bandwidth from nominal:

   less than 2% from 125 Hz - 8 KHz;
   less than 3% throughout range

3. Smoothly sweepable to accompany primary pure tone throughout range

4. Passband ripple: 2.1 - 3.1 dB within 75 Hz - 12.8 KHz range

5. Rolloff: better than 12 dB per octave to noise floor

6. Noise floor: ≤ -38 dB for all maskers

7. Fixed level: varies less than ± 2 dB throughout range

Note: All masking noise data presented is consistent with terms summarized in figure III-3. Masker level, and S/N ratios mentioned here are estimates.

APPENDIX I PROGRAM DOCUMENTATION

Following is the assembly level program listing for the software used in this project. It is suggested that reference be made to the Zilog Z-80 Assembly Language Programming Manual for a complete explanation of instructions. Adequate comments and simple mnemonics should aid in understanding the program details.

FIG. AI-1: ASSEMBLY LEVEL PROGRAM LISTING


```
LOC     STMT    SOURCE                  ;COMMENTS

        1       ;THIS IS THE UPDATE OF JULY 15, 1978
        2
        3
        4       ;HOUSEKEEPING FIRST
2000    5       ORG     2000H
2000    6   BEGIN       DI              ;INTERRUPT SETUPS FOLLOW
2001    7       IM      2
2003    8       LD      A,13H
2005    9       LD      I,A
2007   10       LD      HL,ISERVT
200A   11       LD      (1300H),HL
200D   12       LD      HL,ISERVB
2010   13       LD      (1304H),HL
2013   14       LD      HL,ISERVA
2016   15       LD      (1308H),HL
2019   16       LD      HL,PBSERV
201C   17       LD      (130AH),HL
       18
201F   19       LD      HL,10C0H
2022   20       LD      SP,HL           ;SET UP STACK POINTER
       21
       22       ;PIO SETUPS FOLLOW
2023   23       LD      HL,CON1A        ;ENAB RST PB ONLY
2026   24       LD      B,5
2028   25       LD      C,PIO1AC        ;PIO1A: MSD=OPMODE
202A   26       OTIR                    ;A3,2,1,0=PBS
202C   27       LD      A,00
202E   28       OUT     (PIO1AD),A      ;SET INITIAL MODE TO 'WAIT'
2030   29       LD      HL,CON0A
2033   30       LD      B,5
2035   31       LD      C,PIO0AC        ;PIO0A: MSD=SPARE,A3=SYNCA
2037   32       OTIR                    ;A1/A0=CTRA MSBITS
2039   33       LD      A,0FH
203B   34       OUT     (PIO0AD),A
203D   35       LD      HL,CON0B
2040   36       LD      B,4
2042   37       LD      C,PIO0BC
2044   38       OTIR                    ;PIO0B: CTR A MID DIGITS
2046   39       LD      A,0D9H
2048   40       OUT     (PIO0BD),A      ;SET FREQA TO 1K
204A   41       LD      HL,CON1B
204D   42       LD      B,4
204F   43       LD      C,PIO1BC
2051   44       OTIR                    ;PIO1B: CTRA LS DIGITS
2053   45       LD      A,9AH
2055   46       OUT     (PIO1BD),A
       47
```

```
                48      ;CTC SETUPS FOLLOW
2057            49      LD      C,CTC0
2059            50      LD      A,0
205B            51      OUT     (C),A           ;CTC INT VECTOR
205D            52      LD      A,00110111B
205F            53      OUT     (C),A           ;CTC0 TIMER WAITING FOR TC
2061            54      INC     C
2062            55      LD      A,01010111B
2064            56      OUT     (C),A
2066            57      LD      A,154
2068            58      OUT     (C),A           ;CTC1 IS CTRB,  NO INT
206A            59      INC     C               ;CTC2 IS SQB POSTDIVIDER
206B            60      LD      A,01010111B
206D            61      OUT     (C),A           ;CTC2 INT DISAB
206F            62      LD      A,4
2071            63      OUT     (C),A           ;SET FREQB TO 1K
                64
2073            65      EI
2074            66      LD      HL,28
2077            67      LD      (LLOUT),HL      ;SETS UP MSG LENGTH OUT
207A            68      LD      HL,5
207D            69      LD      (LLIN),HL       ;SETS UP MSG LENGTH IN
2080            70      LD      IY,TTYOUT-1
2084            71      CALL    0BE8H           ;WRITES STARTUP MESSAGE
2087            72      LD      IY,TTYIN-1
208B            73      CALL    0BE8H           ;READS IN 4 CHARACTERS
                74
                75
                76      ;ROUTINE ASSOCIATES 4 INPUT CHARS W TABLES
                77      ;FREQA, FREQB, SWEEP MODE, OPMODE
208E            78      LD      A,4
2090            79      LD      (STAT),A        ;(STAT) HOLDS CHAR COUNTER
2093            80      SCF                     ;CARRY SET (GET 2BYTES)
                81                              ;FOR OPMODE & SWEEP MODE
2094            82      CCF                     ;CARRY CLEAR (GET 3BYTES)
                83                              ;FOR FREQA & FREQB
2095            84      LD      IY,TABLES
2099            85      LD      IX,AINPUT
209D            86      LD      DE,TCA
20A0            87  LOOP        LD      BC,19
20A3            88      PUSH    IY              ;PUSH CURRENT TABLE ADDR
20A5            89      LD      A,(IX+0)        ;LOAD CHARACTER
20A8            90      LD      HL,ASCII$+18
20AB            91      CPDR
20AD            92      POP     HL
20AE            93      JR      C,ONLY2
20B0            94      ADD     HL,BC
20B1            95      LDI                     ;FIRST LOAD OF THREE
20B3            96      LD      BC,18
20B6            97  ONLY2       ADD     HL,BC
20B7            98      LDI                     ;2ND LD OF THREE (1 OF 2)
20B9            99      LD      BC,18
```

```
20BC      100     ADD   HL,BC
20BD      101     LDI                   ;FINAL LOAD
20BF      102     INC   IX              ;NEXT CHARACTER SET UP
20C1      103     LD    HL,STAT
20C4      104     DEC   (HL)
20C5      105     JR    Z,PATCH1        ;JUMP OUT IF THRU
20C7      106     LD    A,2
20C9      107     CPI
20CB      108     JP    M,IYSAME        ;IYSAME FOR FREQB
20CE      109     LD    BC,38
20D1      110     ADD   IY,BC
20D3      111     DEC   HL              ;BECAUSE CPI INCREMENTS HL
20D4      112     CPI
20D6      113     SCF
20D7      114     JR    NZ,LOOP         ;JUMP BACK FOR 4TH CHAR
20D9      115     LD    BC,19
20DC      116     ADD   IY,BC
20DE      117     SCF
20DF      118     JR    LOOP            ;JUMP BACK FOR 3RD CHAR
20E1      119 IYSAME    SCF
20E2      120     CCF
20E3      121     JR    LOOP            ;JUMP BACK FOR 2ND CHAR
          122
          123
          124     ;THREE 'PATCH' ROUTINES FOLLOW
          125
          126     ;PATCH1 FORCES MODE 1(A) IF FREQA=FREQB
          127     ;AND MODE 6(F) OR 7(G) WAS CHOSEN
          128     ;NOTE: LOWER 4 BITS OF (MODE) AND (STAT)
          129     ;ARE FOR STATUS PURPOSES
20E5      130 PATCH1    LD    IX,NCTR
20E9      131     LD    A,00
20EB      132     LD    (STAT),A        ;INIT STAT WORD
20EE      133     LD    A,(MODE)        ;MODE=IX+2, STAT=IX+4
20F1      134     BIT   3,A             ;IS THIS A PATCHABLE MODE?
20F3      135     JR    Z,PATCH2
20F5      136     LD    A,(AINPUT)
20F8      137     LD    B,A
20F9      138     LD    A,(AINPUT+1)
20FC      139     SUB   B               ;DOES FREQA=FREQB?
20FD      140     JR    NZ,PATCH2
20FF      141     LD    A,(MODE)
2102      142     AND   0FH             ;FIXUP
2104      143     ADD   A,50H
2106      144     LD    (MODE),A
          145
          146     ;PATCH2:
          147     ;SETS UP FOR ASWEEP OR BSWEEP (IY=TCA OR TCB)
2109      148 PATCH2    LD    HL,MODE
210C      149     BIT   2,(HL)          ;WILL ASWEEP OR BSWEEP?
210E      150     JR    Z,SETBSW
2110      151     LD    IY,TCA
```

```
2114      152     LD    A,(AINPUT)
2117      153     CP    30H           ;DONT SWEEP DOWN FROM 75HZ
2119      154     JR    NZ,PATCH3
211B      155     SET   0,(HL)
211D      156     JR    PATCH3
211F      157 SETBSW    LD    IY,TCB
2123      158     LD    A,(AINPUT+1)
2126      159     CP    30H           ;DONT SWEEP DOWN FROM 75HZ
2128      160     JR    NZ,PATCH3
212A      161     SET   0,(HL)
          162
          163     ;PATCH3 LOADS CTC0 TIME CONSTANT
          164     ;STANDARD=21MS,FAST=5.3MS(*FOR MODEA CHAR=D,I)
212C      165 PATCH3    LD    A,(AINPUT+2)
212F      166     LD    C,CTC0
2131      167     CP    44H
2133      168     JR    NZ,COMP49
2135      169     LD    B,51
2137      170     JR    OUTT
2139      171 COMP49    CP    49H
213B      172     JR    NZ,OUTT-2
213D      173     LD    B,51
213F      174     JR    OUTT
2141      175     LD    B,203
2143      176 OUTT      OUT   (C),B
          177
          178
          179     ;NOW SET UP PRIME REGS
2145      180 SETCTR    EXX
2146      181     LD    HL,00         ;HL'=STEPS FROM 'BEGIN'
2149      182     LD    B,(IX+1)      ;B' =INTS SINCE 'AGAIN'
214C      183     LD    C,CTC0        ;C', D' SET FOR EASY KILL
214E      184     LD    D,00110001B   ;OF CTC0 INT CAPABILITY
2150      185     EXX
          186
          187
          188     ;ROUTINES INITS LOGIC AND START SYS PLAYING
2151      189     LD    A,01010101B
2153      190     OUT   (CTC1),A
2155      191     OUT   (CTC2),A      ;SQB GEN WAITS FOR NEW TCS
2157      192     LD    HL,(TCB)
215A      193     LD    A,(RNGB)
215D      194     LD    C,A
215E      195     CALL  PREPB         ;RETURNS CTC2 TC, CTC1 TC
2161      196     LD    A,E
2162      197     OUT   (CTC2),A      ;PROG SQB POSTDIVIDER
2164      198     LD    A,H
2165      199     OUT   (CTC1),A      ;PROG CTRB   SQB RUNS
          200
2167      201     LD    HL,(TCA)
216A      202     LD    A,(RNGA)
216D      203     LD    C,A
```

```
216E    204     CALL   PREPA          ;RETURNS PIO WRDS 0A,0B,1B
2171    205     LD     A,E
2172    206     OUT    (PIO0AD),A
2174    207     LD     A,H
2175    208     OUT    (PIO0BD),A
2177    209     LD     A,L
2178    210     OUT    (PIO1BD),A     ;SQ A RUNS
        211
217A    212     LD     A,(MODE)
217D    213     OUT    (PIO1AD),A     ;SYS IS NOW PLAYING
        214
        215
        216     ;'AGAIN' IS REENTRY POINT AFTER EACH STEP
        217     ;CHECK AND SET UP FOR STEPPING OR SWEEPING
        218     ;'GO' AFTER CRITERIA IS MET
217F    219 AGAIN      POP    HL       ;BALANCE STACK
2180    220     LD     A,10110111B
2182    221     OUT    (PIO1AC),A     ;PIO1A WAITING FOR MASK
2184    222     IN     A,(PIO1AD)
2186    223     BIT    2,A            ;CHECK SWEEP PB
2188    224     JR     Z,STEPST       ;NZ:SET UP FOR SWEEPING
218A    225     LD     A,11110110B
218C    226     OUT    (PIO1AC),A     ;MONITOR RESET AND CHDIR
218E    227     LD     A,10110001B
2190    228     OUT    (CTC0),A       ;ENABLE CTC0 INT (SWEEP)
2192    229     JR     WAIT
        230
2194    231 STEPST     LD     A,11110000B
2196    232     OUT    (PIO1AC),A     ;ENABLE ALL 4 PBS
        233                           ;STEP OR EXIT TO SWEEP
        234
2198    235 WAIT       BIT    3,(IX+4)
219C    236     JR     Z,WAIT         ;BIT3=1 WHEN CRITERIA MET
        237
        238
219E    239 GO         LD     A,10110111B
21A0    240     OUT    (PIO1AC),A
21A2    241     LD     A,11110110B
21A4    242     OUT    (PIO1AC),A     ;NOW MONITOR RESET & CHDIR
21A6    243     RES    3,(IX+4)
        244
        245     ;DECIDE ON CURRENT STEP DIRECTION
21AA    246     SRL    (IX+4)         ;BIT0 OF (IX+4):CURRENT DIR
21AE    247     RRC    (IX+2)         ;BIT0 OF (IX+2):STORED DIR
21B2    248     RLC    (IX+2)         ;(IX+2) CHANGED BY CHDIR PB
21B6    249     RL     (IX+4)         ;1=UP  0=DOWN
        250
21BA    251     LD     B,(IX+0)       ;(IX+0) HOLDS STEP SIZE
21BD    252     LD     C,(IY+2)       ;LOAD 3 BYTE TC: CHL
21C0    253     LD     H,(IY+1)
21C3    254     LD     L,(IY+0)
        255
```

```
                256     ;CHECK IF TC IS AT UPPER OR LOWER LIMITS
                257     ;75HZ TO 12.8KHZ
21C6            258     LD      A,C
21C7            259     CP      20H             ;C=20H FOR LOWER LIM
21C9            260     JR      NZ,LIMCHT
21CB            261     SET     0,(IX+2)
21CF            262     SET     0,(IX+4)        ;CHANGE DIRECTION
21D3            263     JR      XMULT
21D5            264 LIMCHT    CP    0           ;C=00 AND H=2F, UPPER LIM
21D7            265     JR      NZ,XMULT
21D9            266     LD      A,H
21DA            267     CP      2FH
21DC            268     JR      NZ,XMULT
21DE            269     RES     0,(IX+2)
21E2            270     RES     0,(IX+4)        ;CHANGE DIRECTION
                271
                272     ;THIS IS THE REPETITIVE MULT ROUTINE, B TIMES
21E6            273 XMULT     LD      D,C       ;DE WILL =  TC DIV BY 2048
21E7            274     LD      E,H
21E8            275     SRL     D
21EA            276     RR      E
21EC            277     SRL     D
21EE            278     RR      E
21F0            279     SRL     D
21F2            280     RR      E
21F4            281     EXX
21F5            282     INC     HL
21F6            283     EXX
21F7            284     BIT     0,(IX+4)
21FB            285     JR      NZ,SUB
21FD            286     ADC     HL,DE           ;ADD FOR STEP DOWN
21FF            287     JR      NC,CHKB
2201            288     INC     C
2202            289     JR      CHKB
2204            290 SUB       SBC     HL,DE     ;SUB FOR STEP UP
2206            291     JR      NC,CHKB
2208            292     DEC     C
2209            293 CHKB      DJNZ,XMULT
                294
220B            295     LD      (IY+0),L
220E            296     LD      (IY+1),H
2211            297     LD      (IY+2),C        ;UPDATE AFTER STEP
                298
2214            299     LD      A,10110111B
2216            300     OUT     (PIO1AC),A
2218            301     LD      A,11110111B
221A            302     OUT     (PIO1AC),A      ;MONITOR RESET PB ONLY
                303
221C            304     BIT     2,(IX+2)        ;UPDATE A OSC OR B OSC?
2220            305     JR      NZ,UPDATA       ;NZ: ASWEEP, Z:BSWEEP
2222            306     CALL    PREPB
2225            307     LD      D,01010101B     ;SET UP FOR SYNCB INT KILL
```

```
2227      308     LD     A,D
2228      309     OUT    (CTC1),A       ;CTC1 WAITING FOR NEW TC
222A      310     LD     A,11010001B
222C      311     LD     C,CTC2
222E      312     OUT    (C),A          ;CTC2 INT NOW ACTIVE
2230      313     HALT                  ;JUMPS BACK TO 'AGAIN'
          314
2231      315 UPDATA  CALL PREPA
2234      316     LD     D,3            ;SET UP FOR SYNC A INT KILL
2236      317     LD     A,83H
2238      318     LD     C,PIO0AC
223A      319     OUT    (C),A          ;SYNCA INT NOW ACTIVE
223C      320     HALT                  ;JUMPS BACK TO 'AGAIN'
          321
          322
          323
          324     ;THIS ROUTINE CONVERTS 3 BYTE TCA (C,H,L)
          325     ;FOR PIO0A, PIO0B, PIO1B  (E,H,L)
223D      326 PREPA   LD     B,4
223F      327 SHIFA   SRL    C
2241      328     RR     H
2243      329     RR     L
2245      330     DJNZ   SHIFA          ;SHIFT TCA 4 PLACES RIGHT
2247      331     LD     A,L            ;COMPLIMENT SHIFTED TCA
2248      332     CPL
2249      333     LD     L,A
224A      334     LD     A,H
224B      335     CPL
224C      336     LD     H,A
224D      337     LD     A,C
224E      338     CPL
224F      339     LD     C,A
2250      340     CCF
2251      341     LD     DE,00
2254      342     ADC    HL,DE
2256      343     LD     E,A
2257      344     RET    NC             ;ROUND APPROPRIATELY
2258      345     INC    E
2259      346     RET
          347
          348     ;THIS ROUTINE CONVERTS 3 BYTE TCB (C,H,L)
          349     ;FOR CTC1 (H) AND CTC2 (E)
225A      350 PREPB   LD     B,1
225C      351     LD     A,C
225D      352 COMPZ   CP     0
225F      353     JR     Z,SHIFED       ;SHIFT CHL RIGHT TILL C=00
2261      354     SRL    A
2263      355     RR     H
2265      356     RR     L
2267      357     SLA    B              ;B=1 FOR NO SHIFT NECESSARY
2269      358     JR     COMPZ          ;B=64 FOR 6 PLACE SHIFT
226B      359 SHIFED  BIT    7,L        ;ROUND APPROPRIATELY
```

```
226D      360     JR     Z,BDONE
226F      361     INC    H
2270      362     CP     H
2271      363     JR     NZ,BDONE
2273      364     LD     H,80H
2275      365     SLA    B
2277      366 BDONE     LD     E,B
2278      367     RET
          368
          369
          370     ;CTC0 TIMER INT SERVICE ROUTINE
          371     ;WORKS WITH BCDEHL' ONLY
2279      372 ISERVT    EXX
227A      373     DJNZ   CONT           ;CHECK B' REG FOR NI COUNT
227C      374     SET    3,(IX+4)       ;IF B'=0, THEN STEP NOW
2280      375     LD     B,(IX+1)       ;AND B' RELOADED
2283      376     OUT    (C),D          ;DISABLE INT
2285      377 CONT      EXX            ;UNTIL LOOP BACK AGAIN
2286      378     EI
2287      379     RETI
          380
          381     ;SYNCA  SERVICE ROUTINE
2289      382 ISERVA    OUT    (C),D   ;KILLS SYNCA INTS
228B      383     LD     C,PIOOAD       ;OUTPUT 3 BYTES
228D      384     OUT    (C),E
228F      385     LD     C,PIOOBD
2291      386     OUT    (C),H
2293      387     LD     C,PIO1BD
2295      388     OUT    (C),L
2297      389     LD     HL,AGAIN
229A      390     PUSH   HL             ;FORCE JUMP TO 'AGAIN'
229B      391     EI
229C      392     RETI
          393
          394     ;CTC2 INT SERVICE ROUTINE
229E      395 ISERVB    OUT    (C),D   ;CTC1&2 WAIT FOR NEW TCS
22A0      396 CNTIS?    IN     B,(C)   ;WAIT TILL CTC2=1
22A2      397     DJNZ   CNTIS?
22A4      398     OUT    (C),E          ;NEW TC FOR CTC2
22A6      399     DEC    C
22A7      400     OUT    (C),H          ;NEW TC FOR CTC1
22A9      401     LD     HL,AGAIN
22AC      402     PUSH   HL             ;FORCE JUMP TO 'AGAIN'
22AD      403     EI
22AE      404     RETI
          405
          406     ;PB INT SERVICE ROUTINE, WORKS WITH AF' ONLY
22B0      407 PBSERV    EX     AF,AF'
22B1      408     IN     A,(PIO1AD)
22B3      409     BIT    3,A
22B5      410     JR     Z,CHDIR?
22B7      411     LD     HL,BEGIN
```

```
22BA     412     PUSH  HL              ;RESET FORCES JP TO BEGIN
22BB     413     RETI
22BD     414 CHDIR?   BIT   0,A
22BF     415     JR    Z,STEP
22C1     416     RR    (IX+2)
22C5     417     CCF                   ;CHDIR PB: CPL STORED DIR
22C6     418     RL    (IX+2)
22CA     419     JR    BACKI
22CC     420 STEP      SET   3,(IX+4)
         421                           ;STEP NOW (STEPPING
         422                           ;OR EXIT TO SWEEP)
22D0     423 BACKI     EX    AF,AF'
22D1     424     EI
22D2     425     RETI
         426
         427
         428     ;TTY SERVICE PARAMETERS
22D4     429 TTYOUT    DEFB      10H
22D5     430           DEFW      ATEXT
22D7     431 LLOUT     DEFS      2
22D9     432           DEFW      00
22DB     433           DEFW      00
22DD     434           DEFS      3
22E0     435 ATEXT     DEFM      '4 CHARACTERS: 0-9,A-I ONLY'
22FB     436           DEFB      0DH
22FC     437 TTYIN     DEFB      0CH
22FD     438           DEFW      AINPUT
22FF     439 LLIN      DEFS      2
2301     440           DEFW      00
2303     441           DEFW      00
2305     442           DEFS      3
         443
         444
         445     ;PIO INITIAL SETUP PARAMETERS
2308     446 CON0A     DEFB  11001111B     ;BIT MODE
2309     447     DEFB  00001000B     ;SYNCA
230A     448     DEFB  08H           ;INT VECTOR PIO0A
230B     449     DEFB  00110111B     ;INT DISAB
230C     450     DEFB  11110111B
         451
230D     452 CON0B     DEFB  11001111B     ;BIT MODE
230E     453     DEFB  0             ;NO INPUTS
230F     454     DEFB  00010111B     ;NO INT
2310     455     DEFB  11111111B
         456
2311     457 CON1A     DEFB  11001111B     ;BIT MODE
2312     458     DEFB  00001111B     ;PBS
2313     459     DEFB  0AH           ;INT VECTOR  PIO1A
2314     460     DEFB  10110111B     ;INT CNTRL:RESET ONLY
2315     461     DEFB  11110111B
         462
2316     463 CON1B     DEFB  11001111B     ;BIT MODE
```

```
2317      464     DEFB  0              ;NO INPUTS
2318      465     DEFB  00010111B      ;NO INT
2319      466     DEFB  11111111B
          467
          468     ;16 BYTES (PLUS STACK) OF RAM NECESSARY
231A      469 AINPUT  DEFS  5
231F      470 TCA     DEFS  2
2321      471 RNGA    DEFS  1
2322      472 TCB     DEFS  2
2324      473 RNGB    DEFS  1
2325      474 NCTR    DEFS  1
2326      475 NICTR   DEFS  1
2327      476 MODE    DEFS  1
2328      477         DEFS  1
2329      478 STAT    DEFS  1
          479
          480     ;19 ASCII CHARS FOR COMPARISON
232A      481 ASCIIS  DEFM  '0123456789ABCDEFGHI'
          482
          483     ;6 TABLES FOLLOW: 3 BYTES OF TCS (FREQA&B)
          484     ;STEP SIZE, # OF INTS PER STEP (SWEEP MODE)
          485     ;AND OPMODE TABLE (1 BYTE ONLY)
          486
233D      487 TABLES   DEFB  00      ;LS BYTES OF TCS
233E      488     DEFB  33H
233F      489     DEFB  00
2340      490     DEFB  00
2341      491     DEFB  00
2342      492     DEFB  9AH
2343      493     DEFB  66H
2344      494     DEFB  0CDH
2345      495     DEFB  33H
2346      496     DEFB  66H
2347      497     DEFB  9AH
2348      498     DEFB  33H
2349      499     DEFB  00
234A      500     DEFB  0CDH
234B      501     DEFB  9AH
234C      502     DEFB  66H
234D      503     DEFB  0CDH
234E      504     DEFB  71H
234F      505     DEFB  33H
          506
2350      507     DEFB  00     ;0=75   MID BYTES OF TCS
2351      508     DEFB  00     ;1=100
2352      509     DEFB  33H    ;2=125
2353      510     DEFB  00     ;3=150
2354      511     DEFB  00     ;4=200
2355      512     DEFB  99H    ;5=250
2356      513     DEFB  66H    ;6=375
2357      514     DEFB  0CCH   ;7=500
2358      515     DEFB  33H    ;8=750
```

```
2359    516     DEFB   66H     ;9=1000
235A    517     DEFB   99H     ;A=1500
235B    518     DEFB   33H     ;B=2000
235C    519     DEFB   00      ;C=2400
235D    520     DEFB   0CCH    ;D=3000
235E    521     DEFB   99H     ;E=4000
235F    522     DEFB   66H     ;F=6000
2360    523     DEFB   4CH     ;G=8000
2361    524     DEFB   3DH     ;H=10000
2362    525     DEFB   33H     ;I=12000
        526
2363    527     DEFB   20H             ;MS BYTES OF TCS
2364    528     DEFB   18H
2365    529     DEFB   13H
2366    530     DEFB   10H
2367    531     DEFB   0CH
2368    532     DEFB   09H
2369    533     DEFB   06H
236A    534     DEFB   04H
236B    535     DEFB   03H
236C    536     DEFB   02H
236D    537     DEFB   01H
236E    538     DEFB   01H
236F    539     DEFB   01H
2370    540     DEFB   00
2371    541     DEFB   00
2372    542     DEFB   00
2373    543     DEFB   00
2374    544     DEFB   00
2375    545     DEFB   00
        546
        547
        548     ;STEP SIZE TABLE FOLLOWS
2376    549     DEFB   1
2377    550     DEFB   1
2378    551     DEFB   1
2379    552     DEFB   2
237A    553     DEFB   2
237B    554     DEFB   2
237C    555     DEFB   4
237D    556     DEFB   4
237E    557     DEFB   4
237F    558     DEFB   8
2380    559     DEFB   8
2381    560     DEFB   8
2382    561     DEFB   8
2383    562     DEFB   8
2384    563     DEFB   16
2385    564     DEFB   16
2386    565     DEFB   16
2387    566     DEFB   16
2388    567     DEFB   16
```

```
                568
                569     ;TABLE OF NUMBER OF INTS PER STEP FOLLOWS,
                570     ;SWEEP MODES DESCRIBED
2389            571     DEFB   4    ;0=RATE .5   FINE STEPS
238A            572     DEFB   2    ;1=RATE 1    FINE STEPS
238B            573     DEFB   1    ;2=RATE 2    FINE STEPS
238C            574     DEFB   8    ;3=RATE .5   DOUBLE STEPS
238D            575     DEFB   4    ;4=RATE 1    DOUBLE STEPS
238E            576     DEFB   2    ;5=RATE 2    DOUBLE STEPS
238F            577     DEFB   16   ;6=RATE .5   QUAD STEPS
2390            578     DEFB   8    ;7=RATE 1    QUAD STEPS
2391            579     DEFB   4    ;8=RATE 2    QUAD STEPS
2392            580     DEFB   32   ;9=RATE .5   OCT STEPS
2393            581     DEFB   16   ;A=RATE 1    OCT STEPS
2394            582     DEFB   8    ;B=RATE 2    OCT STEPS
2395            583     DEFB   2    ;C=RATE 8    OCT STEPS
2396            584     DEFB   2    ;D=RATE 32*  OCT STEPS
2397            585     DEFB   64   ;E=RATE .5   HEXD STEPS
2398            586     DEFB   32   ;F=RATE 1    HEXD STEPS
2399            587     DEFB   16   ;G=RATE 2    HEXD STEPS
239A            588     DEFB   4    ;H=RATE 8    HEXD STEPS
239B            589     DEFB   4    ;I=RATE 32*  HEXD STEPS
                590
                591
                592     ;TABLE OF OPMODE LOOKUP WORDS FOLLOWS
                593     ;MSDIGIT=MODE, BIT3=PATCH?
                594     ;BIT2=ASWEEP (1) OR BSWEEP
                595     ;BIT1=SPARE
                596     ;AND BIT0=UP-DN INITIAL (1=UP)
                597
239C            598     DEFB   00000101B   ;0=WAIT
239D            599     DEFB   01010101B   ;1=AA   UP
239E            600     DEFB   10100001B   ;2=BB   (B SWEEPS)
239F            601     DEFB   11110101B   ;3=NN
23A0            602     DEFB   01110101B   ;4=AN
23A1            603     DEFB   11010101B   ;5=NA
23A2            604     DEFB   01101101B   ;6=AB   (PATCHABLE)
23A3            605     DEFB   10011101B   ;7=BA   (PATCHABLE)
23A4            606     DEFB   01100101B   ;8=AB'
23A5            607     DEFB   01100001B   ;9=AB''(B SWEEPS)
23A6            608     DEFB   01010100B   ;A=AA   DOWN
23A7            609     DEFB   10100000B   ;B=BB   (B SWEEPS)
23A8            610     DEFB   11110100B   ;C=NN
23A9            611     DEFB   01110100B   ;D=AN
23AA            612     DEFB   11010100B   ;E=NA
23AB            613     DEFB   01101100B   ;F=AB   (PATCHABLE)
23AC            614     DEFB   10011100B   ;G=BA   (PATCHABLE)
23AD            615     DEFB   01100100B   ;H=AB'
23AE            616     DEFB   01100000B   ;I=AB''(B SWEEPS)
                617
                618 CTC0    EQU    0F0H
                619 CTC1    EQU    0F1H
```

```
620 CTC2     EQU    0F2H
621 PIO1AD   EQU    0E4H
622 PIO1BD   EQU    0E5H
623 PIO1AC   EQU    0E6H
624 PIO1BC   EQU    0E7H
625 PIO0AD   EQU    0E0H
626 PIO0BD   EQU    0E1H
627 PIO0AC   EQU    0E2H
628 PIO0BC   EQU    0E3H
629
630     END

0 ASSEMBLY ERRORS
```

APPENDIX II SCHEMATIC DIAGRAMS

Schematic diagrams for the entire prototype system, excluding the MCB and MDC boards within the microcomputer, follow. The IC types are standard and noncritical with the exceptions listed below:

1). Interdesign 1511 Waveform Generator: low distortion, high linearity--

2). Motorola MC14046B Phaselocked loop: used as a digital phase detector--

3). Intersil ICL 8049 Antilog generator

4). Signetics NE527 comparator: very fast for use in noise generator clock circuitry

5). Analog Devices AD533 Multiplier: four quadrant device needs trimming, higher quality pretrimmed type recommended

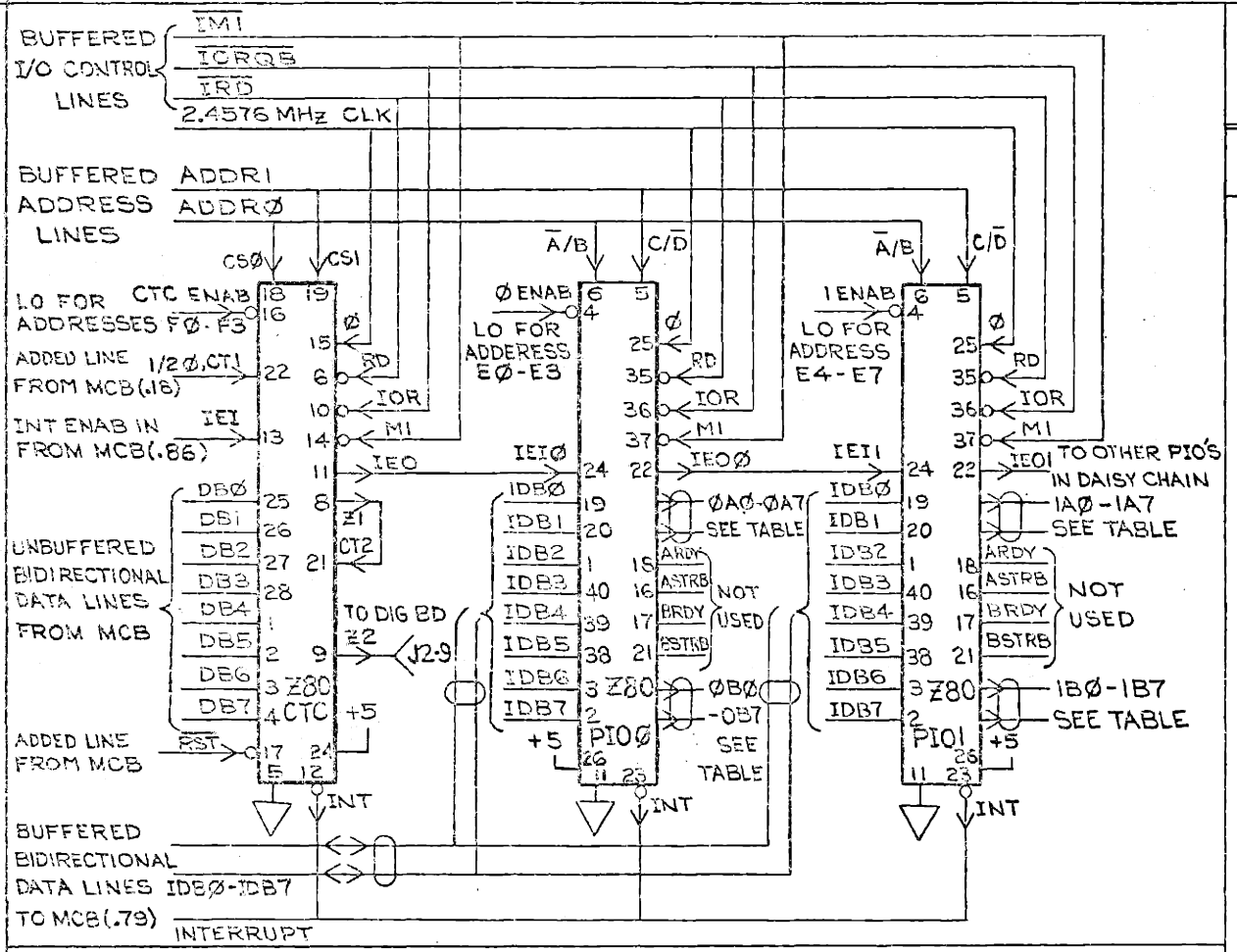

FIG. AII-1: PARTIAL SCHEMATIC: MICROPROCESSOR INPUT/OUTPUT

(SEE Z80 IOB HARDWARE USER'S MANUAL)

TABLE OF I/O INTERCONNECTIONS FROM IOB TO DIGITAL BD

NAME	PIO CONN	I/O JACK CONN
ØAØ	PIOØ: pin 15	J3 pin 9
ØA1	14	10
ØA2	13	11
ØA3	12	12
ØA4	10	13
ØA5	9	14
ØA6	8	15
ØA7	7	16
ØBØ	pin 27	pin 8
ØB1	28	7
ØB2	29	6
ØB3	30	5
ØB4	31	4
ØB5	32	3
ØB6	33	2
ØB7	34	1
1AØ	PIO1: pin 15	J4 pin 9
1A1	14	10
1A2	13	11
1A3	12	12
1A4	10	13
1A5	9	14
1A6	8	15
1A7	7	16
1BØ	pin 27	pin 8
1B1	28	7
1B2	29	6
1B3	30	5
1B4	31	4
1B5	32	3
1B6	33	2
1B7	34	1

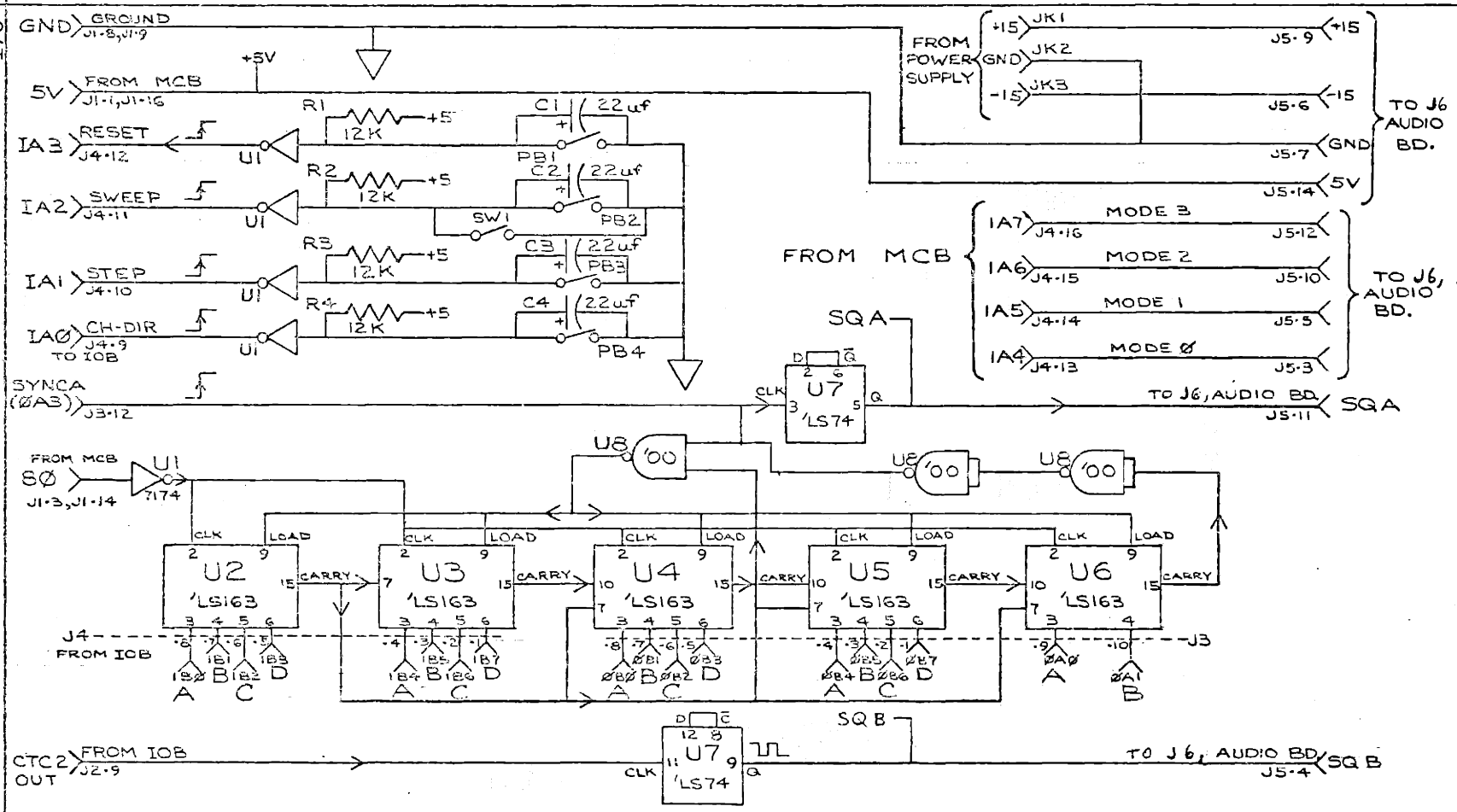

FIG. AII-2: SCHEMATIC OF SQUARE WAVE GENERATORS (DIGITAL BOARD)

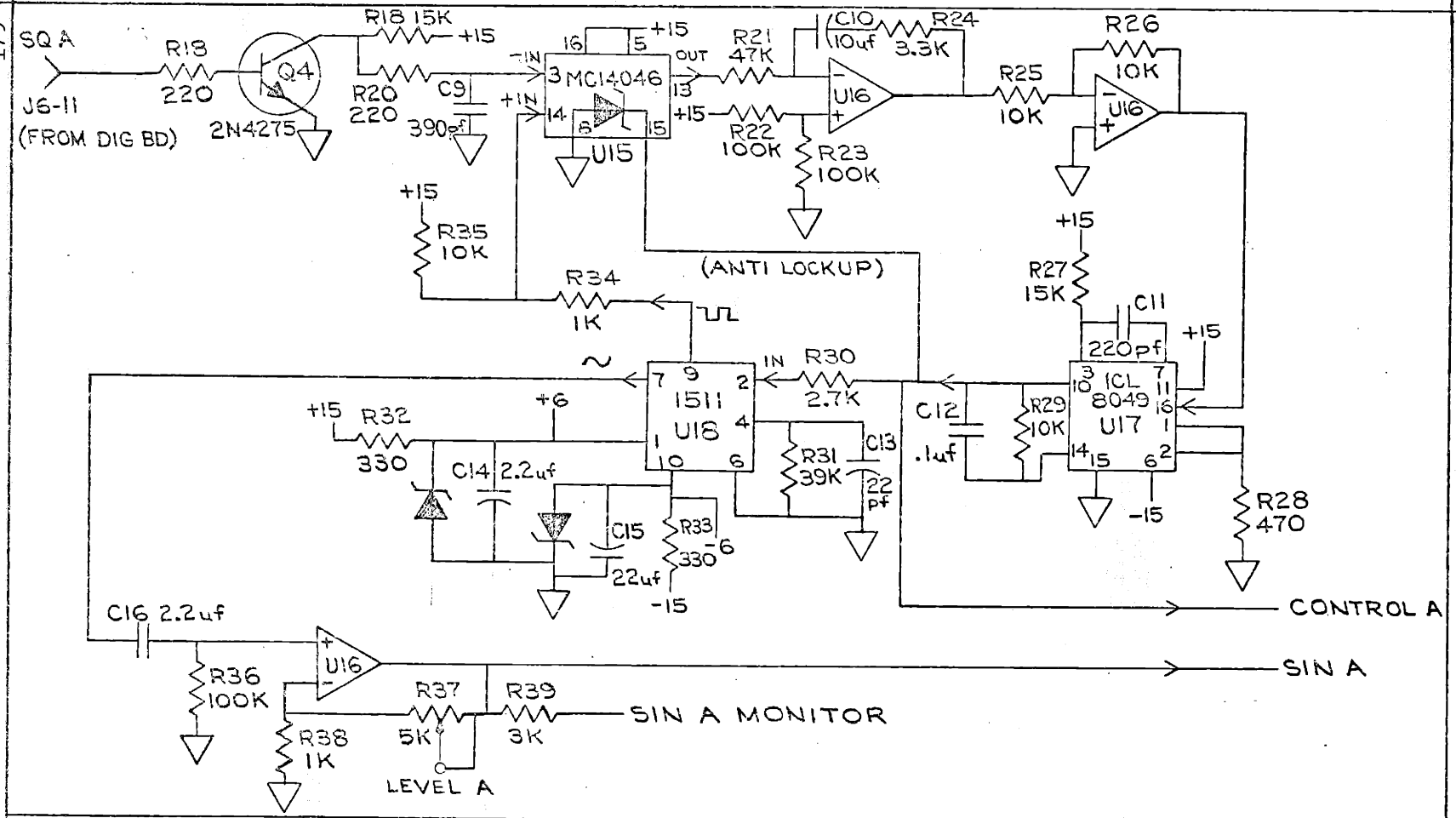

FIG. AII-3: SCHEMATIC OF PHASE-LOCKED LOOP A (AUDIO BOARD)

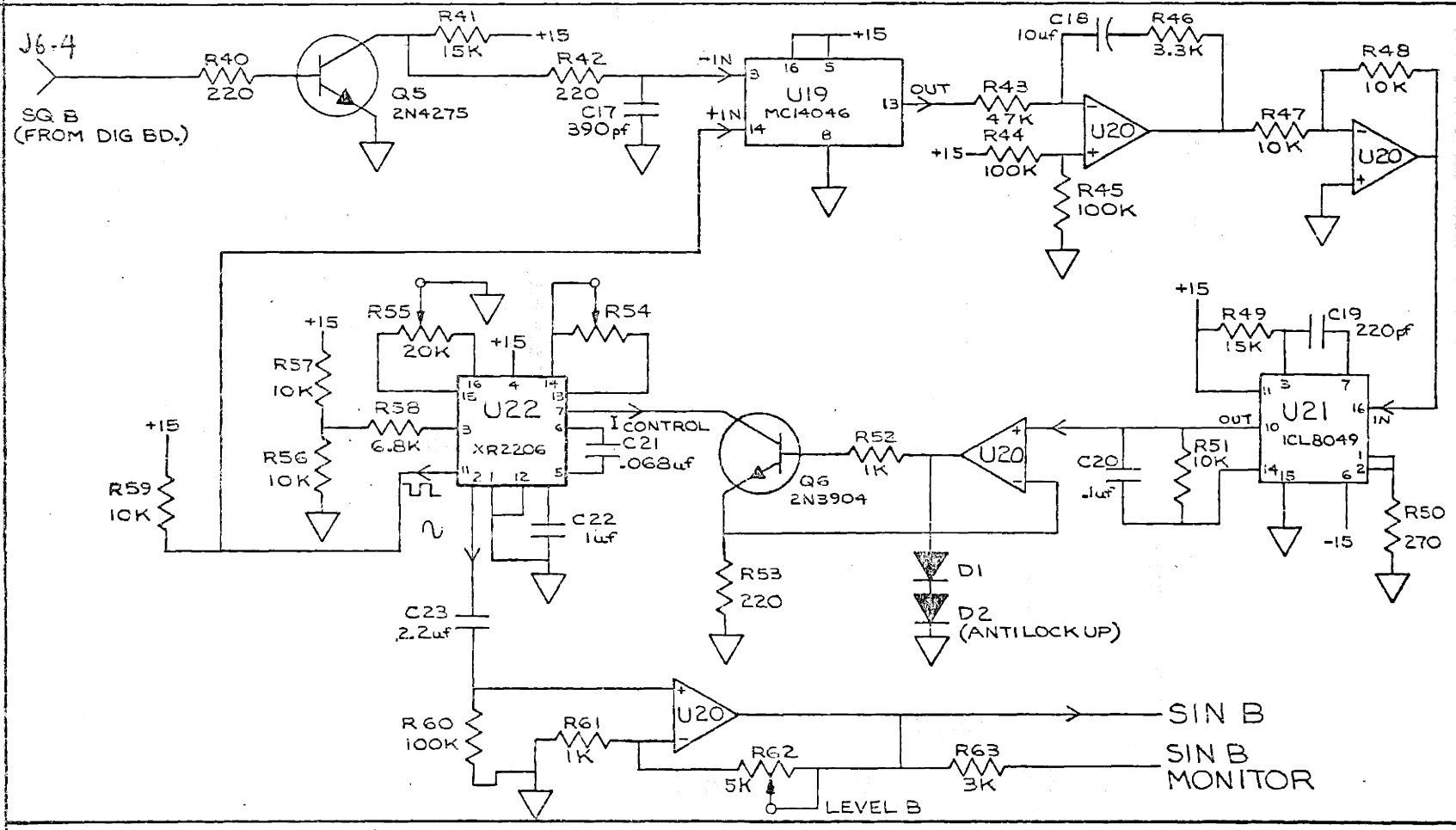

FIG. AII-4: SCHEMATIC OF PHASE-LOCKED LOOP B (AUDIO BOARD)

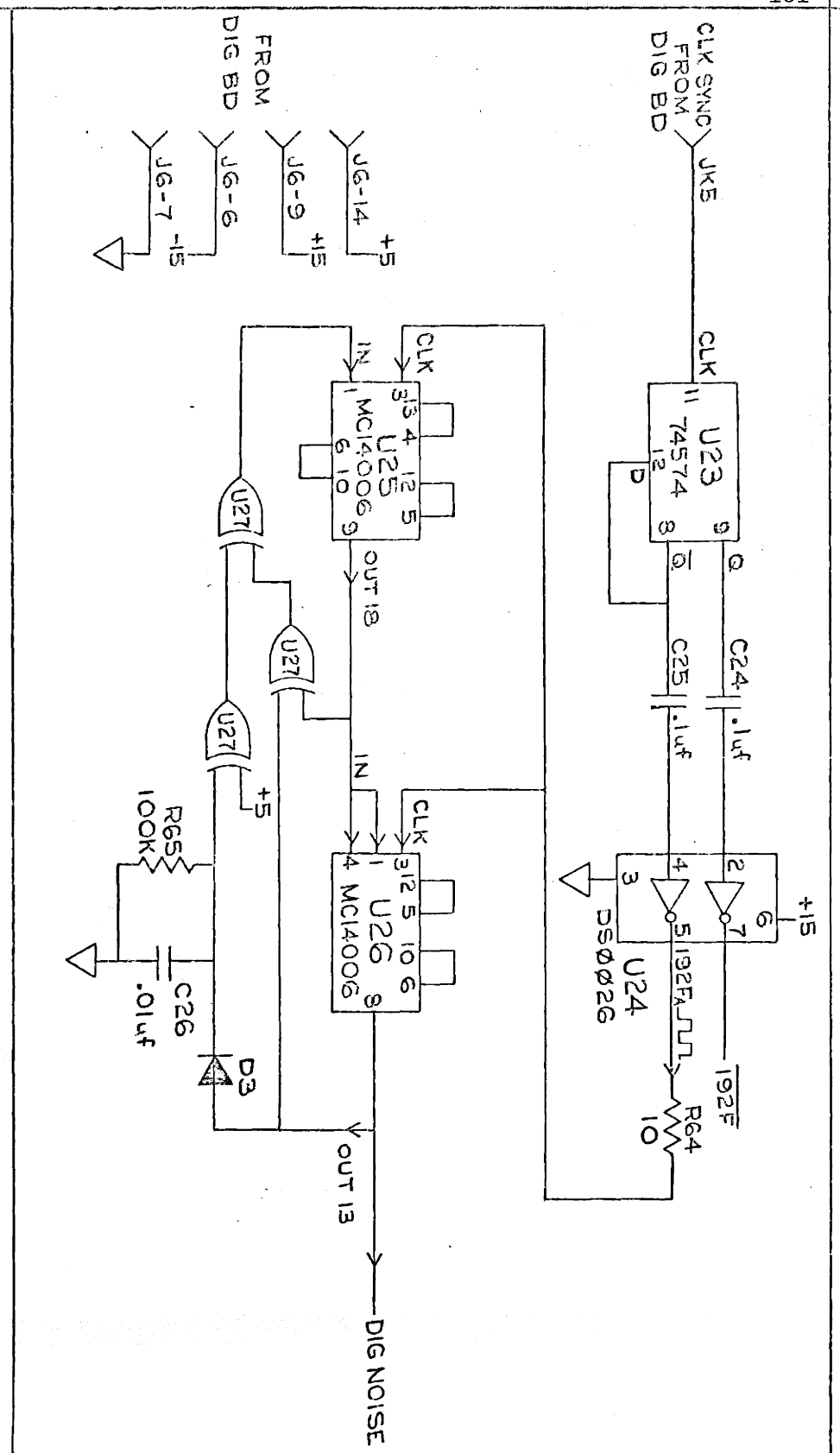

FIG. AII-5: SCHEMATIC OF DIGITAL NOISE GENERATOR (AUDIO BOARD)

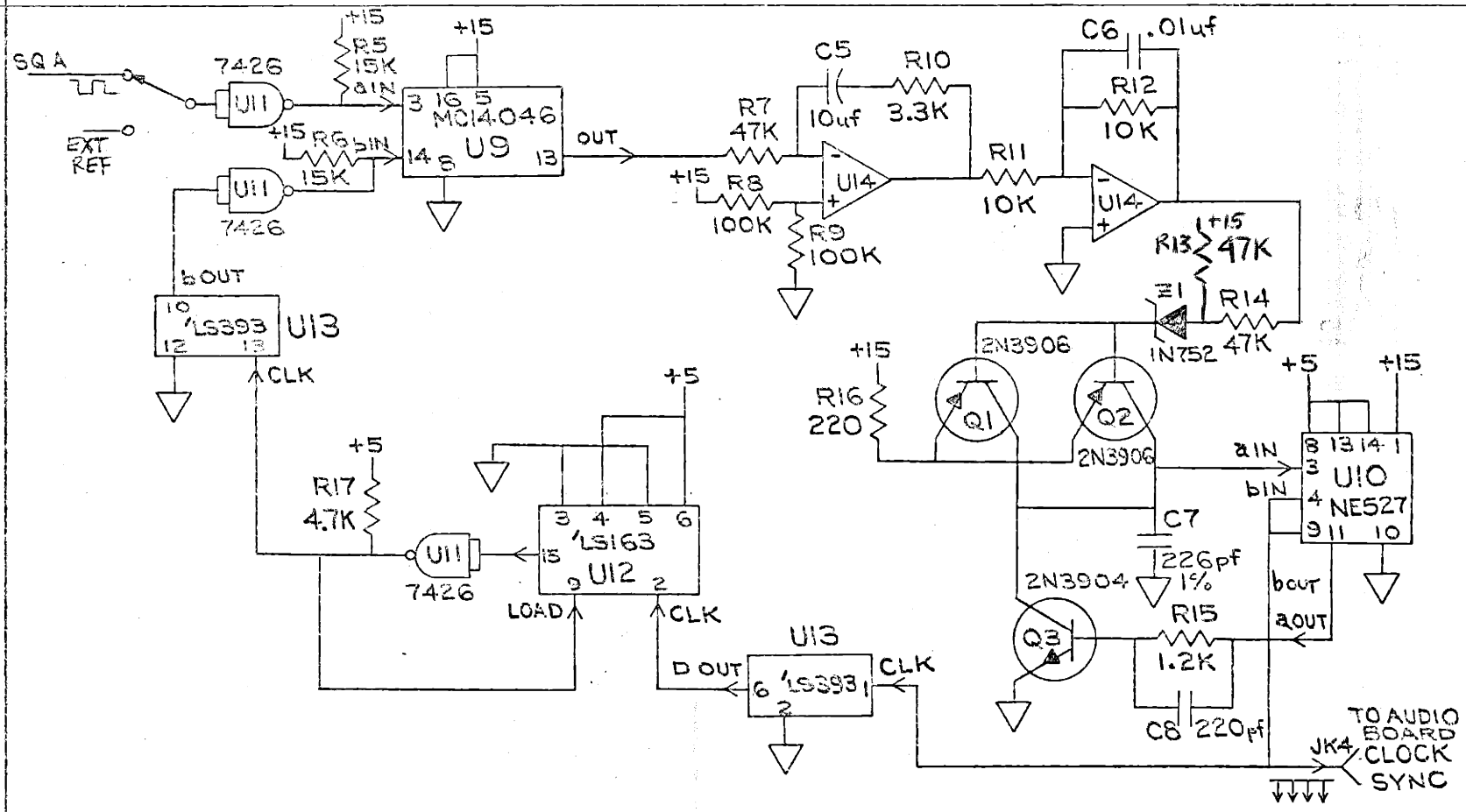

FIG. AII-6: SCHEMATIC OF CLOCK GENERATOR (DIGITAL BOARD)

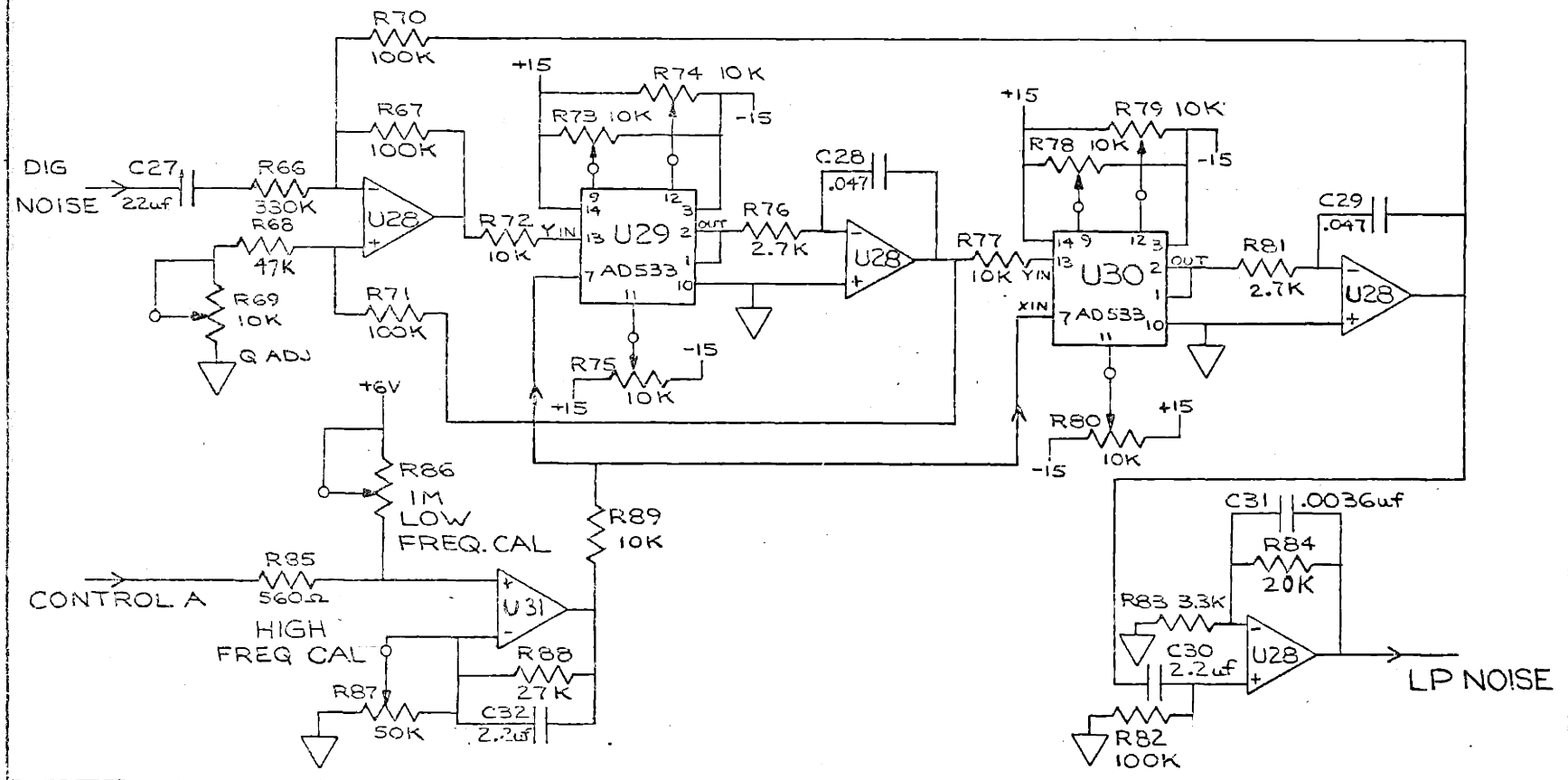

FIG. AII-7: SCHEMATIC OF VOLTAGE CONTROLLED FILTER (AUDIO BOARD)

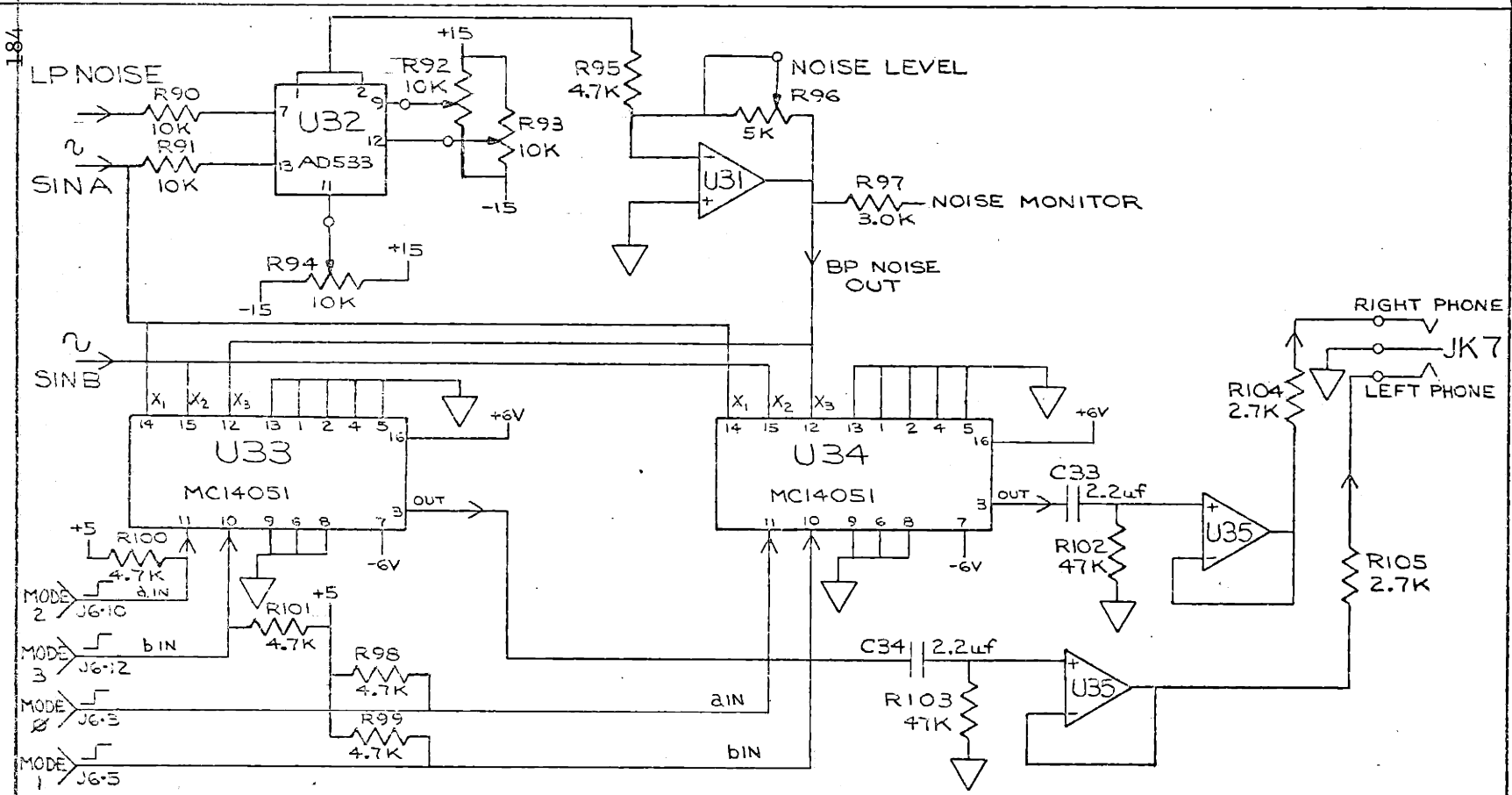

FIG. AII-8: SCHEMATIC OF MULTIPLIER AND SWITCHING (AUDIO BOARD)

HISTORICAL AND CLINICAL REFERENCES

American National Standards Institute. Specifications for Audiometers, ANSI S3.6, 1969.

American National Standards Institute. Draft Specifications for Audiometers, May, 1978.

Aristotle. De Audibilibus. Trans. T. Loveday and E.S.Forster (1913) reproduced in Lindsay, R.Bruce, ed. Acoustics: Historical and Philosophical Development, q.v.

Bekesy, Georg von. "A new audiometer". Acta Otolaryngol. Vol. 35, 411-422, 1947

Beranek, Leo L. Acoustic Measurements. New York: John Wiley & Sons, 1949.

Bunch, C.C. "The development of the audiometer", Laryngoscope, Vol. 51, 1100-1118, 1941.

Bunch, C.C. and Dean, L.W. "The use of the pitch range audiometer in otology", Laryngoscope, Vol. 29, 453-462, 1919.

Davis, Audrey B. and Merzbach, Uta C. Early Auditory Studies. Activities in the Psychology Laboratories of American Universities. Washington, D.C.: Smithsonian Institution Press, 1975.

Fletcher, Harvey. Speech and Hearing in Communication. New York: Van Nostrand, 1953.

Grason-Stadler Co., Littleton, Mass. Bekesy Audiometer, Model E800 Instructions., 1965.

Grason-Stadler Co., Littleton, Mass. 1701 Audiometer Instruction Manual, 1978.

Green, David M. An Introduction to Hearing. New York: John Wiley & Sons, 1976.

Harris, J. Donald, ed. Forty Germinal Papers in Human Hearing, Groton, CN: J. Aud. Res. Publ., 1969.

Hirsh, Ira J. The Measurement of Hearing. New York: McGraw-Hill, 1952.

Johnson, E.W. "Tuning forks to audiometers and back again", Laryngoscope, Vol. 80, 49-68, 1970.

Katz, Jack, ed. Handbook of Clinical Audiology. Baltimore, MD: Williams and Wilkins, 1972.

Lindsay, R. Bruce, ed. Acoustics: Historical and Philosophical Development. Stroudsburg, PA: Dowden, Hutchinson & Ross, 1966.

Lindsay, R.Bruce. "The story of acoustics", J. Acoust. Soc. Amer, Vol. 39, 629-644, 1966.

Lucretius. T. The Nature of the Universe. Book IV. Baltimore, MD: Penguin, 1952.

Macfarlan, Douglas. "History of audiometry". Arch. of Otolaryngol, Vol. 29, 514-519, 1939.

Mackintosh, John. Principles of Pathology and Practice of Physic. Washington, D.C.: Register and Library of Medical and Chirurgical Science, 1834.

Martin, Frederick N. Introduction to Audiology. Englewood Cliffs, NJ: Prentice-Hall, 1975.

Raue, C.G. Special Pathology and Diagnostics with Therapeutic Hints. Philadelphia, PA: Hahnemann Publishing House, 3rd ed., 183-212, 1885.

Richards, Alan M. Basic Experimentation in Psychoacoustics. Baltimore, MD: University Park Press, 1976.

Schroeder, Manfred R. "Models of hearing". Proc. IEEE, Vol. 63, 1332-1350, 1975.

Stevens, S.S. and Davis, Hallowell. Hearing: Its Psychology and Physiology. New York: John Wiley & Sons, 1938.

Susskind, Charles. "American contributions to electronics: coming of age and some more", Proc. IEEE, Vol. 64, 1300-1305, 1976.

Ventry, Ira M., Chaiklin, Joseph B. and Dixon, Richard F., eds. Hearing Measurement: A Book of Readings. New York: Appleton Century Crofts, 1971.

Watson, Leland A. and Tolan, Thomas. Hearing Tests and Hearing Instruments. Baltimore, MD: Williams and Wilkins, 1949,

Selger, Donna J., consulting audiologist, private correspondence.

BIBLIOGRAPHY FOR ELECTRONIC DESIGN

Analog Devices, Inc., Norwood, MA. Product Guide, 1975.

Baertsch, R.D., Engeler, W.E., Goldberg, H.S., Puckette, C.M. and Teimann, J.J. "The design and operation of practical charge transfer transversal filters". IEEE J. of Solid State Circuits, Vol. SC-11, 65-74, 1976.

Burr-Brown Research Corp., Tucson, AZ. Universal Active Filter: UAF-31 Specifications and Design Notes.

Buss, D.D., Collins, D.R., Bailey, W.H. and Reeves, C.R. "Transversal filtering using charge transfer devices". IEEE J. of Solid State Circuits, Vol. SC-8, 138-146, 1973.

Buss, R.R., and Tanaka, S.C. "Implementation of discrete time analog filter and processing systems", Reticon Corp., Application Note #111, Sunnyvale, CA., 1977.

Cantarano, S. and Pallattino, G.V. "Approximate results for networks containing periodically operated switches". Proc. IEEE, Vol. 57, 2070, 1969.

Caves, J.T., Copeland, M.A., Rahim, C.F. and Rosenbaum, S.D. "Sampled analog filtering using switched capacitors as resistor equivalents". IEEE J. of Solid State Circuits, Vol. SC-12, 592-599, 1977.

Cumming, I.G. "Autocorrelation function and spectrum of a filtered pseudorandom binary sequence". Proc. IEE, Vol. 114, 1360-1362, 1967.

Delegrange, A.D. "It could be the 'ideal' filter". Electronic Design, Vol. 24, no. 4, 156-161, 1976.

Dove, Webster P. A Digitally Controlled Precision Oscillator. Thesis for BSEE, Mass. Inst. of Technology, January 1978.

Drake, Alvin W. Fundamentals of Applied Probability Theory. New York: McGraw-Hill, 1967.

Exar Integrated Systems, Inc., Sunnyvale, CA. XR-2206 Monolithic Function Generator Specifications, 1975.

Gardner, Floyd M. Phaselock Techniques. New York: John Wiley & Sons, 1966.

Gorski-Popeil, Jerzy, ed. Frequency Synthesis: Techniques and Applications. New York: IEEE Press, 1975.

Gray, A.H. and Markel, J.D. "A computer program for designing digital eliptical filters". IEEE Trans. on Acoustics, Speech & Signal Processing, Vol. ASSP-24, 529-535, 1976.

Intersil Corp., Cupertino, CA. Analog Products Catalog, Volume I, 1976.

Jung, Walter G. "Applications of the two quadrant transconductance amplifier/multiplier in audio signal processing". J. of the Audio Eng. Soc., Vol. 23, 207-212, 1975.

Kaiser, J.F. "Nonrecursive ditigal filter design using the I -SINH window function." Proc. 1974 IEEE Int. Symp. on Circuits and Systems, 20-23.

Knapton, James H. "Waveform Generator". Monochip Application Note APN-8, Interdesign Corp., Sunnyvale, CA, 1976.

Lee, Y.W. Statistical Theory of Communication. New York: John Wiley & Sons, 1960.

Lindsey, William C. and Simon, Marvin K., eds. Phase-Locked Loops and Their Application. New York: IEEE Press, 1978.

McClellan, J.H., Parks, T.W., and Rabiner, L.R. "A computer program for designing optimum FIR linear phase digital filters". IEEE Trans. Audio & Electroacoust., Vol. AU-21, 506-526, 1973.

Motorola Semiconductor Products, Inc., Phoenix, AZ. Semiconductor Data Library - CMOS. Vol. 5, 1976.

Oppenheim, Alan V. and Schafer, Ronald W. Digital Signal Processing. Englewood Cliffs, NJ: Prentice-Hall, 1975.

Patangia, H.C. and Blostein, M.L. "A digitally controlled tunable N-path filter". IEEE Trans. on Circuits & Systems, Vol. CAS-25, 135-144, 1978.

Rabiner, L.R. "Approximate design relationships for low pass FIR digital filters". IEEE Trans. Audio & Electroacoust., Vol. AU-21, 456-460, 1973.

Rabiner, L.R., Kaiser, J.F., Herrmann, O. and Dolan, M.T. "Some comparisons between FIR and IIR digital filters". Bell System Tech. J., Vol. 53, 305-331, 1974.

Rabiner, L.R., McClellan, J.H. and Parks, T.W. "FIR digital filter design techniques using weighted Chebyshev approximation". Proc. IEEE, Vol. 63, 595-610, 1975.

Roberts, P.D. and Davis, R.H. "Statistical properties of smoothed maximal-length linear binary sequences". Proc. IEE, Vol. 113, 1360-1362, 1966.

Saha, Sisir K. "Electronically tunable RC sinusoidal oscillators". IEEE Trans. on Instrumentation & Measurement, Vol. IM-24, 156-159, 1975.

Schwartz, Mischa. Information Transmission, Modulation, and Noise. New York: McGraw-Hill, 492-499, 1970.

Signetics Corp., Sunnyvale, CA. Data Manual, 1976.

Texas Instruments, Inc., Dallas, TX. The TTL Data Book for Design Engineers, 2nd ed., 1976.

Thomas, Lee C. "The biquad: Part 1 - some practical design considerations". IEEE Trans Circuit Theory, Vol. CT-18, 350-357, 1971.

Tow, J. "A step-by-step active filter design", IEEE Spectrum, Vol. 6, 64-68, 1969.

Weaver, C.S. "A new approach to the linear design and analysis of phase-locked loops". IRE transactions on Space Electronics and Telemetry, Vol. SET-5, 166-178, 1959.

Weckler, Gene P. "A tapped analog delay for sampled data signal processing". Proc. of the 19th Midwest Symposium on Circuits & Systems, Univ. of Wisconsin, 1976.

Wozencraft, J.M. and Jacobs, I.M. Principles of Communication Engineering. New York: John Wiley & Sons, 1965.

Zilog, Inc., Cupertino, CA. Z-80 Series of Technical and User's Manuals. a)Z-80-CPU Technical Manual (1977); b)Z-80-CTC Technical Manual (1977); c)Z-80-PIO Technical Manual (1977); d)Z-80-OS2.1 Software User's Manual (1978); e)Z-80-PDS Hardware User's Manual (1978); f)Z-80 MCB Hardware User's Manual (1978); g)Z-80-IOB Hardware User's Manual (1977); h)Z-80 Assembly Language Programming Manual (1978).

Zilog, Inc., Cupertino, CA. "Application Note: The Z-80 family interrupt structure", 1977.

Goldberg, Hyman, Dyn-Aura Eng. Labs, San Diego, CA., private correspondence.

Steele, John M., GenRad Inc., Bolton, MA., private correspondence.